INVESTIGATION OVER ''COMPETITIVE GROWTH" IN SEED POLYMERIZATION OF VINYL CHLORIDE

Master thesis 1970 by

Finn Knut Hansen

This work is done in the autumn
1970 at the Department of
Industrial Chemistry, NTH
under the leadership of
Professor J.Ugelstad

I hereby declare that this task
is performed independently and
in accordance with the Norwegian Institute of Technology's master regulations.

Trondheim 20.12.1970

Finn Knut Hansen (sign.)

Note: This report is a digitized translation of the original written thesis from 1970. The content is the same as in the original thesis and no later knowledge has been added. Some of the mathematical derivations have been used in later publications. The original graphs have been redrawn by the Origin graphing program from the original numerical data. Simulated models have been recomputed to render the same data as in in the original. The appendices have not been translated nor included in this version.

Oslo, May 5, 2018

1 Contents

2 Abstract

In this work, the relative growth of two particle sizes was studied by emulsion polymerization of vinyl chloride (seed polymerization). Particles with diameters of about 1000 and 2000 Å were used. The total particle number was varied between 0.9 and 5.4 1016 particles per L water, and the ratio of the number of small and large particles between 1:1 and 13:1. The initiator concentration was varied in three runs between 6 10^{-3} and 7.5 10^{-4} moles of potassium persulfate per. L water. In the experiments, sodium lauryl sulfate was used as an emulsifier in 80% coverage at start and the temperature was 50 °C.

The experiments gave an experimental order of the volume growth of the particles with respect to diameter between 2 and 3. This increased with increasing total PVC content in the seed latex, but was almost independent of the ratio of the number of large and small particles. The variation of the initiator concentration gave no clear trend, but a possible slight increase in the order could be observed. The uncertainty in this order was quite large (± 0.2 on average), which was due to uncertainty in the particle diameters.

A mechanism of desorption and reabsorption of radicals was adapted to the system, which gave an explanation of the experimental order, while the conformity was not complete.

3 Introduction

3.1 Earlier work

Competitive growth in emulsion polymerization has so far only been studied with styrene as monomer. Ewart and Carr (7) studied the growth in step II of a regular emulsion polymerization using statistical expressions developed on the basis of a mean radical number in the particles, $\bar{n}$ equal to 0.5 (case 2 in Smith and Ewart's theory, see also section 4.1). Using measurements of images of the latex particles taken with electron microscopes, they determined the distribution of the particles on the particles and could correlate the test results with their statistical expressions using the spread on this and the volume distribution. They found that the distribution curves for the diameter and for the volume expand during the polymerization, i.e. that the spread increases over time (Tables I and II). The spread on the volume showed a strong increase, the relative spread, as Ewart and Carr denote $\Delta d / \bar{d}$ and $\Delta d^3 / \bar{d}^3$, respectively (diameter and volume), showed a slight decreasing trend (Table II). However, they do not have any good quantitative explanation of their results.

Sample no.	Potassium laurate, g./100 cc. water	Styrene, g./100 cc. water	$\bar{d}$, cm. × 10^4	$\overline{d^3}$, cm.^{3} × 10^{14}	No. of particles/ cm.^{3} water × 10^{-14}
2	0.10	2.64	0.2219	1.109	0.433
3	.10	8.90	.3177	3.305	0.490
4	.15	1.1	.1117	0.1430	1.40
5	.15	8.8	.1743	0.5515	2.90
6	.15	29.6	.2756	2.135	2.52
7	.21	3.3	.0998	0.1073	5.59
8	.21	26.4	.1754	0.5747	8.03
9	.21	63	.2394	1.429	8.01

Table I. Experimental conditions and results from Ewart and Carr (7).

Sample no.	Δd, cm. × 10^4	Δd^3, cm.^{3} × 10^{14}	$\Delta d/\bar{d}$	$\Delta d^3/\bar{d}^3$
2	0.0175	0.201	0.079	0.182
3	.0356	.650	.112	.197
4	.0104	.0331	.094	.232
5	.0215	.156	.123	.284
6	.0231	.463	.084	.217
7	.0175	.0404	.176	.377
8	.0269	.208	.154	.363
9	.0285	.443	.120	.310

Table II. Absolute and relative spread from Ewart and Carr (7).

The method used by Ewart and Carr gives little quantitative results. Another method was developed by Vanderhoff et al. (4), (5). These used a seed polymerization by a mixture of two monodisperse latexes of different particle size. In this case, approximately uniform particles

of different size will compete with each other for free radicals and possibly monomer in the same system. This has given rise to the name of competitive growth.

Vanderhoff et al. conducted the polymerization in closed bottles at temperatures of 50, 70 and 90 ° C (thermostat bath). The reactions went to virtually complete sales. Particle sizes were used at 1260, 2640, 5570, and 11710 Å (see Table III). As an initiator, potassium persulfate was used in different concentrations. Polymerizations initiated by benzoyl peroxide and γ-radiation were also performed.

Run No.	Average particle diameter, A	Standard deviation, A	No. of measurements	Designation used hereafter
LS-052-A	1,260	52	97	52
LS-057-A	2,640	60	577	57
LS-063-A	5,570	108	373	63
LS-067-A	11,710	133	315	67

Table III. Data for seed latexes used by Vanderhoff et al. (5).

The study was conducted thoroughly by varying the following sizes: seed diameter, number of seed particles, ratio of number of large and small particles (between 1/9 and 9/1, mostly 1/1), initiator concentration (between 0, 05 and 10 g $K_2S_2O_8$/ L H2O), the temperature, monomer / polymer ratio (1, 2, 5 and 10) and emulsifier concentration (usually no additional emulsifier was added).

By means of the expression $\frac{dv}{dt} = kD^x$, (3:1)

they could set up curves for the ratio D_b/D_a as a function of D_a/D_a^0 and x during polymerization. Here is

v - volume of a particle without monomer
D - diameter, if any, a particle without monomer
t - time
k - constant depending on time, but not by D
x - order with respect to diameter
index a - small particles
index b - large particles
Index 0 - seed particles

(A more thorough investigation is given in the theoretical section, section 4.3.2).

In all their experiments with persulfate as initiator, they got the x between 2 and 2.5. The accuracy of the determination of their x was not better than +/- 0.1 and often higher. Experiments with particles of diameter 1260 and 2640 Å gave an x which increased with increasing initiator concentration (from x = 2.0 at 0.2 g/L H_2O to x = 2.4 at 10 g/L H_2O) (see figure 1) while larger diameter particles gave a constant or decreasing x (see Figure 2). (Vanderhoff et al. used the letter n for the exponent, which is here called x). The number of particles was not the same for these experiments (Table IV). They also found that x was

almost independent of the temperature and the ratio N_a^w/N_b^w, where N_i^w is the number of small, large parties per unit volume of water, respectively.

Pair	Particles per ml. H_2O, $\times 10^{-10}$	Particles per ml. H_2O, $\times 10^{-10}$	Total particles per ml. H_2O, $\times 10^{-10}$	Total no. of particles per seed charge, $\times 10^{-12}$
52–57	106–52	88.2–57	194	384
52–63	12.6–52	10.5–63	23.1	45.8
52–67	1.37–52	1.14–67	2.52	4.98
57–63	8.95–57	10.5–63	19.3	38.6
57–67	1.13–57	1.13–67	2.26	4.48
63–67	1.03–63	1.03–67	2.06	4.09

Table IV. Experimental conditions of Vanderhoff et al. (5).

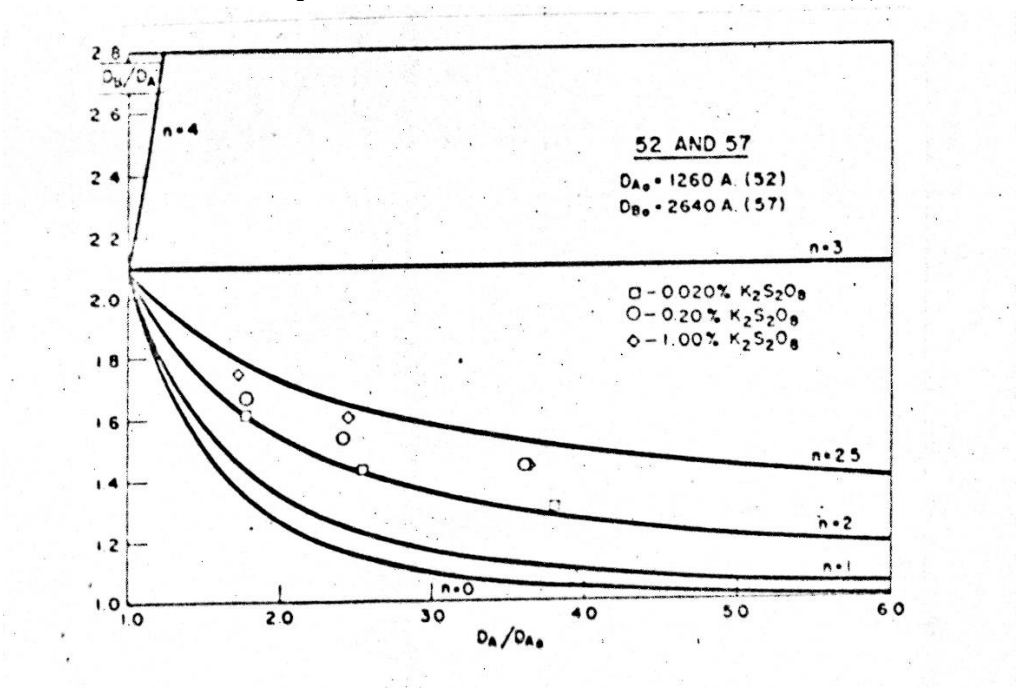

Figure 1. Some results from Vanderhoff et al. (5).

Upon initiation with γ-radiation, x they found between 2 and 2.7, depending on temperature and particle sizes. Their experiments with benzoyl peroxide as initiator (2 g/L monomer, 70 ° C) (suspension polymerization) gave an x which increased from about 2 to 4 with increasing conversion.

As mentioned, they did not usually use extra emulsifiers added as they operated with highly diluted emulsions. They did not get any new particles, but a weak coagulation. Attempts at which additional emulsifier was added gave no new formation with less than about 2 g/L H_2O. They do not specify the type of emulsifier used. Vanderhoff et al. have only to a small degree attempted to give a physical explanation of their results. For discussion of these, see section 8.

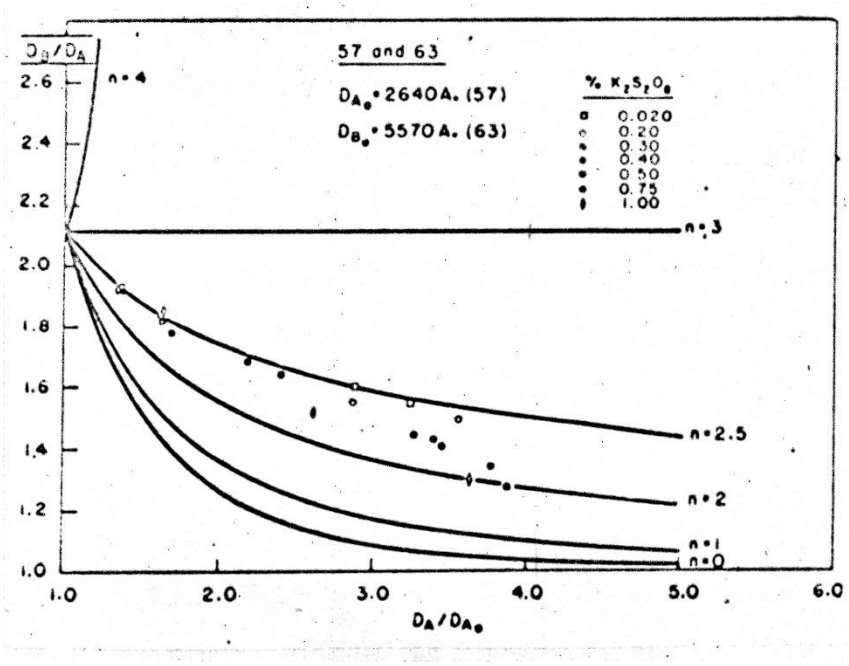

Figure 2. Some results from Vanderhoff et al. (5).

Gerrens (7) states that unpublished results from further investigations made by the same authors have given an x between 1 and 2 for smaller particles (800-1400 Å). He also states that Vanderhoff and Bradford have used the method of competing growth on co-polymerization in the systems styrene-divinylbenzene and styrene-acrylonitrile (also unpublished results). At the beginning of the polymerization, they have found x = 2 while increasing with increasing turnover. Further experimental conditions are not specified.

3.2 Execution of the work

The work has been carried out in close cooperation with Professor J. Ugelstad and personnel at the Department of Industrial Chemistry, NTH, and can be considered as a supplement to and continuation of some of their work on emulsion polymerization of vinyl chloride. The experiments are thus carried out on fixed appliances (glass autoclave, see section 5, and experimental section 6) at the department, and according to the conditions and procedures partly used in completed and ongoing work.

Preparation of samples for electron microscopy and image magnification and copying were carried out by personnel at the department following well-established methods (see section 6.4.2).

Therefore, in the choice of experimental methods and conditions it is considered that the results should as far as possible be comparable with the previous work at the institute and that calculations should be able to use data (eg constants) found in these works. This applies to the choice of temperature, emulsifier, initiator, buffer, stirrer speed, etc.

Most experiments were therefore made with sodium lauryl sulfate as emulsifier. In connection with ongoing work at the institute, some experiments were also carried out with

the addition of fatty alcohol (hexadecanol) in consultation with Professor Ugelstad. Here, everything was experimentally due to the time restrictions done by staff at the department. The designation of the experiments shows who they are performed by, as all experiments designated by B-, are performed by the author, while all others are performed by departmental staff.

3.3 Plan for the work

The time frame for the assignment was 15 weeks (1.9. - 14.12.1970). As a first plan for the work, one could put:

I Introductory literature studies and training in experimental methodology.
II Preparation of seed.
III Experiments with competitive growth
IV Final treatment of experimental results.
V Report writing

Literature studies will of course be included in all the points to a greater or lesser extent. It was found that point II took longer than expected (about 3 weeks) due to waiting for electron microscope images and dialysis of the seed latexes, partly because it was somewhat uncertain how to best produce sufficient monodispers seed. The polymerization under point III could be carried out at in about 5 weeks, while microscopy and particle measurements (which were partially performed simultaneously with the experiments) took another 2 weeks. Treatment of the results and theoretical derivations were conducted in parallel with this. Computer processing was delayed due to machine failure and reduced operation. Therefore, it was applied for a week's extension of the submission deadline, which was granted. The report writing took approximately the planned time (about 3 weeks).

Regarding the competitive growth experiments, the plan was to vary the factors that were believed to have the greatest impact on relative growth, such as total number of particles, the ratio of large to small particles (in number), and concentration of initiator. In terms of variation of particle size on seed, it was found that this would require more than the planned 12-15 experiments in addition to the above mentioned factors to get a satisfactory number of experiments with variation of the other factors. After part of point II was completed, it was found that it would take too long to produce seeds with a diameter substantially above 2300 Å, which must be manufactured in two stages with intermediate dialysis, and that there would be very few particles from one such manufacturing method (about 10^{16} per L H2O per run in the 2nd stage to about 3500 Å). Substantially smaller particles than about 1000 Å diameter will also be difficult to measure, and could give great uncertainty in D_a^0 (at 24000x magnification). It was therefore decided that the experiments should be done with only two substantially different particle sizes.

4 Theoretical

4.1 Ordinary emulsion polymerization

The major features of the mechanism of emulsion polymerization are clarified by Harkins et al. (12) and are treated quantitatively in the work of Smith and Ewart (13). An overview of these works is, among other things, given by Bowey et al. (14) and by Gerrens (7). Harkins' theory is based on the initiation of polymeric radicals in micelles swollen with monomer. Micelles are small aggregates of emulsifier molecules formed when the concentration of emulsifier in the water exceeds the solubility of free emulsifier molecules, the critical micellar concentration (c.m.c.), which among other factors is depending on the nature of the emulsifier. The monomer is present as its own dispersed phase (with down to 1 μm drop size) and monomer molecules diffuse from it through the aqueous phase to the micelles.

Free radicals initiated in the water phase from the initiator diffuse into the micelles and initiate growing polymer chains within them. Micelles are rapidly changing to polymer particles swollen with monomer, and emulsifier from the water phase and from micelles that have not formed polymer particles are adsorbed on them. The initiation of new particles therefore stops after a certain period of time. This is stage I in the polymerization. In stage II, no new particles are formed, while those already formed grow by the absorption of new radicals and monomers. The particles will usually be in the form of spheres due to swelling with monomer.

The growing polymer chains in the particles are terminated by the usual mechanisms applicable to radical polymerization; combination, disproportionation and chain transfer, the latter does not change the number of radicals and is usually not considered termination. A termination of radicals in a particle can only occur if the particle contains at least two radicals. Radicals can also disappear by diffusion out of a particle.

Polymerization takes place at a certain rate (which may vary with time) as long as free monomer is present. The concentration of monomer in the particles will then usually be constant. Once all free monomer in the water phase is exhausted, the monomer concentration in the particles will decrease and the viscosity will increase. One would then usually get an abnormal increase in polymerization rate, or a slight decrease, as monomer concentration decreases (see Equation 4:4). For example, vinyl chloride observes a strong increase in speed ("max" effect). This is called the so-called Tromsdorff effect and it is believed it is because the viscosity of the particles increases so that termination is prevented (possibly also desorption). This gives an increase in the mean radical number per. particle and an increase in velocity that outweighs the decrease in monomer concentration (Equation 4: 4). However, this last factor becomes crucial after a while, and the reaction stops when all monomer is exhausted.

Smith and Ewart (13) have treated the particle growth by assuming that at one given time there is distribution of particles containing 0, 1, 2, ... n radicals, and that this distribution

is constant (semi-stationary). Thus an equation can be drawn up taking into account diffusion of radicals in and out of the particles and termination

$$\frac{dN_n}{dt} = \rho_A \frac{N_{n-1}}{N} - \rho_A \frac{N_n}{N} + k_d N_{n+1}(n+1) - k_d N_n n + \frac{k_{tp}}{v} N_{n+2}(n+2)(n+1) - \frac{k_{tp}}{v} N_n n(n-1) = 0 \qquad (4:1)$$

(Some modified version of their original equation).

Here are

ρ_A - absorption rate of radicals per volume of water (L^{-1})
N_n - number of particles containing n radicals (L^{-1})
k_d - rate constant for desorption of radicals from a particle (s^{-1})
k_{tp} - rate constant for termination of radicals in a particle (L/molec. s)
v - volume of one particle (L)

The equation expresses the rate of change of the number of particles with n radicals (N_n) , and this is set equal to 0 according to the assumption of a semi-static state. It is based on the formation of n-particles by:

a) Diffusion of a radical into (n-1) particles
b) Diffusion of a radical out of (n + 1) particles
c) Termination of two radicals in (n + 2) particles

n-particles disappear by the same mechanisms:

d) Diffusion of a radical into n-particles
e) Diffusion of a radical out of n particles
f) Termination in n-particles (assuming $n \geq 2$)

Smith and Ewart derived solutions of equation (4:1) for three special cases:

1. $\bar{n} << 1$
This is the case when desorption rate (and/or possible termination rate with monomer due to allyl formation or the like) is much higher than the absorption rate.

2. $\bar{n} = 0.5$
is the case when the termination rate is much higher than the absorption rate and one can ignore desorption.

3. $\bar{n} >> 1$
is the case when the absorption rate is much higher than the termination rate and desorption rate.

Smith and Ewart also assume that any desorbed radicals cannot be reabsorbed.

Based on the rate expression for propagation, one has in the usual way

$$r_p = k_p C_M^{\ p} C_R^{\ p} \qquad (4:2)$$

where r_p – reaction rate (mol/L s)
k_p – rate constant (L/mol s)
C_M^p- concentration of monomer in the particles (mol/L)
C_R^p - concentration of radicals in the particles (mol/L)

C_R^p can be written $C_R{}^p = \frac{\bar{n}N^w}{N_A}$ (4:3)

where $\bar{n}$ - mean number of radicals (-)
N^w – total number of particles per volume of water (L^{-1})
N_A – Avogadro's number

Which gives the equation:

$$r_p = \frac{k_p C_M{}^p}{N_A}\bar{n}N^w \qquad (4:4)$$

The general solution of equation (4:1) is prepared by Stockmayer (10), and this solution regards Smith and Ewart's cases as border cases. When no desorption or reabsorption occurs, the mean radical number $\bar{n}$ depends only on the parameter α:

$$\alpha = \frac{\rho_A v}{N^w k_{tp}} = \frac{\rho_A V_p}{(N^w)^2 k_{tp}} \qquad (4:5)$$

as $V_p = N^w v$ = total volume of latex particles per volume of water (L^{-1})

At values of $\alpha < 5\ 10^{-2}$, $\bar{n}$ is independent of α and is constant equal to 0.5 (Smith-Ewart, case 2). With increasing α, $\bar{n}$ increases beyond 0.5 and when $\alpha > 1$

$$\bar{n} = \left(\frac{\alpha}{2}\right)^{\frac{1}{2}} \qquad (4:6)$$

(Smith-Ewart, case 3).

If desorption of radicals from the particles is significant, O'Toole (11) has shown that Stockmayer's equations are not physically correct, taking no account of the desorbed radicals. The recursion equation used by O 'Toole is

$$\left(\frac{\rho_A}{N^w}\right)P_n = \left(k_d + n\frac{k_{tp}}{v}\right)(n+1)P_{n+1} + \frac{k_{tp}}{v}(n+1)(n+2)P_{n+2} \qquad (4:7)$$

P_n here is the probability that a particle will have n radicals. The solution provided by O'Toole is

$$\bar{n} = \frac{a}{4}\frac{I_m(a)}{I_{m-1}(a)} \qquad (4:8)$$

Here, I_m og I_{m-1} are modified Bessel functions. (For calculation of av $\bar{n}$, see 4.3.4).

In addition

$$a = (2\alpha)^{\frac{1}{2}} \qquad (4:9)$$

$$m = \frac{k_d v}{k_{tp}} \qquad (4:10)$$

Equation (4:8) applies to all values of $\alpha \geq 0$ and $m \geq 0$.

Smith and Ewart also have derived in their theory an expression for the number of particles formed during stage I in a common emulsion polymerization. This expression is

$$N^w = k\left(\frac{\rho^w}{\mu_v}\right)^{\frac{2}{5}} (a_s S)^{\frac{3}{5}} \qquad (4:11)$$

Here $0.37 < k < 0.53$, which can be found by theoretical considerations (see, for example, (13)).

ρ^w - formation rate of radicals in the water phase (molec./L s), $\rho^w = 2k_i C_i^w$ (4:12)
where k_i is the rate constant (s^{-1}) and C_i^w is the initiator concentration (molec./L)
μ_v - rate of volume increase (L/ s)
a_s - surface occupied by an adsorbed emulsifier molecule (dm^2)
S - emulsifier concentration (molek./L)

4.2 The case of vinyl chloride

4.2.1 General theory

All authors who have studied the emulsion polymerization of vinyl chloride agree that the reaction does not follow Case 2 in Smith and Ewart's theory. The main deviations are:

a) The number of latex particles varies greatly with the emulsifier concentration, while the rate of polymerization changes relatively little.
b) The number of particles is independent of the initiator concentration (Equation 4:11)
c) The reaction rate increases with increasing initiator concentration with constant number of particles (the order is found between 0.5 and 0.8 by different authors).
d) The conversion as a function of time shows an autocatalytic increase up to high turnover.

These discrepancies have been explained differently by different authors. These explanations are discussed by Ugelstad et al. (9) which considers that the deviations should neither be explained by significant termination of radicals in the water phase nor a chain transfer to polymer as assumed by, respectively, Giskehaug and Gerrens et al. (ref. in (9)). Ugelstad and Mørk (3) have calculated the number of radicals per. particle from equation (4:4), having used values for k and C_M^p found experimentally in the literature and from experimental determination. They have used $k_p = 3{,}6\ 10^7$ L/mol h and $C_M^p = 6$ mol/L. In the given

experimental conditions, they found $\bar{n}$ in the range 0.001-0.1. $\bar{n}$ increased by the number of particles and with increasing conversion. These values are somewhat uncertain, as the value for k_p is measured in bulk. If k_p is significantly lower in emulsion polymerization, this will yield a significantly higher value for (inverse proportional). Ugelstad and Mørk have, however, with other experiments (3) where the rate was varied during the reaction, shown that the calculated values are approximately correct. Their explanation for the low value is a mechanism of desorption and reabsorption of radicals, considering that the radicals desorbed from a particle are completely reabsorbed in other (or the same) particles. There is also a possibility for termination in the water phase. They believe that desorption and reabsorption is a likely mechanism of polymerization of vinyl chloride because it is known that in this case a chain transfer to monomer easily takes place and these radicals will easily diffuse.

The case of radical desorption is treated in Smith and Ewart Case 1. This, however, is considered to be little suitable for describing kinetics here, since it does not take into account the reabsorption of the desorbed radicals, and one must therefore have an unusually high termination (and polymerization) in the water phase, which has not been observed (see also (2)).

4.2.2 General rate expressions

From the assumption of desorption and reabsorption, Ugelstad et al. (1) could express the rate of absorption, ρ_A, by

$$\rho_A = \rho^w + k_d \sum_{n=1}^{\infty} nN_n - 2k_{tw}\left(C_R{}^w\right)^2 \qquad (4:13)$$

k_{tw} - termination constant for radicals in the water phase (L/molec. s)

$C_R{}^w$ - concentration radicals in the water phase (molec./L)

They also set the rate of absorption of radicals proportional to the concentration of radicals in the water phase,

$$\rho_A = k_a C_R{}^w \qquad (4:14)$$

By inserting $C_R{}^w = \rho_A/k_a$ in equation (4:13) and multiplication of the equation with $v/k_{tp}N^w$ we get

$$\alpha = \alpha' + m\bar{n} - Y\alpha^2 . \qquad (4:15)$$

Here $$\alpha' = \frac{\rho^w v}{k_{tp} N^w} \qquad (4:16)$$

$$m = \frac{k_d w}{k_{tp}} \qquad (4:17)$$

$$Y = 2N^w \frac{k_{tp} k_w}{k_a{}^2 v} \qquad (4:18)$$

α is the same as in equation (4:5).

If termination in the water phase is negligible, then we can set Y = 0 (k_{tw} = 0). Ugelstad et al. has calculated $\bar{n}$ as a function of α with m and Y as parameters. Figure 3 shows their results with Y = 0 with $\bar{n}$ calculated from equation (4:8). At values of Y greater than 0, the curves will get a somewhat different shape. The main difference is that the variation of $\bar{n}$ with m for m> 1 becomes larger. Ugelstad et al. has calculated that Y for most monomers will be less than 10^{-4} when $N^w \approx 10^{17}$ part./L H_2O and V_p = 0.1. Y can therefore often be neglected by common emulsion polymerizations with vinyl chloride (depending on conditions).

The equations described here and below apply to all monomers when the correct constants are used (Figure 3 below).

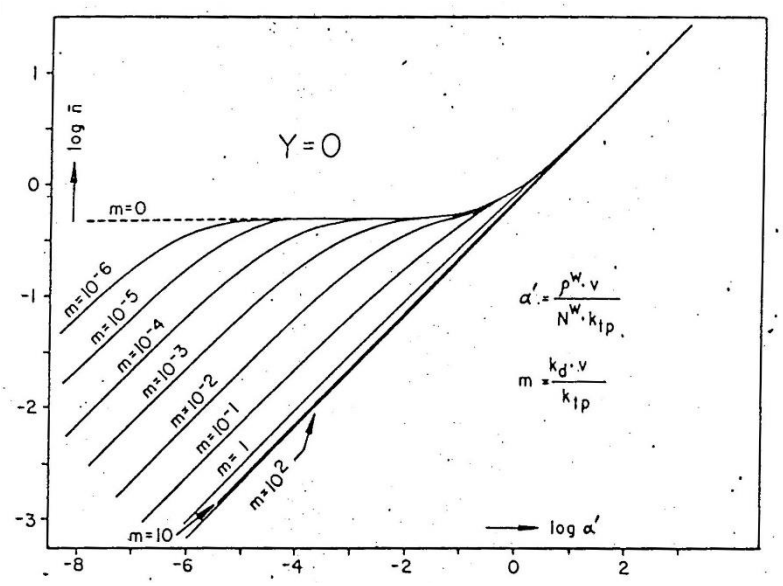

Figure 3. Log $\bar{n}$ as function of log α' for Y= 0. From Ugelstad et al. (1).

4.2.3 The special case $\bar{n} << 1$

For the case of $\bar{n} << 1$, Ugelstad et al. (2) developed an approximate expression for the polymerization rate. At low $\bar{n}$, only particles with 0, 1 and 2 radicals need to be considered, they have set the following equations when considering a semi-stationary state,

$$\frac{dN_1}{dt} = \frac{\rho_A}{N^w}\left[N^w - \left(N_1 + N_2\right)\right] + 2k_d N_2 - k_d N_1 - \rho_A \frac{N_1}{N_2} = 0 \qquad (4:19)$$

$$\frac{dN_2}{dt} = \frac{\rho_A}{N^w} N_1 - 2k_d N_2 - 2\frac{k_{tp}}{v} N_2 = 0 \qquad (4:20)$$

$$\frac{dn_t}{dt} = \rho^w - 4\frac{k_{tp}}{v} N_2 - 2k_{tw}\left(C_R{}^w\right)^2 = 0 \qquad (4:21)$$

n_t – total number of radicals in the system

By inserting $\rho_A = k_a C_R{}^w$ fra (4:14) and supposing that $N^w >> N_1 >> N_2$ we obtain the equations (4:19), (4:20), and (4:21).

$$N_1 = \left(\rho^w\right)^{\frac{1}{2}}\left[\frac{\left(V_p k_d + N^w k_{tp}\right)k_a{}^2}{2k_{tp}k_d k_a{}^2 + 2k_{tw}k_d{}^2\left(V_p k_d + N^w k_{tp}\right)}\right]^{\frac{1}{2}} \qquad (4:22)$$

By ignoring termination in the water phase, (4:22) and (4:4) and $N_1 = N^w \bar{n}$ ($N_1 >> N_2$) (4:23) result in

$$r_p = \frac{k_{tp} C_M}{N_A}\left(\rho^w\right)^{\frac{1}{2}}\left[\frac{V_p}{2k_{tp}} + \frac{N^w}{2k_d}\right]^{\frac{1}{2}} \qquad (4:24)$$

They have found an experimental order with respect to N^w in the range of 0.05 - 0.15, increasing with increasing numbers of particles, decreasing slightly with increasing conversion, and an order with respect to V_p from 0.3 to 0.5, increasing with decreasing particle numbers and increasing conversion. They have therefore proposed to express k_d in the form

$$k_d = k_d{}'\left(\frac{N^w}{V_p}\right)^{2/3} = \frac{k_d{}'}{v^{2/3}} \qquad (4:25)$$

k_d' – constant (dm^2/s)

This is the same as saying that the desorption is diffusion controlled where

$$k_d = 4\pi D_p \frac{r}{v} \qquad (4:26)$$

D_p - diffusivity of radicals out of a particle (dm^2/s)
r – radius of a particle (dm)

(See also section 4.4)

This means that

$$k_d{}' = 4\pi\left(\frac{3}{4\pi}\right)^{1/3} D_p = 7{,}82\ D_p \qquad (4:27)$$

The volume v comes here into (4:26) because it is the concentration of radicals in the particles n/v that is included in the calculation of diffusion rate.

The final expression of r_p derived from Ugelstad et al. is then

$$r_p = \frac{k_{tp} C_M}{N_A} \left(\rho^w\right)^{\frac{1}{2}} \left[\frac{V_p}{2k_{tp}} + \frac{(N^w)^{1/3}(V_p)^{2/3}}{2k_d'} \right]^{\frac{1}{2}} \qquad (4:28)$$

They have found that this expression is consistent with experimental data from cases when $\bar{n} << 1$. They can therefore also conclude that termination in the water phase is negligible (see further discussion in ref. (2)).

4.2.4 Different types of radicals

All derivations made in the foregoing have assumed that all the radicals existing in the system are equal and have the same reactivity and diffusion rates. However, in a recent work, Ugelstad and Mørk (3) have assumed that this is not the case. They distinguish between monomer and polymer radicals, where polymer is defined as molecules with chain length 2 or greater. The particles considered are in addition to particles without radical particles with

a) 1 monomer radical, denoted by 1m
b) 1 polymer radical, denoted by lp
c) 2 monomer radicals, denoted by 2m
d) 2 polymer radicals, denoted by 2p
e) 1 monomer- and 1 polymer radical, denoted by pm

For n <0,1, one does not need to consider particles with three radicals. Radicals can react and absorbed/desorbed in the following ways:

	rate	
Absoption of M·	$\rho_A N_j / N^w$	(4:29)
Desorption of M·	$k_{dm} N_j$	(4:30)
Transfer to monomer:		
$P\cdot + M \rightarrow M\cdot + P$	$k_f N_j C_M^p$	(4: 31)
Propagation of monomer radical:		
$M\cdot + M \rightarrow P\cdot$	$k_p' N_j C_M^p$	(4:32)
Termination between two polymer radicals:		
$P\cdot + P\cdot \rightarrow P$	$(2k_t/v)\, N_j$	(4:33)
Termination between polymer- and monomer radical:		
$M\cdot + P\cdot \rightarrow P$	$(k_t'/v)\, N_j$	(4:34)
Termination between two monomer radicals:		
$M\cdot + M\cdot \rightarrow P$	$(2k_t''/v)\, N_j$	(4:35)

Here, N_j denotes the number of particles with radicals of the respective black. Table V below gives an overview of the types of particles the different mechanisms provide from

particles of type 1m, 1p, etc. The mechanisms are represented by their respective velocity constants (velocities).

Rate.const.> V Start type	ρ_A	k_{dm}	k_f	k_p’	k_t	k_t’	k_t’’
1m	2m	0	-	1p	-	-	-
2m	-(3m)	1m	-	pm	-	-	0
1p	pm	-	1m	-	-	-	-
2p	- (2pm)	-	pm	-	0	-	-
pm	- (p2m)	1p	2m	2p	-	0	-
0	1m	-	-	-	-	-	-

Table V. Result-type particles from different output types and reaction mechanisms.

This system cannot be solved in the same way as if only one kind of radical is considered, as stated in Section 4.2.2 (Bessel functions, Equations 4:8 and 4:13) because it becomes too complicated, but the method of semi-stationary state (section 4.2.3) can be used. This probably applies to $\bar{n} = 0.5$ at least for $\bar{n} < 0.1$. Particles with more than two radicals can then be ignored and gives the following equations (according to the same principle as in clause 4.2.3)

$$\frac{dN_{1m}}{dt} = 2k_{dm}N_{2m} + k_f N_{1p}C_M{}^p - \rho_A \frac{N_{1m}}{N^w} - k_p' N_{1m}C_M{}^p - k_{dm}N_{1m} + \rho_A \frac{N_0}{N^w} = 0 \quad (4:36)$$

$$\frac{dN_{2m}}{dt} = \rho_A \frac{N_{1m}}{N^w} + k_f N_{pm}C_M{}^p + 2k_p' N_{2m}C_M{}^p - \frac{2k_t''}{v} N_{2m} - 2k_{dm}N_{2m} = 0 \quad (4:37)$$

$$\frac{dN_p}{dt} = k_p' N_{1m}C_M{}^p + k_{dm}N_{pm} - \rho_A \frac{N_{1p}}{N^w} - k_f N_{1p}C_M{}^p = 0 \quad (4:38)$$

$$\frac{dN_{2p}}{dt} = k_p' N_{pm}C_M{}^p - 2k_f N_{2p} - \frac{k_t}{v} N_{2p} = 0 \quad (4:39)$$

$$\frac{dN_{pm}}{dt} = 2k_p' N_{2m}C_M{}^p + \rho_A \frac{N_{1p}}{N^w} + 2k_f N_{2p}C_M{}^p - k_f N_{pm}C_M{}^p - k_p' N_{pm}C_M{}^p - \frac{k_t'}{v} N_{pm} - k_{dm}N_{pm} = 0 \quad (4:40)$$

$$\frac{dn_t}{dt} = \rho^w - \frac{4k_t}{v} N_{2p} - \frac{2k_t'}{v} N_{pm} - \frac{4k_t''}{v} N_{2m} = 0 \quad (4:41)$$

Ugelstad et al. have in their treatment disregarded particles with two monomer radicals when $\bar{n} << 1$, and all terms indicating the formation of or formation from such particles are omitted. The reason for this is that the probability of formation of 2m particles is assumed to be small relative to the formation of pm particles. Therefore, among other things, the whole of equation (4:37) is imitted. For small $\bar{n}$, $N_2 << N_1 << N_0$ and equation (4:36) and (4:38) give (when 2m loop is omitted),

$$\rho_A = k_{dm} N_{1m} \qquad (4:42)$$

By setting $\bar{n} = N_{1p}/N^w$, Ugelstad et al. developed an analytical expression for $\bar{n}$. This expression is too complicated to be directly comparable to experimental data, but can be simplified by further assumptions. First, by using an assumption of the relationship between ρ^w / N^w and three parameters A, B and C (these are functions of the rate constants and C_M^p and v, see (3)) they arrive at two, in the form equal, expressions for $\bar{n}$ by further assumptions.

$k_p' C_M^p >> \frac{k_t}{v} + k_f C_M^p$ and $k_p' C_M^p >> k_{dm}$ give

$$\bar{n} = \frac{(\rho^w)^{\frac{1}{2}}}{N^w}\left[\frac{V_p}{2k_t} + \frac{N^w}{2k_{dm}k_f / k_p'}\right]^{\frac{1}{2}} \qquad (4:43)$$

$k_t' >> k_t$ gives

$$\bar{n} = \frac{(\rho^w)^{\frac{1}{2}}}{N^w}\left[\frac{V_p}{2k_t' k_f / k_p'} + \frac{N^w}{2k_{dm}k_f / k_p'}\right]^{\frac{1}{2}} \qquad (4:44)$$

By inserting in equation (4:4), an expression that in the form is identical to equation (4:24), which is based on the assumption that all radicals are the same. By using equation (4:25), an expression equal to equation (4:28) is obtained, which differs only from this by k_t and k_d' being replaced by expressions composed of other constants. Compliance with the experimental data will then be the same.

4.3 Competitive growth

4.3.1 Seeding and competitive growth

The term seeding was introduced by Smith (13b). By this is meant that monomer is polymerized in a previously prepared latex under such conditions that no new particles are formed. The particles will then grow in the usual manner as in Step II of a typical emulsion polymerization (regarding new nucleation, see section 4.5.2). The growth of particles of different diameters may be different, so that the distribution curve of the diameter (number of particles with a given diameter as a function of this diameter, assuming discrete diameter sizes, see point 4.5.3) may change shape over time as exemplified in Figure 4.

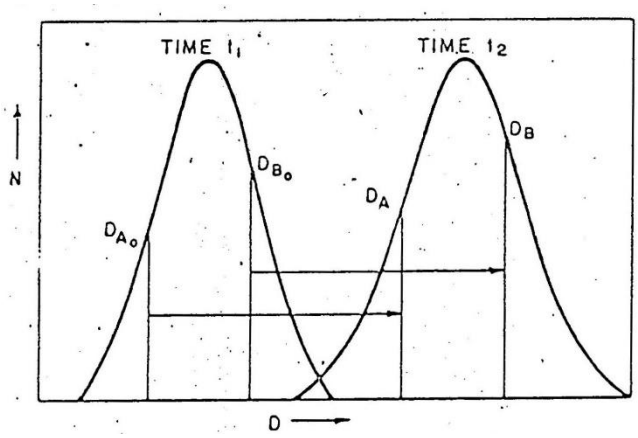

Figure 4. Particle size distribution at two different times t_1 and t_2. From Vanderhoff and Bradford (5).

The growth during this step has been studied by Ewart and Carr (8). They consider the distribution of the particle diameter as a function of time and they have developed a statistical expression of probability dP because a particle contains a free radical for a part of its time between f and f+df.

$$dP = \frac{(2a-1)!}{(a-1)!} f^{a-1}(1-f)^{a-1}\,df \qquad (4:45)$$

Here $f=t/t_0$

t – The time a particle contains a free radical

t_0 – total polymerization time

2a – the number of free radicals that are absorbed during the time t_0

The prerequisite for the expression is that $\bar{n} = 0.5$ (Smith-Ewart case 2). They can from (4:45) derive that

$$\left(\frac{\Delta f}{f}\right)^2 = \frac{\overline{(f-\bar{f})^2}}{\bar{f}^2} = \frac{1}{2a} \qquad (4:46)$$

Δf is the spread on f

They think that there is a possibility that random variations in the radical concentration in a particle from the mean $\bar{n} = 0.5$, which gives the expression (4:45) above, may affect the distribution function of the particle diameter (-volume), so that the distribution becomes wider during polymerization than it would otherwise do for $\bar{n} = 0.5$. As they assume that the volume growth is constant, i.e that $D^3 \sim k \cdot t$, they can set

$$\frac{\Delta D^3}{\bar{D}^3} = \frac{\Delta f}{f} = \left(\frac{1}{2a}\right)^{\frac{1}{2}} \qquad (4:47)$$

ΔD^3 is the spread of the mean particle volume $\bar{D}^3$. As 2a increases over time, $D^3/\ \bar{D}^3$ should decrease over time, even if the distribution becomes wider (the spread on $\bar{D}$ increases).

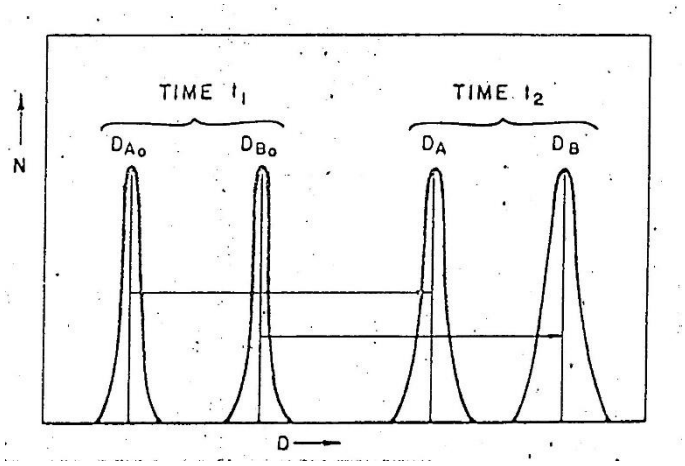

Figure 5. Hypothetical particle size distributions for a mix of seeds with different particle sizes at two different times t_1 and t_2. From Vanderhoff and Bradford (5).

This method of studying growth gives only a qualitative impression, and is bound to the assumption of $\bar{n} = 0.5$, which often does not apply. Vanderhoff and Bradford therefore introduced a more direct method of competitive growth. The method is to polymerize with a seed which is a mixture of two monodisperse latexes of different particle size. In this case, particles of different sizes will compete for radicals (and possibly monomer) in the same system. Both sizes will grow, but the growth may be different for the small ans large particles. Figure 5 shows how growth may take place. The particle size can be determined by electron microscopy (see section 4.5.4) (for the preparation of monodisperse latexes, see section 4.5.1).

4.3.2 Mathematical treatment

Vanderhoff et al. have treated the growth out of the assumption of an exponential relationship between the volume v of the polymer in a particle and the corresponding diameter D:

$$\frac{dv}{dt} = kD^x \qquad (4:48)$$

The exponent x is thus the order of the volume growth with respect to the diameter. k is a constant that can vary with the initiator concentration, with temperature, and over time. However, it is assumed that k is the same for particles of both sizes at a given time. The equation can then be set for both small and large particles:

$$\frac{dv_a}{dt} = kD_a^{\ x} \qquad (4:49)$$

$$\frac{dv_b}{dt} = kD_b^{\,x} \tag{4:50}$$

Here a denotes small particles and b large. By eliminating the time, we get

$$\frac{dv_b}{dv_a} = \left(\frac{D_b}{D_a}\right)^x \tag{4:51}$$

Now $v = \frac{\pi}{6}D^3$, so that $dv = \frac{\pi}{2}D^2 dD$, which gives

$$\frac{dv_b}{dv_a} = \left(\frac{D_b}{D_a}\right)^2 \cdot \frac{dD_b}{dD_a} \tag{4:52}$$

Giving $\frac{dD_b}{dD_a} = \left(\frac{D_b}{D_a}\right)^{x-2}$ (4:53)

This equation can then be integrated from time to time 0 (D_a^0, D_b^0) to t (D_a, D_b):

$$\int_{D_a^{\,0}}^{D_a} D_a^{\,2-x} dD_a = \int_{D_b^{\,0}}^{D_b} D_b^{\,2-x} dD_b \tag{4:54}$$

Which gives $D_a^{\,3-x} - D_a^{\,0\;3-x} = D_b^{\,3-x} D_b^{\,0\;3-x}$ (4:55)

By rearranging and dividing on $D_a^{\,0\;3-x}$ we get

$$\frac{D_b}{D_a} = \frac{D_a^{\,0}}{D_a}\left[\left(\frac{D_a}{D_a^{\,0}}\right)^{3-x} + \left(\frac{D_b^{\,0}}{D_a^{\,0}}\right)^{3-x} - 1\right]^{\frac{1}{3-x}} \tag{4:56}$$

The integration assumes that x is constant and ≠3. For given values of D_a^0 and D_b^0, D_b/D_a can be calculated as a function of D_a/D_a^0 and x. A value of x = 3, will from (4:53) give

$$\frac{dD_b}{dD_a} = \frac{D_b}{D_a} \tag{4:57}$$

Or, integrated,

$$\frac{D_b}{D_a} = \frac{D_b^{\,0}}{D_a^{\,0}} \tag{4:58}$$

The ratio between D_b og D_a will thus be constant. Figure 6 shows the function D_b/D_a at different values of x at a starting value $D_b^0/D_a^0 = 2$. When x = 3, the volume growth rate (4:48) will be proportional to the volume and the diameter will increase with the same ratio. When x = 2, the rate of diameter increase will be constant and the difference between the diameter, $D_b - D_a$, will be constant equal to $D_b^0 - D_a^0$. When x = 0, the volume growth rate

will be constant and the difference between the diameters will decrease rapidly as the difference between the volumes, $v_b - v_a$, will be constant, equal to $v_b^0 - v_a^0$.

It will easily be realized that equation (4:48) is not a correct model for the physical conditions during growth (one has not taken into account, for example, the particle number), but the treatment method gives a very good overview, as x can be determined experimentally from D_b and D_a using a figure (or equivalent table) as Figure 6 where D_b/D_a is set as a function of D_a/D_a^0.

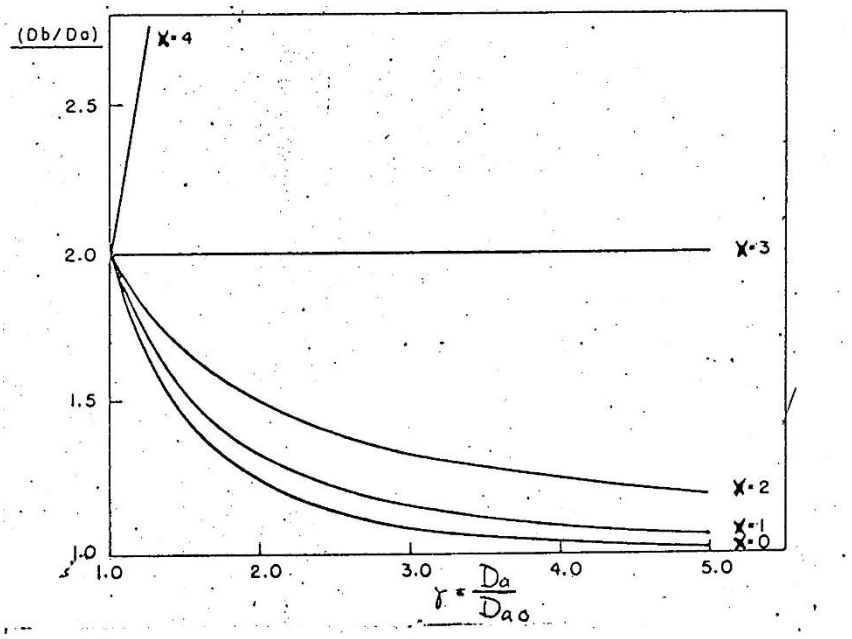

Figure 6. Reference curves for D_b/D_a as function of D_a/D_a^0 and x with $D_b^0/D_a^0 = 2$. From Vanderhoff et al. (4).

The magnitude of x will therefore be a good measure of the relative growth; to what extent and how quickly the diameters will approach or deviate from each other. Equation (4:51) may be considered as a defining equation of x. One must be aware that if x is not constant, x found from equation (4:56) will not be the same as in equation (4:51), because (4:51) gives the differential velocity at a given point, while (4:56) gives an integral value, that is, a mean value. x will therefore vary more strongly from equation (4:51) than from (4:56).

To find x from equation (4:51) or (4:53), it is necessary to differentiate v_b as a function of v_a (or D_b as a function of D_a), graphically or analytically by fitting an equation (e.g. a polynomial) to the function. If one as an approximation sets

$$D_b = C_1 + C_2 D_a + C_3 D_a^2 \qquad (4:59)$$

where C_1, C_2 og C_3 are constants, differentiation gives

$$\frac{dD_b}{dD_a} = C_2 + 2C_3 D_a \qquad (4:60$$

Together with (4:53), this gives

$$C_2 + 3C_3D_a = \left(\frac{D_b}{D_a}\right)^{x-2} \tag{4:61}$$

E.g. $$x = \frac{\log\left(C_2 + 2C_3D_a\right)}{\log\left(D_b / D_a\right)} + 2 \tag{4:62}$$

(4:59) can be found by using the method of least square, and the parable one may be forced to pass through the point (D_a^0, D_b^0), so that one gets the same starting diameters for all experiments with the same seeds a and b. It is also possibly to use higher-order polynomials, however, this requires many experimental points (D_a, D_b); optionally, other functional relationships may be used. Such a method will produce better results than a graphical derivative but will not be able to provide exact values.

4.3.3 Theoretical derivation of x

Vanderhoff et al. do not give any theoretical derivation of x, but they write that according to Smith and Ewart's theory, Case 2, x = 0.

Since the reaction rate r_p is defined as moles of monomer reacted per liter of water per unit time, we have from (4: 4)

$$\frac{dV_p}{dt} \sim r_p = \frac{k_p C_M{}^p}{N_A} \bar{n}\, N^w \tag{4:63}$$

I.e. $$\frac{dV_{pb}}{dV_{pa}} = \frac{C_{Mb}{}^p}{C_{Ma}{}^p} \cdot \frac{\bar{n}_b}{\bar{n}_a} \cdot \frac{N_b{}^w}{N_a{}^w} \tag{4:64}$$

because (4:63) is also valid for a- and b-particles separately. Now

$$V_p = N^w \tfrac{\pi}{6} D^3 \tag{4:65}$$

so that $$\frac{dV_p}{dt} = N^w \tfrac{\pi}{2} D^2 \frac{dD}{dt} \tag{4:66}$$

because N^w do not change with time. This gives:

$$\frac{N_b{}^w D_b{}^2}{N_a{}^w D_a{}^2} \cdot \frac{dD_b}{dD_a} = \frac{C_{Mb}{}^p}{C_{Ma}{}^p} \cdot \frac{\bar{n}_b}{\bar{n}_a} \cdot \frac{N_b{}^w}{N_a{}^w} \tag{4:67}$$

We then introduce the parameter $\eta = D_a/D_b$ which gives

$$\frac{dD_b}{dD_a} = \frac{C_{Mb}{}^p}{C_{Ma}{}^p} \eta^2 \frac{\bar{n}_b}{\bar{n}_a} \tag{4:68}$$

Regarding the monomer concentration in polymer particles, this will be highly dependent on which system we are working with (what kind of monomer). Generally, we may

assume that there is an equilibrium between monomer dissolved in the polymer and the surface energy of the particle so that the chemical potential of monomer dissolved in the polymer (Flory-Huggin equation) equals the surface potential (Thomson's equation) as indicated by Gerrens (7) and Ugelstad et al. (9).

$$-RT\left[\ln\varphi_1+\left(1-\tfrac{1}{x}\right)\varphi_2+{\varphi_2}^2\lambda\right]=\frac{2V_1\sigma}{r} \qquad (4:69)$$

φ_1 og φ_2 - volume fraction of monomer and polymer in the particles, respectively.
λ - interaction constant
x - here equal to the degree of polymerization. 1-1/x can approximately be set to 1
V_1 - molar volume of the monomer
σ - interfacial tension
r - particle radius
R - gas constant and T temperature

The significance of the surface energy term depends on the size of the interaction constant. For vinyl chloride at 50°C, Ugelstad indicates that $\lambda = 0.88$, corresponding to 6 mol/L, and it can be shown that the significance of the interfacial energy term is negligible so that one can set $C_{Ma}^{p} = C_{Mb}^{p}$, regardless of r and σ. (4:68) then gives:

$$\frac{dD_b}{dD_a}=\eta^2\frac{\bar{n}_b}{\bar{n}_a} \qquad (4:70)$$

Equatiuon (4:53) can be written

$$\frac{dD_b}{dD_a}=\left(\frac{D_b}{D_a}\right)^{x-2}=\eta^{2-x}=\eta^2\cdot\eta^{-x} \qquad (4:71)$$

Together with (4:70) we then get

$$x=\frac{\log\left(\bar{n}_a/\bar{n}_b\right)}{\log\eta} \qquad (4:72)$$

If $\bar{n}_a / \bar{n}_b$ is known, x can therefore be calculated from (4:72), and this value can be directly compared to values from (4:53), possibly (4:62) (differential values), but not with values from (4:56) as mentioned earlier. If $n_a = \bar{n}_b = 0.5$, will obviously x become 0, as mentioned by Vanderhoff et al.

4.3.4 Calculation of $\bar{n}_a$ and $\bar{n}_b$

If $\bar{n} \neq 0.5$, we must derive $\bar{n}_a$ og $\bar{n}_b$ from the physical conditions under competing growth. We may then use calculation methods similar to those used by Ugelstad et al. (1), (2) and (3). The first assumption that is made is that the termination of radicals in the water phase is ignored. During seed experiments, we will already have a significant particle volume from

the beginning, and Ugelstad et al. have found that we then can set Y = 0 by good approximation (equation 4:15 and 4:18). In analogy with (4:13) we can then set

$$\rho_A = \rho_{Aa} + \rho_{Ab} = \rho^w + k_{da}\sum_{n=1}^{\infty} nN_{na} + k_{db}\sum_{n=1}^{\infty} nN_{nb}\,, \qquad (4:73)$$

as the total rate of absorption of radicals ρ_A will be the sum of the velocities of a- and b-particles, ρ_{Aa} and ρ_{Ab} . k_d will be independent of r, and we therefore must distinguish between k_d for the two particle sizes. (4:73) can be written,

$$\rho_A = \rho^w + k_{da}\bar{n}_a N_a{}^w + k_{db}\bar{n}_b N_b{}^w \qquad (4:74)$$

It is assumed that ρ_A is proportional to the particle radius r. This assumes diffusion controlled absorption with an infinitely thick diffusion layer (see section 4.4). ρ_A will also be proportional to the particle number N^w so that we can set

$$\rho_{Aa} = \frac{r_a N_a{}^w}{r_a N_a{}^w + r_b N_b{}^w}\cdot\rho_A \qquad (4:75)$$

$$\rho_{Ab} = \frac{r_b N_b{}^w}{r_a N_a{}^w + r_b N_b{}^w}\cdot\rho_A \qquad (4:76)$$

By division above and below the fraction bar with $r_b N_b{}^w$ we get

$$\rho_{Aa} = \frac{\eta F}{\eta F + 1}\rho_A \qquad (4:77)$$

$$\rho_{Ab} = \frac{1}{\eta F + 1}\rho_A \qquad (4:78)$$

as we have set $F = N_a{}^w / N_b{}^w$ (4:79), and as earlier is $r_a/r_b = D_a/D_b$.

(4:74) og (4:77) then give

$$\rho_{Aa} = \left(\rho^w + k_{da}\bar{n}_a N_a{}^w + k_{db}\bar{n}_b N_b{}^w\right)\frac{\eta F}{\eta F + 1} \qquad (4:80)$$

As in section 4.2.2, the equation is multiplied by $\dfrac{v_a}{k_{tp} N_a{}^w}$ which gives

$$\frac{\rho_{Aa} v_a}{k_{tp} N_a{}^w} = \left(\frac{\rho^w v_a}{k_{tp} N_a{}^w} + \frac{k_{da} v_a}{k_{tp}}\bar{n}_a + \frac{k_{db} v_b}{k_{tp}}\cdot\frac{v_a}{v_b}\cdot\frac{N_b{}^w}{N_a{}^w}\bar{n}_b\right)\frac{\eta F}{\eta F + 1}\,. \qquad (4:81)$$

This can be written

$$\alpha_a = \left(\alpha_a ' + m_a \bar{n}_a + \frac{\eta^3}{F} m_b \bar{n}_b \right) \frac{\eta F}{\eta F + 1} \tag{4:82}$$

α_b can if desired, be expressed in the same way. We have

$$\alpha_a = \frac{\rho_{Aa} v_a}{k_{tp} N_a{}^w} \tag{4:83}$$

$$\alpha_a ' = \frac{\rho^w v_a}{k_{tp} N_a{}^w} \tag{4:84}$$

$$m_a = \frac{k_{da} v_a}{k_{tp}} \tag{4:85}$$

From (4:77) and (4:78) we have

$$\frac{\rho_{Aa}}{\rho_{Ab}} = \eta F \tag{4:86}$$

If the desorption is also diffusion controlled, we can express k_d from equation (4:26).

$$k_{da} = 4\pi D_p r_a / v_a \tag{4:87}$$

$$k_{db} = 4\pi D_p r_b / v_b \tag{4:88}$$

This gives $m_a = \frac{4\pi D_p r_a}{k_{tp}}$ (4:89)

The corresponding parameter for b become

$$\alpha_b = \frac{\rho_{Ab} v_b}{k_{tp} N_b{}^w} = \alpha_a \frac{\rho_{Ab}}{\rho_{Aa}} \cdot \frac{v_b}{v_a} \cdot \frac{N_a{}^w}{N_b{}^w} = \alpha_a \frac{1}{\eta F} \cdot \frac{F}{\eta^3} = \alpha_a \frac{1}{\eta^4} \tag{4:90}$$

$$\alpha_b ' = \frac{\rho^w v_b}{k_{tp} N_b{}^w} = \alpha_a ' \frac{v_b}{v_a} \cdot \frac{N_a{}^w}{N_b{}^w} = \alpha_a ' \frac{F}{\eta^3} \tag{4:91}$$

$$m_b = \frac{4\pi D_p}{k_{tp}} r_b = m_a \frac{r_b}{r_a} = m_a \frac{1}{\eta} \tag{4:92}$$

The recursion equations (4:1) and (4:7) can be set up for a- and b-particles separately, as there are no linked terms in these equations. For a- particles (4:7) gives

$$\left(\frac{\rho_{Aa}}{N^w} \right) P_n = \left(k_{da} + n \frac{k_{tp}}{v_a} \right) (n+1) P_{n+1} + \frac{k_{tp}}{v_a} (n+1)(n+2) P_{n+2} \tag{4:93}$$

b particles give the same equation when index a is replaced by b. The solution becomes analogous to equation (4:8).

$$\bar{n}_a = \frac{a_a}{4}\frac{I_{ma}(a_a)}{I_{ma-1}(a_a)} \qquad (4:94)$$

Where $\alpha_a = (8\alpha_a)^{\frac{1}{2}}$ (4:95)

and corresponding for b-particles. (4: 8) was developed by Ugelstad et al. (1) and $\bar{n}_a$ can be written

$$\bar{n}_a = \frac{1}{2}\cfrac{2\alpha_a}{m_a + \cfrac{2\alpha_a}{m_a+1+\cfrac{2\alpha_a}{m_a+2+\cfrac{2\alpha_a}{m_a+3+....}}}} \qquad (4:96)$$

This is a continued fraction that converges rapidly for all $\alpha_a \geq 0$ and $m_a \geq 0$. We get a corresponding equation for b-particles.

Calculation of $\bar{n}_a$ and $\bar{n}_b$ can be done in several ways, common to these is that a computer should be used to save computational work. Curves for $\bar{n}_a$ and $\bar{n}_b$ as a function of α_a' (and α_b') for given m_a, η, and F can be produced by assigning a number of values to α_a, then α_b is calculated from (4:90). By a given m_a, m_b is also given by (4:92), and $\bar{n}_a$ and $\bar{n}_b$ can then be calculated from (4:96). By inserting these values into (4:82), we can find α_a'

$$\alpha_a' = \alpha_a\left(1+\frac{1}{\eta F}\right) - m_a\bar{n}_a - m_b\bar{n}_b\frac{\eta^3}{F} \qquad (4:97)$$

α_b' is found from (4:91).

If one instead wants to find $\bar{n}$ directly with given values for α ', m, η, and F, this cannot be done directly analytically, since $\bar{n}$ cannot be solved explicitly from (4:82) and (4:96). On a computer, however, this can be done by an iteration routine. One then assumes a value for α_a (or ρ_{Aa}). α_b is calculated from (4:90), and $\bar{n}_a$ and $\bar{n}_b$ are calculated from these and from m_a and m_b, which are known. The calculated values for $\bar{n}$ are inserted into (4:82) which gives a new value for α_a. It can be shown that this value is closer to the correct one than the original so that the routine will converge. This is also clearly apparent from the calculations (Appendix 11). By performing the routine a sufficient number of times, the desired accuracy in α can be achieved (e.g., 10^{-5} relative).

Once $\bar{n}$ is found, x can also be calculated from equation (4:72). With competitive growth, we are less interested in the absolute values of n_a and $\bar{n}_b$ than the ratio $\bar{n}_b / \bar{n}_a$ and how this (or x) changes with time (the conversion). If $x \neq 3$, η will change with α, α', m, and $\bar{n}$, while F will be constant (assuming negligible agglomeration and reactor fouling). To calculate how x will change over time, we can do a numerical integration of (4:70). With

initial values of D_a^0 and D_b^0 and given values for rate constants, ρ_w and F, $\bar{n}_b / \bar{n}_a$ can be calculated by the method specified above. dD_b/dD_a can be approximately written $\Delta D_b/\Delta D_a$, where ΔD_a and ΔD_b are small increments in D_a and D_b. ΔD_a can be fixed or can optionally be varied to achieve a desired accuracy, e.g. by using the Kutta-Merson integration method. We obtain

$$\Delta D_b = \eta^2 \frac{\bar{n}_b}{\bar{n}_a} \Delta D_a \qquad (4:98)$$

Values for ΔD_a and ΔD_b are added to D_a og D_b, and new values for α', m, and η are calculated, giving new values for $\bar{n}_a$ and $\bar{n}_b$, etc. The value of x can be calculated after each step from (4:72).

4.3.5 Limiting cases for x, treatment for $\bar{n}$<<1

If $\alpha < 5\ 10^{-2}$, then $\bar{n} = 0.5$ and x = 0 as mentioned earlier. This applies if there is no desorption and reabsorption of radicals (m = 0). In this case, we will have $\bar{n} = (\alpha/2)^{\frac{1}{2}}$ for α>1 (equation 4:6) (Smith-Ewart Case 3). We then obtain

$$\frac{\bar{n}_a}{\bar{n}_b} = \left(\frac{\alpha_a}{\alpha_b}\right)^{\frac{1}{2}} = \left(\eta^4\right)^{\frac{1}{2}} = \eta^2 \qquad (4:99)$$

(4:72) gives $x = \dfrac{\log(\bar{n}_a / \bar{n}_b)}{\log \eta} = 2$ (4:100)

A value for $\bar{n}$>>0.5 therefore givers a constant value of x = 2, even if $\bar{n}$ can vary in this interval, and independent of η and F.

If desorption and reabsorption takes place, we can find the limiting value for x when $\bar{n}$ << 1. We then use the expressions developed by Ugelstad et al. (2) given in section 4.2.3. Equations corresponding (4:19), (4:20), and (4:21) are written for both a and b particles (semi stationary state):

$$\frac{dN_{1a}}{dt} = \rho_{Aa} \frac{N_{0a}}{N_a{}^w} + 2k_{da}N_{2a} - k_{da}N_{1a} - \rho_{Aa} \frac{N_{1a}}{N_a{}^w} = 0 \qquad (4:101)$$

$$\frac{dN_{1b}}{dt} = \rho_{Ab} \frac{N_{0b}}{N_b{}^w} + 2k_{db}N_{2b} - k_{db}N_{1b} - \rho_{Ab} \frac{N_{1b}}{N_b{}^w} = 0 \qquad (4:102)$$

$$\frac{dN_{2a}}{dt} = \rho_{Aa} \frac{N_{1a}}{N_a{}^w} - 2k_{da}N_{2a} - 2\frac{k_{tp}}{v_a} N_{2a} = 0 \qquad (4:103)$$

$$\frac{dN_{2b}}{dt} = \rho_{Ab}\frac{N_{1b}}{N_b{}^w} - 2k_{db}N_{2b} - 2\frac{k_{tp}}{v_b}N_{2b} = 0 \qquad (4:104)$$

$$\frac{dn_t}{dt} = \rho^w - \frac{4k_{tp}}{v_a}N_{2a} - \frac{4k_{tp}}{v_b}N_{2b} - 2k_{tw}\left(C_R{}^w \cdot\right)^2 \qquad (4:105)$$

An exact solution to this equation set should give the same result as the solution with Bessel functions in section 4.3.4 up to $\bar{n} = 0.5$, at least for $\bar{n} < 0{,}1$. However, for $\bar{n} << 1$ we can set

$N_a{}^w >> N_{1a} >> N_{2a}$

and $N_b{}^w >> N_{1b} >> N_{2b}$

The equations (4:101) and (4:102) then give

$$\rho_{Aa} = k_{da}\,N_{1a} \qquad (4:106)$$

$$\rho_{Ab} = k_{db}\,N_{1b} \qquad (4:107)$$

If we use the same dependency of ρ_A and k_d as before, we get from (4:106), (4:107), (4:86), (4:87), (4:88), and (4:23):

$$\frac{\rho_{Aa}}{\rho_{Ab}} = \eta F = \frac{k_{da}}{k_{db}}\frac{N_{1a}}{N_{1b}} = \frac{r_a}{r_b}\frac{v_b}{v_a}\frac{\bar{n}_a}{\bar{n}_b}\frac{N_a{}^w}{N_b{}^w} = \frac{1}{\eta^2}\frac{\bar{n}_a}{\bar{n}_b}F \qquad (4:108)$$

I.e. $$\frac{\bar{n}_a}{\bar{n}_b} = \eta^3 \qquad (4:109)$$

And $$x = \frac{\log\eta^3}{\log\eta} = 3 \qquad (4:110)$$

Again x becomes independent of η og F.

$\bar{n}_a$ (eller $\bar{n}_b$) can be found from the equation set above in the same way as Ugelstad et al. (4:102) and (4:104) give together with (4:106) and (4:107)

$$N_{2a} = \frac{\rho_{Aa}N_{1a}/N_a{}^w}{2k_{da} + 2k_{tp}/v_a} = \frac{k_{da}N_{1a}{}^2/N_a{}^w}{2k_{da} + 2k_{tp}/v_a} = \frac{N_{1a}{}^2/N_a{}^w}{2 + 2m_a} \qquad (4:111)$$

$$N_{2b} = \frac{N_{1b}{}^2/N_b{}^w}{2 + 2m_b} \qquad (4:112)$$

If we disregard termination in the water phase, we can insert N_{2a} og N_{2b} in equation (4:105), giving

$$\rho^w = \frac{4k_{tp}}{v_a}\cdot\frac{N_a{}^w\bar{n}_a{}^2}{2 + 2m_a} + \frac{4k_{tp}}{v_b}\cdot\frac{N_b{}^w\bar{n}_b{}^2}{2 + 2m_b}, \qquad (4:113)$$

as we set $\bar{n} = N_1/N^w$. Multiplication of the equation with $v_a/k_{tp}N_a{}^w$ gives

$$\alpha_a' = \frac{2\bar{n}_a^{\,2}}{1+1/m_a} + \frac{2\bar{n}_b^{\,2}}{1+1/m_b}\frac{\eta^3}{F} \qquad (4:114)$$

As from (4:107) $\bar{n}_b = \bar{n}_a/\eta^3$ we obtain

$$\alpha_a' = \frac{2\bar{n}_a^{\,2}}{1+1/m_a} + \frac{2\bar{n}_a^{\,2}}{1+1/m_b}\frac{1}{\rho^3 F}, \qquad (4:115)$$

and accordingly

$$\bar{n}_a = \left[\frac{\alpha_a'}{\frac{2}{1+1/m_a} + \frac{2}{1+1/m_b}\cdot\frac{1}{\eta^3 F}}\right]^{\frac{1}{2}}. \qquad (4:116)$$

By inserting the parameters α_a', m_a, m_b, η, and F we can if get $\bar{n}_a$ expressed by ρ^w, k_{tp}, V_p, etc. We immediately see that $\bar{n}_a \sim (\rho^w)^{1/2}$ and therefore also $\bar{n}_b \sim (\rho^w)^{1/2}$. For small m, m<<1, $\bar{n}$<<1 is hardly valid, as for large m, 1/m <<1 so that

$$\bar{n}_a = \left[\frac{1}{2}\cdot\frac{\alpha_a'}{1+(1/\eta^3 F)}\right]^{\frac{1}{2}} \qquad (4:117)$$

If $\rho^3 F << 1$ then $\bar{n}_a = \left(\frac{1}{2}\eta^3 F\alpha_a'\right)^{\frac{1}{2}}$, (4:118)

as for $\rho^3 F >> 1$, $\bar{n}_a = \left(\frac{1}{2}\alpha_a'\right)^{\frac{1}{2}}$ (4:119)

In this last case, either $N_a^w >> N_b^w$ or a is designated as the large particles, so that $D_a^3 >> D_b^3$.

The case (4:119) is the same as obtained for large values of m when we only operate with one kind of particles (the boundary line in Figure 3 for m >> 1). These special cases are of lesser interest in the study of competitive growth.

4.3.6 Different types of radicals

In the case of two particle sizes we can also set up equations when distinguishing between monomer and polymer radicals as in point 4.2.4. This way of thinking will be more realistic than those used above, but the disadvantage is that an analytical solution of the equation system becomes very difficult, if not impossible, at least when we cannot assume that ın << 1. Such an assumption will likely produce the same result as already found (x = 3), so the interesting case is whether we get any difference from the Bessel function model if $\bar{n}$ < 0.5 while $\bar{n}$ << 1 does not apply. According to Ugelstad, such a difference would be possible because it is not certain that the ratio between monomer and polymer radicals is the same in large and small particles. The equation system can only be solved numerically. The system corresponds to the equations (4:36) - (4:40) for a and b particles separately, as ρ_A is exchanged by ρ_{Aa} and ρ_{Ab} , and k_{dm} by k_{dma} and k_{dmb}. The rest of the constants are the same

for both particle sizes. We use the equations (4:26) and (4:84) ($k_d=4\pi D_p r/v$ and $\rho_{Aa}/\rho_{Ab} = \eta F$). When we ignore the termination in the water phase, equation (4:41) gets the same form as (4:105):

$$\frac{dn_t}{dt} = \rho^w - \frac{4k_t}{v_a} N_{2pa} - \frac{2k_t'}{v_a} N_{pma} - \frac{4k_t''}{v_a} N_{2ma} - \frac{4k_t}{v_b} N_{2pb} - \frac{2k_t'}{v_b} N_{pmb} - \frac{4k_t''}{v_b} N_{2mb} \qquad (4:120)$$

We have 11 equations with 11 unknowns. The unknowns are N_{1ma}, N_{2ma}, N_{1pa}, N_{2pa}, N_{pma}, N_{1mb}, N_{2mb}, N_{1pb}, N_{2pb}, N_{pmb}, and ρ_{Aa}, as ρ_{Ab} is given by ρ_{Aa} and η. In addition, N_a^w and F are given in addition to values for all the constants. Solution of the equation system is programmed for computer by Lervik (15) in consultation with the author. Here, the method of Bessel functions described in section 4.3.4 is used to calculate a value for ρ_{Aa} close to the correct one. This is then put into the equation system, and it becomes linear in all N_j. To solve N_j, we use 10 of the equations, while the one containing ρ_{Aa} is not used. The last equation is solved with respect to ρ_{Aa} and all N_j contained in this are inserted. The value of ρ_{Aa} that is obtained is reintroduced into the rest of the equation system, and the routine is repeated. The routine will by convergence give the values of N_j and ρ_{Aa} with the desired accuracy. We can then calculate both and $\bar{n}_a$ and $\bar{n}_b$ by

$$\bar{n}_a = \left(N_{1ma} + 2N_{2ma} + N_{1pa} + 2N_{2pa} + 2N_{mpa} \right) / N_a^w \qquad (4:121)$$

$$\bar{n}_b = \left(N_{1mb} + 2N_{2mb} + N_{1pb} + 2N_{2pb} + 2N_{mpb} \right) / N_b^w \qquad (4:122)$$

x can be calculated according to the previously described equation (4:72) and equation (4:70) can be integrated numerically by the method described in section 4.3.4 (the same computer program).

4.4 The diffusion model

In the foregoing, the rate of absorption and desorption (radicals per unit time) is assumed to be proportional to the particle radius r and the concentration of radicals in the water phase C_R^w, or in the particles, n/v. Here will be given a calculation of the rate, especially for the absorption, based on the mathematical contexts that apply to such a system.

For transport into a sphere of a diffusing component A through a stationary medium B, the equation applies:

$$\dot{N}_A = -D_{AB} 4\pi R^2 C \left.\frac{dx_A}{dr}\right|_{R=r} \quad (mol/s) \qquad (4:123)$$

D_{AB} – diffusivity of A in B (m^2/s)

R – particle radius (m)

r - radius of the spherical surface considered (outside the particle, see Figure 7) (m)

C - total koncentration of A and B (mol/m^3)

x_A – molar fraction of A

$\frac{dx_A}{dr}$ - gradient in the surface on molar fraction basis (m^{-1})

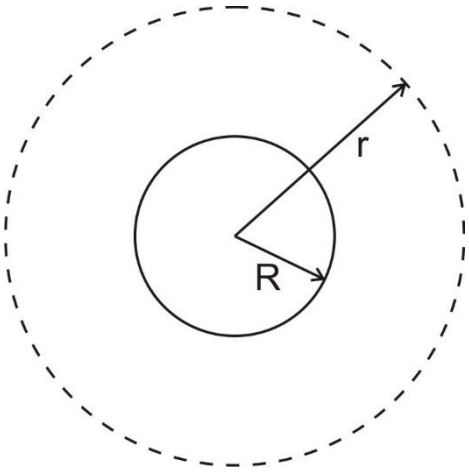

Figure 7.

The considered model.

The task is therefore to determine $\frac{dx_A}{dr} = f(r)$

For stationary diffusion, according to (6) in sperical coordinates,

$$\frac{d}{dr}\left(r^2 \frac{CD_{AB}}{1-x_A} \cdot \frac{dx_A}{dr} \right) = 0 \qquad (4:124)$$

This gives by twice integration:

1) $$\frac{r^2}{dr}\frac{dx_A}{1-x_A} = K_1 \quad (4:125)$$

2) $$\ln(1-x_A) = K_1\frac{1}{r} + K_2 \quad (4:126)$$

as C D_{AB} is included in K_1. K_1 and K_2 are integration constants that must be determined from boundary conditions.

$$r = \infty \text{ gir } x_A = x_{Aw} \quad (4:127)$$

$$r = R \text{ gir } x_A = x_{AR} \quad (4:128)$$

x_{Aw} corresponds to the molar fraction of initiator in the water phase and x_{AR} is equivalent to the molar fraction at the surface of the particle. This provides:

$$K_2 = \ln(1-x_{Aw}) \quad (4:129)$$

$$K_1 = R\ln\left(\frac{1-x_{AR}}{1-x_{Aw}}\right) \quad (4:130)$$

Inserted in (4:126) we get,

$$\ln(1-x_A) = \frac{R}{r}\ln\left(\frac{1-x_{AR}}{1-x_{Aw}}\right) + \ln(1-x_{Aw}) \quad (4:131)$$

I.e. $$\frac{1-x_A}{1-x_{Aw}} = \left(\frac{1-x_{AR}}{1-x_{Aw}}\right)^{\frac{R}{r}} \quad (4:132)$$

This expression gives a molar fraction profile from the water phase r=∞ to the particle surface r=R. x_A must be derived to find for å find $\left.\frac{dx}{dr}\right|_{r=R}$:

$$\frac{dx_A}{dr} = -(1-x_{Aw})\left(\frac{1-x_{AR}}{1-x_{Aw}}\right)^{\frac{R}{r}}\ln\left(\frac{1-x_{AR}}{1-x_{Aw}}\right)\cdot\left(-\frac{R}{r^2}\right) \quad (4:133)$$

Now, x_{AR} and x_{Aw} are very small, as x_{Aw} is of the order of 10^{-4} (the concentration of water in water is 55.5 mol/L, and of initiator between 10^{-2} and 10^{-4} mol/L). We can then write

$$\ln\left(\frac{1-x_{AR}}{1-x_{Aw}}\right) = \ln\left(\frac{1-x_{Aw}+x_{Aw}-x_{AR}}{1-x_{Aw}}\right) = \ln\left(1+\frac{x_{Aw}-x_{AR}}{1-x_{Aw}}\right) \approx x_{Aw}-x_{AR} \quad (4:134)$$

as generally $\ln(1+\varepsilon) \approx \varepsilon$ for small ε ($\varepsilon<10^{-2}$) and x_{Aw} can be neglected compared to 1.

(4:131) then gives

$$\frac{dx_A}{dr} = \frac{R}{r^2}\left(x_{Aw} - x_{AR}\right) \qquad (4:135)$$

for r=R, then $\left.\frac{dx_A}{dr}\right|_{r=R} = \frac{1}{R}\left(x_{Aw} - x_{AR}\right)$ (4:136)

(4:123) gives

$$\dot{N}_A = -D_{AB}\,4\pi RC\left(x_{Aw} - x_{AR}\right) = \underline{-D_{AB}\,4\pi R\left(C_{Aw} - C_{AR}\right)} \qquad (4:137)$$

(negative sign because diffusion is in the opposite direction of the coordinate system as in Fick's 1st law)

C_A is the concentration of A (mol/m^3)

We see that $\dot{N}_A$ is proportional to the particle radius, and C_A^w - C_{AR}.

A prerequisite for $\dot{N}_A$ (ρ_A) to be proportional to $C_A^w = (C_R^w)$ is that $C_A^w >> C_{AR}$, i.e. that concentration of radicals at the surface of the particle is very small. In addition, the boundary condition $x_A = x_{Aw}$ when $r = \infty$ must be met. This assumes that there is no mechanical mixing in the system for $R < r < \infty$, which seems unrealistic. Equation (4:137) can therefore only be approximately correct. If we set $x_A = x_{Aw}$ for $r = R_1 > R$, we will in an analogue manner as above get the following expression

$$\dot{N}_A = -D_{AB}\,4\pi R\,\frac{R_1}{R_1 - R}\left(C_{Aw} - C_{AR}\right) \qquad (4:138)$$

which gives (4:137) when $R \to \infty$. If $R_1 \to R$, the absorption rate will no longer be diffusion-controlled, but will be collision-controlled and proportional to R^2. It all depends, therefore, on the mixing in the system and the number and size of the particles. However, it is not certain that the mixing in the system will be so effective that, for example, the stirring intensity is important for the absorption rate (one operates with small Reynolds numbers, because of very small particle sizes). However, the possibility is present for the particles to come so close that the direct transition of a radical may be of importance. Even if not $R_1 >> R$, it may be possible that $\dot{N}_A \sim R$. If we set $R_1 - R = \Delta$, we get

$$\frac{R_1}{R_1 - R} = \frac{R + \Delta}{\Delta} = \frac{R}{\Delta} + 1 \qquad (4:139)$$

If $\Delta \sim R$, R/Δ will be constant, and $\dot{N}_A \sim R$. If Δ = constant, then $(R/\Delta) + 1$ will be independent of R_1 and the dependency will vary with the size of Δ. For $\Delta << R$, $(R/\Delta) >> 1$ and the absorption proportional to the surface.

If this is the case, the expressions for ρ_{Aa} and ρ_{Ab} we be different. (4:75) will be changed to

$$\rho_{Aa} = \frac{r_a{}^2 N_a{}^w}{r_a{}^2 N_a{}^w + r_b{}^2 N_b{}^w}\rho_A = \frac{\eta^2 F}{\eta^2 F + 1}\rho_A \qquad (4:140)$$

(4:76) will be changed correspondingly, so that

$$\frac{\rho_{Aa}}{\rho_{Ab}} = \eta^2 F \qquad (4:141)$$

which gives $\alpha_b = \alpha_a \frac{\rho_{Ab}}{\rho_{Aa}} \frac{v_b}{v_a} \frac{N_a{}^w}{N_b{}^w} = \alpha_a \frac{1}{\eta^5}$ (4:142)

(4:82) will also change accordingly to (4:75). The expressions for α_b 'and m_b are the same, as the desorption rate is still assumed to be proportional to the radius. If this is also proportional to the surface as assumed by Smith and Ewart (13), m_b becomes:

When m = 0, $\bar{n} = (\alpha/2)^{1/2}$ for $\alpha>1$ according to equation (4:6), and we then get

$$\frac{\bar{n}_a}{\bar{n}_b} = \left(\frac{\alpha_a}{\alpha_b}\right)^{\frac{1}{2}} = \left(\eta^5\right)^{\frac{1}{2}} = \eta^{2,5} \qquad (4:144)$$

and $x = \frac{\log(\bar{n}_a / \bar{n}_b)}{\log \eta} = 2,5$ (4:145)

When m>0 and $\bar{n}<<1$ we get from (4:108):

$$\frac{\rho_{Aa}}{\rho_{Ab}} = \frac{1}{\eta^2}\frac{\bar{n}_a}{\bar{n}_b} F = \eta^2 F \qquad (4:146)$$

So that $\frac{\bar{n}_a}{\bar{n}_b} = \eta^4$ (4:147)

and $x = \frac{\log(\bar{n}_a / \bar{n}_b)}{\log \eta} = 4.$ (4:148)

If $k_d \sim r^2/v$ w eget in the same way

$$\frac{\rho_{Aa}}{\rho_{Ab}} = \frac{r_a{}^2}{r_b{}^2}\frac{v_b}{v_a}\frac{\bar{n}_a}{\bar{n}_b}\frac{N_a{}^w}{N_b{}^w} = \frac{1}{\eta}\frac{\bar{n}_a}{\bar{n}_b} F = \eta^2 F \qquad (4:149)$$

$$\frac{\bar{n}_a}{\bar{n}_b} = \eta^3 \quad \text{and} \quad \underline{x = 3} \qquad (4:150)$$

The limiting value of x becomes equal to 3 when only the proportionality of the rates of absorption and desorption is the same (with r or r^2). x can be calculated for all values of $\bar{n}$, using the method described in section 4.3.4 (Bessel functions). This can also be used just like that when $\rho_A \sim r^2$, using (4:140) and (4:142) instead of (4:77) and (4:90). If the desorption rate is proportional to the surface, the expression for k_{da} in (4:87) and k_{db} in (4:88) must be changed so that $k_d \sim r^2/v$. We then get another constant instead of $4\pi D_p$, and this is not known

(it may be determined from experimental data). According to Ugelstad, $k_d \sim r^2/v$ does not match the experimental data for the total velocity by ordinary emulsion polymerization, while the dependency of ρ_A is not important (with only particle size).

4.5 Principles for experimental execution

4.5.1 Monodisperse latexes

In competitive growth experiments, according to Vanderhoff and Bradford (5), two different seed latexes with a relatively small spread should be used, so that the distribution curves will in no case overlap, either at the start or during of the reaction. Determining average particle diameters for each size would otherwise be uncertain. The distributions should also not be too wide, the accuracy of the mean diameter will be less the wider the distribution is (in that case, more particles must be measured), in addition, uncertainty may occur due to big difference between the different diameter averages (see point 4.5.3). The distribution curves should therefore be as narrow as possible.

With regard to the production of monodispers seed, it can be calculated from Smith and Ewart's theory what influence the various variables like concentration of emulsifier, initiator, and monomer, and temperature will have on the distribution. One then uses equation (4:11) and the equations used for its derivation. Such a calculation has been made by Gerrens (7) and shall not be reproduced here. It is primarily the type and concentration of emulsifier that is important for the distribution, as increasing amount of emulsifier provides wider distribution (in addition to more particles). According to Gerrens, the width of the distribution curve will decrease (the spread decreases) when the number of particles initiated in Stage I decreases. In order to produce a monodisperse latex, one should then use a low starting concentration of an emulsifier that gives few particles (few micelles). Such an emulsifier is e.g. sodium octyl sulfate ($C_8H_{17}SO_4Na$). The solubility of this in water is relatively high (high critical micelle concentration) and it produces small micelles. According to Gerrens, the spread should also decrease with increasing initiator concentration, but the impact is small. Ugelstad et al. has found that the initiator concentration has no effect on the number of particles formed in Step I (Section 4.2.1.) for PVC, and then the distribution function should neither change significantly.

Although Smith and Ewart's theory do not apply to vinyl chloride, one should expect a similar effect in terms of the importance of the emulsifier amount. Vanderhoff et al. used a standard polystyrene latex (Dow) in their experiments, and the production method is not provided. Gatta et al. (6) utilized monodisperse PVC latexes in their experiments with new nucleation, but only stated that the latexes were prepared according to a well-known batch procedure. Their largest particles had an average diameter of 4200 Å with a spread of 120 Å, and the particle number was $1.0\ 10^{16}$ per. L water.

The results of competitive growth experiments will also show how one can expect the distribution curve to change during a normal polymerization (also see section 4.3.1).

4.5.2 Amount of latex in seed experiments, new nucleation

Vanderhoff et al. used very few particles in their seed experiments (2 10^{13} - 2 10^{15} per liter of water), but did not get any new nucleation when no additional emulsifier was added. New nucleation in seed experiments with vinyl chloride has been studied by Gatta et al. (6). They showed that a certain amount of seed present at the start of the reaction is required in order not to form new particles and that this amount depends on the particle size.

For different particle sizes, they found regions where growth conditions varied, so that at particle numbers above the regions they did not get any new generation. The regions were given by the particle surface and the corresponding particle numbers. Their values for the surface are plotted in Figure 8. They did not give the coverage of emulsifier at startup, only that it was below 100%. The emulsifier was Empicol Ser (Marchon Italiana) containing 88% sodium lauryl sulfate ($C_{12}H_{25}SO_4Na$).

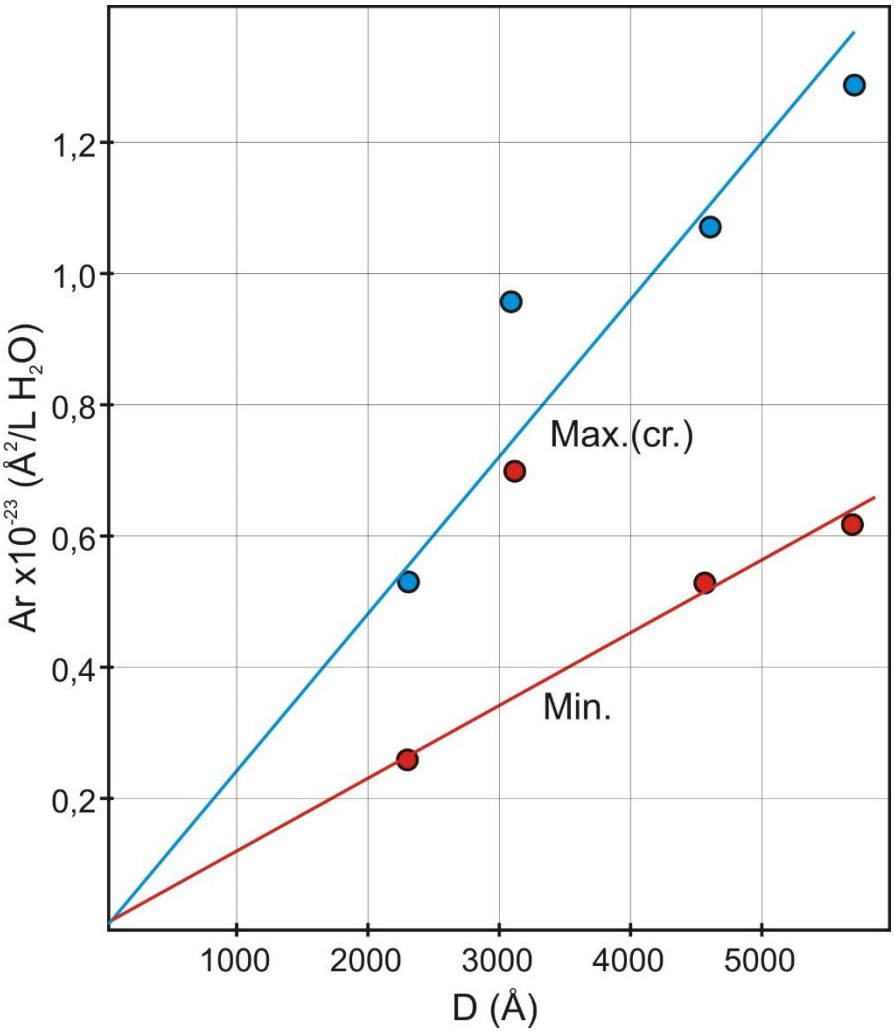

Figure 8. Regions where new nucleation of particles by seed polymerization of vinyl chloride varies. Values from Gatta et al. (6).

They assumed that the new formation was due to that vinyl chloride is somewhat soluble in water, so that polymerization can start in the water phase by initiating dissolved monomer with radicals. These growing radicals they assumed can be absorbed by particles, and this absorption will go faster the more particles present, such that over a certain particle number such radicals will be completely absorbed and one will not get any new generation. At low particle numbers, however, the growing radicals can absorb emulsifier and new particles are formed. They initially set the rate of absorption proportional to the total surface area of the particles, while they set the absorption rate per. unit surface inversely proportional to the radius, so that the actual absorption rate becomes proportional to the radius. Therefore, the critical size of new generation becomes $N^w r$, something Figure 8 indicates. The limiting values for the surface as a function of the diameter can be said to be lying on a straight line through the origin so that

$$N^w r^2 \sim r, \text{ i.e that } N^w r = \text{constant} \qquad (4:151)$$

This gives a good indication that the rate of absorption is proportional to the radius as found in section 4.4. However, the points in Figure 8 are too few and too scattered to provide reliable results. The critical value for $N^w r$ should then be $(N^W r)_{kr.} = 3.8\ 10^{18}$ Å/L H_2O. It is possible that this value will vary with the emulsifier coverage, and as mentioned above, this is not given. In any case, one should operate with values at $N^w r$ that are well above this value if one is to be sure to avoid new nucleation. Gatta et al. also believe that the reason that seed experiments with styrene do not give new nucleation at lower values of $N^w r$, is that styrene is much less soluble in water than vinyl chloride, so that growing radicals in the water phase are not as easily formed. For vinyl chloride, they also found that the monomer/polymer ratio did not have any effect on the new nucleation.

4.5.3 Mean diameter, particle numbers

When measuring average diameters of latex particles, one must use a number of discrete intervals for the distribution. The size of these is determined by the accuracy of measurements, with a high degree of accuracy giving a large number of intervals. It is common to measure the diameter from images taken with an electron microscope. The magnification of the images and the type of the measuring device will then determine the width of the measurement intervals. The calculation of the mean diameter can then be done in several ways according to the desired type of average. The most commonly used means are the following:

Mean number diameter:

$$\bar{D}_n = \frac{\sum N_i D_i}{\sum N_i} \qquad (4:152)$$

This can only be used for uniform latex particles

$\sum \equiv \sum_{i=1}^{n_1}$, where n_1 is the number of measuring intervals

N_i – number of particles of diameter D_i

Mean volume diameter:

$$\bar{D}_v = \left[\frac{\sum N_i D_i^3}{\sum N_i} \right]^{1/3} \quad (4:153)$$

This is the commony used diameter of heterodisperse particles, which corresponds to the diameter of a latex particle having a weight equal to the average number particle weight:

$$\bar{W}_n = \frac{\sum N_i W_i}{\sum N_i} \quad (4:154)$$

$W_i = v_i\, d$ – weight of particle i

d - density

Mean waight diameter:

$$\bar{D}_w = \left[\frac{\sum N_i D_i^6}{\sum N_i D_i^3} \right]^{1/3} \quad (4:155)$$

$\bar{D}_w$ is the average diameter of a particle having a weight equal to the average weight particle weight:

$$\bar{W}_w = \frac{\sum N_i W_i^2}{\sum N_i W_i} \quad (4:156)$$

Mean surface diameter:

$$\bar{D}_{ar} = \frac{\sum N_i D_i^3}{\sum N_i D_i^2} \quad (4:157)$$

This is the diameter found by soap titration (section 4.5.4). Usually, we will have:

$$\bar{D}_n \le \bar{D}_v \le \bar{D}_{ar} \le \bar{D}_w \quad (4:158)$$

If the latex consists of particles with only one diameter, all the average diameters will be the same. As a measure of heterodispersity, one can use the ratio $\bar{D}_n / \bar{D}_v$ which will be less than 1 for heterodisperse latexes. Instead, one can use the spread on $\bar{D}_n$. This is given as

$$\sigma = \left[\frac{\sum N_i \left(D_i - \bar{D}_n \right)^2}{\sum N_i} \right]^{\frac{1}{2}} \quad (4:159)$$

$$= \left[\frac{\sum N_i D_i^2}{\sum N_i} - \bar{D}_w^{\,2} \right]^{\frac{1}{2}} \quad (4:160)$$

The spread (standard deviation) will be independent of the width of the measurement intervals (assuming zero uncertainty in σ, as this will increase with the width of the measurement intervals when the number of particles is the same).

The distribution curve is obtained one by plotting the number of particles in each interval as a function of the average diameter of the interval. In order to compare distribution curves, the same number of particles must be used, i.e. as the ordinate, % of the total number is most commonly used. We get a bar graph (histogram) (the width of the bars is equal to the interval width) and the distribution curve is drawn as a smooth curve so that the area under the curve in each interval becomes equal to the area of the respective bar (the area under the curve becomes 100% • interval width). Curves that are drawn with different interval widths cannot be easily compared, but must be converted so that the area under the curves become the same. We also see that the height of the curve will increase with the interval width, with the limiting values being 100% when all the particles are in a single interval and zero when the number of intervals is infinite.

Knowing $\bar{D}_v$ and the conversion P_t (gPVC/L H_2O) of the latex, the particle number N_w (part./L H_2O) can be calculated.

We have

$$N^w \frac{\pi}{6} \bar{D}_v^3 d = P_t \qquad (4:161)$$

i.e.
$$N^w = \frac{6P_t}{\pi d \bar{D}_v^3} \qquad (4:162)$$

(d [=] g/cm^3)

To calculate average diameter, we can also use soap titration. This is based on the fact that the particles can adsorb emulsifier (soap) until they are 100% covered. Further added emulsifier will then be dissolved in the water and will form micelles when the concentration exceeds the critical micelle concentration. If one knows the latex's content of polymer and emulsifier, the surface area can be determined from the total adsorbed emulsifier, and thus the average surface diameter. This assumes that one knows the surface an emulsifier molecule occupies, a_s. The titration end point is reached at the critical micelle concentration, and this can be measured in several ways; by measuring surface tension, conductivity, dissolution of fluorescent substances or pigments, etc. Surface tension measurement (used here) is based on the fact that the surface tension on the latex will decrease rapidly and (almost) linearly with increasing coverage of emulsifier up to the c.m.c. is reached, then it will only change slowly. By drawing a curve for surface tension as a function of the titration volume, this so-called break point is easily determined, as shown in Figure 9.

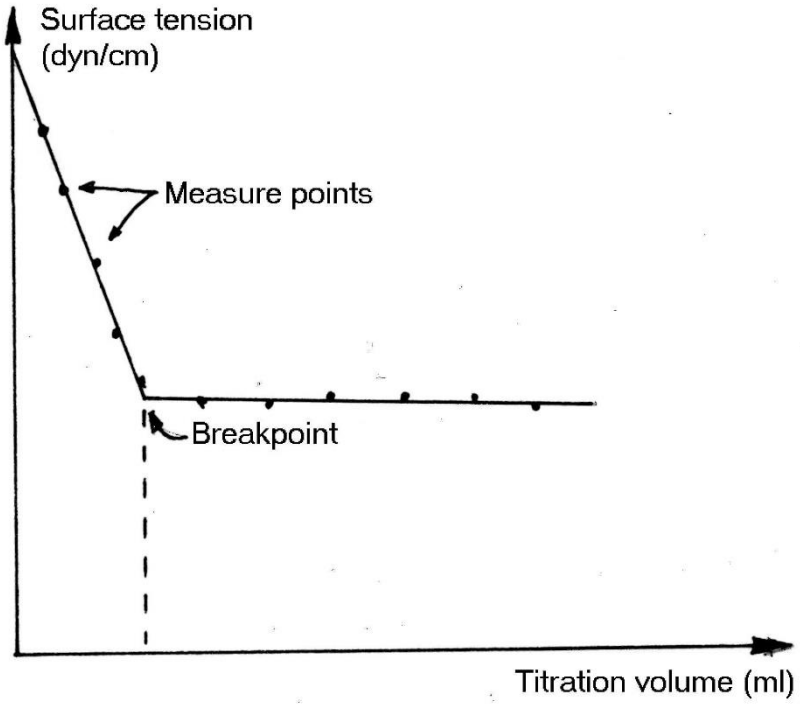

Figure 9. Example of titration curve by soap titration.

When one knows the emulsifier amount at the break-point, one must deduct the critical micellar concentration. This is found by making two or more titrations of the same sample at different dilutions, so that the total amount of emulsifier at the junction becomes different. By drawing a curve (straight line) for the amount of emulsifier as a function of the polymer content of the latex (at the junction), the c.m.c. can be determined by extrapolating the line to zero polymer content. The slope of the line then gives the amount of emulsifier per. gram of polymer, S_a (mol/g). The titration solution and the latex are added salt (NaCl) so that the c.m.c. is as small as possible (ionic effect).

Mean surface diameter can be calculated from

$$\bar{D}_{ar} = \frac{6}{d \cdot a_s \cdot S_a} \qquad (4:163)$$

For PVC (d = 1,41 g/cm^3) this gives

$$\bar{D}_{ar} = \frac{7{,}11}{a_s \cdot S_a} \ (\text{Å}) \qquad (4:164)$$

when a_s [=] Å^2/molecule

S_a [=] mol/g PVC

5 Instrumentation

All polymerizations were carried out in a 1.5 liter glass autoclave (Ingenieurenbureau, SFS, Zurich, Switzerland) fitted with thermostatic water circulation, blade stirrer and power switches, pressure gauge, thermometer and valves for liquid and gas addition and sampling. The autoclave and associated equipment and fluid circuits are shown in Figure 10, while Figure 11 is a photograph of the autoclave fully assembled. (The figure shows the autoclave with turbine stirrers, while in the experiments, two blades were used, about 35 x 15 mm).

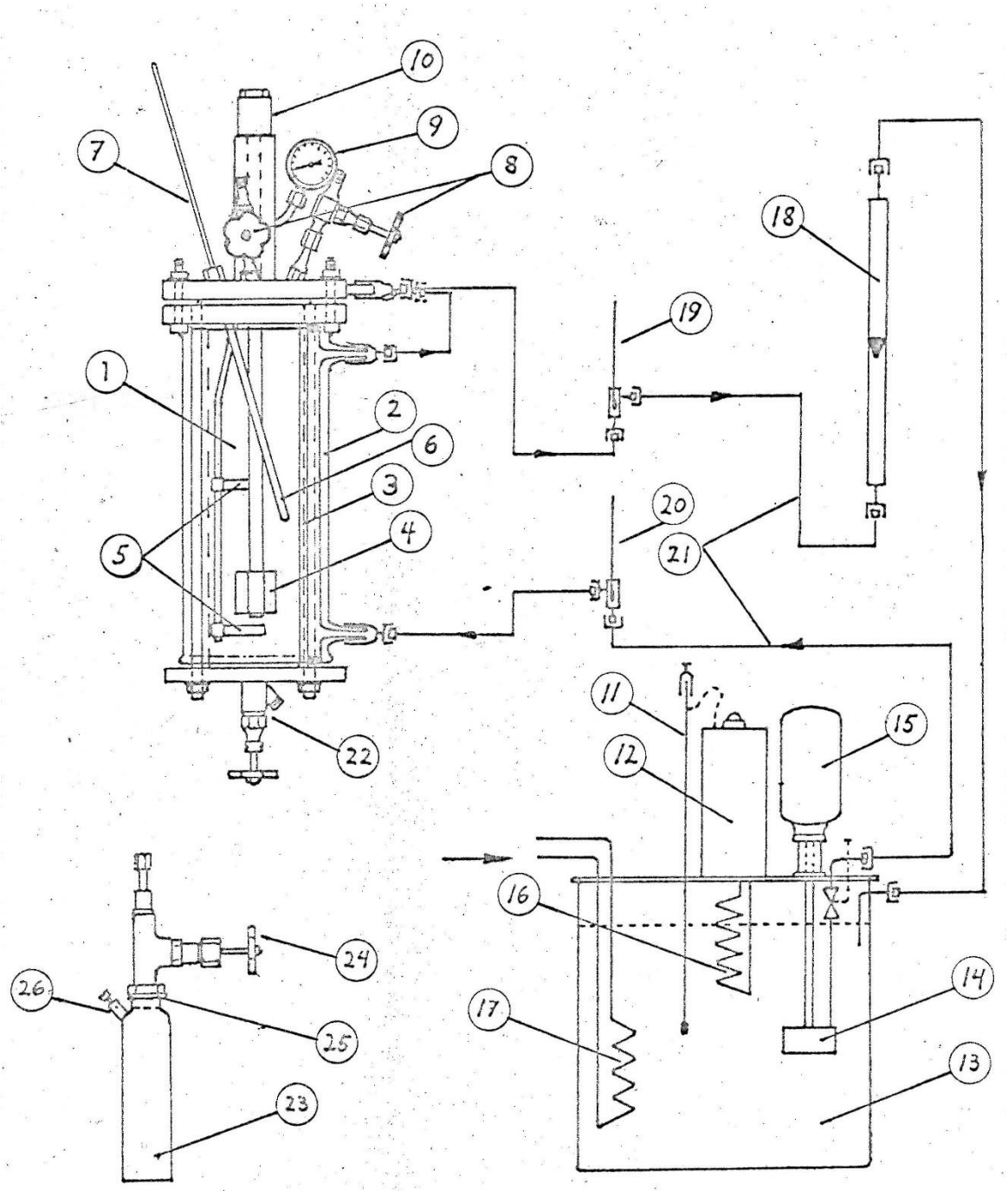

Figure 10. Autoclave with liquid circuit and pressure bottle for sampling.

Caption to Figure 10

1. Autoclave
2. Outer mantel
3. Inner mantel
4. Blade stirrer
5. Current switches
6. Thermometer pocket, can be dismounted for addition of solids
7. Thermometer, 0 - 100° C, ± 0,1 °C
8. Valves for addition of liquids and gas and for gas exhaust
9. Pressure gauge, +1 - 16 ato
10. Cylinder for magnet's follower (mounted on the stirrer's axle)
11. Contact thermometer
12. Thermostat
13. Thermostat bath (water)
14. Centrifugal pump (submerged)
15. Pump motor
16. Heating spiral (electric)
17. Cooling coil (cold water)
18. Rotameter
19. Thermometer for circulation water from the autoclave
20. Thermometer for circulation water to the autoclave
21. Rubber hoses
22. Valve for sampling
23. Pressure flask for sampling to microscope
24. Valve on the pressure flask
25. PTFE gasket
26. Valve for venting of vinyl chloride (manual control by screw)

The power transfer to the stirrer takes place by means of a magnet that rotates around the cylinder 10 and a follower inside the cylinder to which the stirrer shaft is mounted. The autoclave can therefore be kept very tight during the experiments. In front of the autoclave, a steel protection plate was mounted during the experiments. Vinyl chloride was added from a 1.5 liter pressure bottle of steel which was filled from a large pressure cylinder with vinyl chloride supplied by Norsk Hydro. The addition was effected by the pressure bottle being heated in hot water (60-70°C) and then screwed to one of the valves 8 on the autoclave by a reducer.

Initiator was added dissolved in water from a specially designed pressure bottle as shown in Figure 12. (See also section 6.1). The initiator solution was added against nitrogen pressure using a graduated Erlenmeyer flask with a special valve arrangement. See Figure 12.

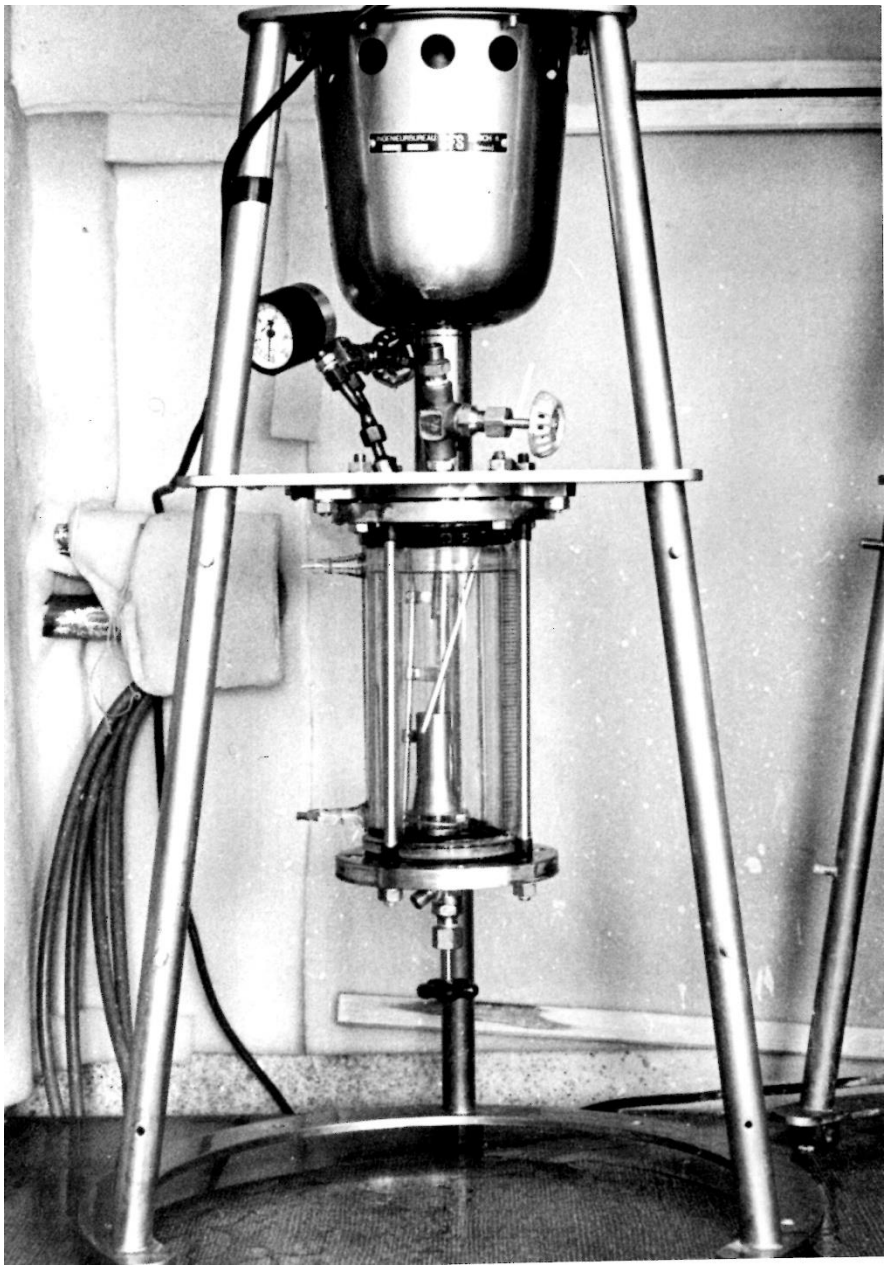

Figure 11. Mounted autoclave, not connected to hoses for circulation water

For the microscopy an electron microscope type Siemens, Elmiskop I (No. 207) was used. The photos, which were captured on photographic plates, were enlarged and copied using a regular magnifier.

For the particle measurements a semi-automatic optic-electronic particle size analyzer, Zeiss TGZ 3 was used. The measurement is done by comparing the particle images with a circular light spot. The diameter of this can be varied continuously from approx. 1 to about 10 mm, divided into 48 discrete intervals. A measurement is automatically recorded in a register

corresponding to the diameter interval. At the same time, the measured particle is labeled so that the same particle is not measured several times.

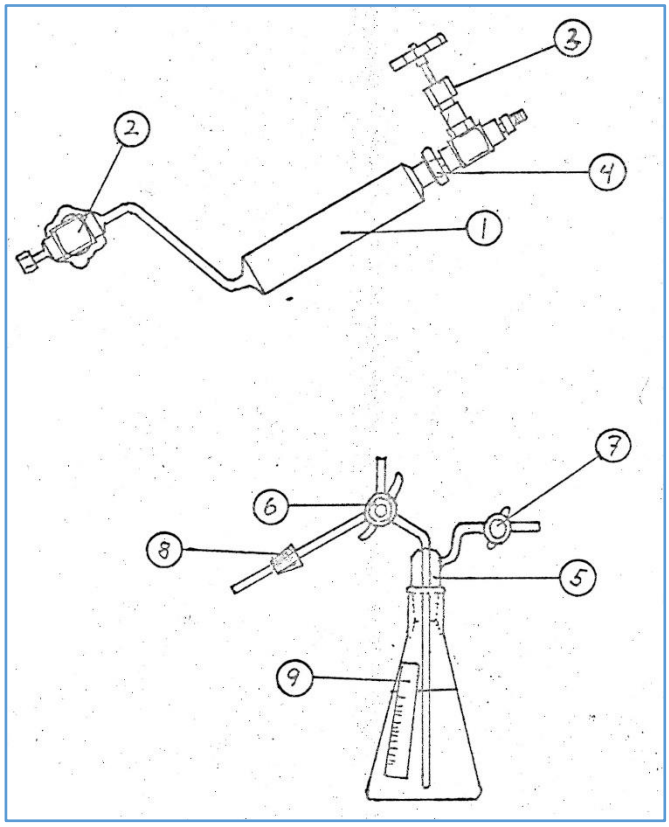

Figure 12. Pressure flask for addition of initiator (top) and flask for addition of water (bottom).

1. Steel cylinder
2. and
3. Valves
4. Detachable part (with valve 3)
5. Glass stopper (ground) with tubes
6. 3-way valve
7. Ordinary glass valve
8. Rubber stopper
9. Scale for volume reading

A tensiometer, type Krüss K8600E, was used for measuring the surface tension by soap titration (section 6.4.3). The instrument is based on the Du Noüy ring method, and the surface tension is read directly in dyn/cm.

6 Experimental

6.1 Preparation of seed

6.1.1 Polymerization

The process of seed preparation was as in a conventional polymerization described by Ugelstad et al. (2). It will nevertheless be given a detailed description here. For experimental conditions, see section 6.3.

The autoclave (Figures 10 and 11) was filled with the given amount of redistilled water (700 or 1000 ml) through the opening of the thermometer pocket, which was removed. It was then evacuated using a water jet pump and 60 ml of water was evaporated with stirring and heating (250 rpm, 30 - 40° C). In this way, dissolved oxygen in the water was removed, which would otherwise act as an inhibitor of the reaction. The reading of the volume was done by a scale on the autoclave. At the end of the evaporation the autoclave was filled with nitrogen, the vacuum pump was shut off and the thermometer pocket removed. Emulsifier and buffer were added from weight ships under a weak counter flow of nitrogen. The thermometer pocket was mounted and emulsifier and buffer were stirred for 10 minutes under low nitrogen overpressure (1 to 2 ato), while the pressure bottle with vinyl chloride (item #5) was heated under running hot water. The vinyl chloride was then added from the pressure bottle at a temperature of about 50°C. The pressure was thus raised to 7.5 - 8.0 ato (saturation pressure for vinyl chloride at 50°C is about 7.5 ata). The vinyl chloride was stirred for 25 minutes at 500 rpm, while the temperature was adjusted to 50°C.

At the same time this stirring, the initiator solution was prepared. The part #4 of the pressure bottle (Figure 12) was turned off and the flask of boiling redistilled water (Figure 12) was mounted to it using the rubber stopper #8. The two bottles were located at the angle shown by the figures and the water bottle was on the cooking plate. The water had previously been boiled for 10-20 minutes with the tap #7 open to remove oxygen. The entire procedure of the addition occurred under low counter flow (back pressure) of nitrogen through the pressure bottle (hose mounted to the other end, to the left of the figure). With the 3-way valve #6, contact was established between the flask and the pressure bottle, and any oxygen in the riser in the flask was removed by the nitrogen flow. The tap #7 was then closed and 60 ml of water was pressed into the pressure bottle through the riser by means of the vapor pressure in the flask. The volume was read on the scale #9.

The flask was then removed and the water in the pressure bottle cooled somewhat using cold water on the outside. The initiator which was weight out in advance was added from a weighing ship and the ship was washed with 1 - 2 ml of water from the flask. The part #4 was again mounted, both taps were closed and the pressure bottle shaken to dissolve the initiator in the water. The bottle was then screwed on to one of the valves #8 on the autoclave with the tap #2 on the bottle down. Using the 8 ato nitrogen pressure on the pressure bottle, the water with the dissolved initiator was pressed into the autoclave (stirring halted). The

stirring was restarted, and pressure, volume, and temperatures noted. This time was set as the start time for the reaction.

Samples for the determination of conversion were withdrawn through the bottom valve #22 at regular intervals (section 6.4.1) (30-60 min). The temperature was kept as close to 50 ° C as possible by adjusting the contact thermometer #11 (Figure 10).

At the end of the reaction, one gets the typical "max" effect (point 4.1). From reactions that were run down to a pressure of 5 ato (especially experiment B-4), one could predict when this "max" effect would occur, and the reactions were stopped before this time.

Upon quenching of the reaction, cooling water was applied to the coil #17 (Figure 10) and residual vinyl chloride was released as quickly as possible through one of the valves #8. This usually took 5-10 minutes, depending on the amount of vinyl chloride left and of the amount of foaming (due to the surfactant, but very little with 1 g/L sodium octyl sulfate).

The autoclave was removed, and the final latex poured onto a bottle. Of this, solids samples and samples for microscopy were taken.

Washing the autoclave with accessories was done with acetone and water, while the stream breakers and blade stirrer were washed in water and cyclohexanone. All parts were washed with boiling redistilled water before reinstallation.

During the experiments, a run form was used in which times, temperatures, pressure, volume, etc. were noted. A typical form from seed production is attached in Appendix 1.1.

6.1.2 Dialyses

In order to be be able to study the kinetics of the reactions with competitive growth, the residual initiator must be removed from the final latex from seed preparation. This was done by dialysis which was performed by filling the latex into a tube of cellulose film (dialysis membrane) which was closed at both ends as a “sausage” (diameter about 5 cm, length 20-30 cm). This (possibly more, maximum 1 liter total volume) was placed in a bath with distilled, deionized water, which was replaced after 2 and 4 days. The bath (3 - 5 liters) was provided with stirring. Following the experience gained at the department, after such a dialysis of 6 days, initiator and buffer will be removed by diffusion through the cellulose membrane. If this also applies to the emulsifier is less certain (see sections 7.2 and 8.2). After dialysis, new solids samples were taken, as the solids content could change somewhat by dialysis.

Some of the dialyzed latexes were also soap titrated to determine the amount of emulsifier to be added in the experiments with competitive growth. Also see section 6.4.3.

6.2 Competitive growth

6.2.1 Ordinary experiments

For the competitive growth experiments, a mixture of latexes with two different particle sizes was used. Additionally, additional water and the usual additives were added (section 6.3). The process of polymerization was in many ways the same as in the production of seed, only the start-up was somewhat different. This also varied somewhat on the basis of experience that was gained gradually.

The experiments B-9 - B-12 differ from the following, because no emulsifier was added to the latexes in advance or together with the latexes and the water. Therefore, 60 ml of water could be evaporated with a subsequent addition of emulsifier and buffer as before.

In experiments B-13 - B-18, all emulsifiers (to 80% coverage) were added to the latex in advance to prevent coagulation upon standing. (Seed B-3+5 and B-6). In experiments B-19 - B-21, not all emulsifiers were added to the seed with the large particles (F-200) because this was also used for experiments with fatty alcohol (section 6.2.2). In all experiments designated B, from B-13, the following procedure was used:

Based on calculations (see section 4.5.3 and Appendix 4.5) seeds a and b were weight out. Extra water minus 60 ml was measured in a graduated cylinder (250 ml) and this was added to the autoclave together with buffer and optional emulsifier. Stirring (250 rpm) was applied and the autoclave evacuated without heating (20-25°C) as far as the foaming allowed (0.1 - 0.2 ata). Nitrogen was filled up to 4 ato, and the liquid stirred for 2 - 4 minutes to wash out oxygen dissolved in the water. This was repeated a total of 4 times. Warm (approximately 60°C) circulating water was then turned on and heated to 45 - 50°C during about 20 minutes. The procedure of the addition of vinyl chloride and initiator was the same as in the preparation of seed (initial stirring with vinyl chloride for 30 minutes).

Samples were taken for the determination of conversion in the usual manner, and for the determination of the diameter of the particles during growth, pressure samples were taken. These were taken by means of a small pressure bottle (about 150 ml) shown in Figure 10. The bottle was screwed to the bottom valve #22 on the autoclave and this valve was opened together with the valve #24 on the bottle. A sample of 40 - 60 ml (read on the autoclave) was taken, and was immediately cooled in running cold water (about 10°C) to stop the reaction. Unreacted vinyl chloride was released within 0.5 - 2 hours by carefully opening valve #26. A number of 4 - 5 pressure samples were taken per experiment.

The reactions were in some experiments run through the "max" region. Pressure samples were then taken a while before the "max" was expected. In other experiments, all from B-15 and on, the reactions were stopped before the "max" and the last microscopic sample taken from the final latex. The reactions were stopped in the same way as in the preparation of seed. A typical run form is attached in Appendix 1.2 (experiment B-13).

6.2.2 Experiments with fatty alcohol addition

At the request of Professor Ugelstad, two mixed emulsifier experiments were also performed, where in addition to sodium lauryl sulfate, a fatty alcohol (hexadecanol) was also added. As mentioned in the introduction, these experiments (F-205 and F-206) were run by staff at the department due to time shortage. The procedures of these experiments were somewhat different from the others in the start-up. An emulsion of the fatty alcohol and emulsifier in the water (added in addition to the water in the seed latex) was initially made at 70 °C (30 minutes at 500 rpm). The seed latexes were then added and the whole was stirred for 30 minutes at 1000 rpm. Evacuation was carried out in 4 series as before, while the vinyl chloride was added in two rounds: First 40% of total with subsequent stirring for 60 minutes at 500 rpm, then the rest with stirring for 20 minutes 50 rpm and finally 2 minutes at 750 rpm. This was done to prevent too much fatty alcohol from being dissolved in the monomer phase. (It dissolves much easier than the emulsifier because the fatty alcohol is much less polar.). Further experimental methodology was as usual for seed experiments.

6.3 Experimental conditions

6.3.1 Chemicals

The water used is designated as “redistilled”. This was made by two times distillation of ion exchanged water taken from one of the chemistry department’s ion exchange taps. The purpose of this was to remove any contaminants that could affect the reaction.

Vinyl chloride came in a steel cylinder from Norsk Hydro, and it had a purity of 99.99%. 80% of the contaminants are ethylene dichloride.

In experiments V-16 and B-1 - B-4, as emulsifier was used sodium octyl sulfate ($C_8H_{17}SO_4Na$) delivered by Norsk Hydro, dissolved in water to a 25% solution. In all other seed production experiments, sodium octyl sulfate was prepared at the institute from octanol and purified by recrystallization from ethanol.

Sodium lauryl sulfate ($C_{12}H_{25}SO_4Na$) (Schuchart) was purified by extraction with ethyl ether and recrystallized from ethanol.

As an initiator, potassium persulfate ($K_2S_2O_8$) (Merck, p.a.) was used in all experiments, and as buffer was used borax ($Na_2B_4O_7 \cdot 10H_2O$) (Merck, p.a.).

In the experiments with fatty alcohol, hexadecanol ($C_{16}H_{33}OH$) (Schuchart) was used. This was also purified by recrystallization from ethanol.

All nitrogen used was “high purity” (99.99%).

6.3.2 Preparation of seed

In order to gain training in the work operations of the polymerization and to investigate the effect of the emulsifier amount on the width of the diameter distribution,

experiments with 1 and 4 grams of sodium octyl sulfate per liter of water were performed. An overview of these experiments and the other experiments for seed production is given in Table VI below. All weight amounts except the amount of water are given in g/L water.

Experiment	Water (g)	Vinyl chloride (g)	Emulsifier (g)	Buffer (g)	Purpose of the experiment
V-16	700	430	1.00	0.30	Test
B-1	700	728	4.00	0.20	Test
B-2	700	850	4.00	0.20	Test
B-3	1000	170	1.00	0.30	Test + seed a
B-4	700	850	1.00	0.30	Test
B-5	1000	170	1.00	0.30	Seed a
B-6	700	850	1.00	0.30	Seed b
B-7	700	850	1.00	0.30	Seed b
B-8	1000	170	1.00	0.30	Seed a
F-200	700	850	1.00	0.30	Seed b

Table IV

The experiments V-16, B-1, B-2, and B-4 were run through the "max" range to 5 ato pressure, the others were stopped before "max" after a predetermined time to achieve a certain particle size.

Other conditions, common to all the experiments were:

Temperature: 50 ± 0,3°C

Pressure: 7,5 – 8.0 ato

Stirrer speed: 500 rpm = 8,33 s^{-1}

pH: 8,1 – 8,2

Initiator concentration: 1,63 g/L = 6,0 10^{-3} mol/L

6.3.3 Competitive growth

An overview of the different seed latexes is given in Table VII. Seed B-3+5 was a mixture of the dialyzed latexes from experiments B-3 and B-5. Seed B-MIX was a mixture of 378 g of seed B-3+5 and 969 g of dialyzed latex from run B-8. Seed B-3+5, B-MIX and B-6 were added sodium lauryl sulfate to 80% coverage (found by soap titration, see section 7.2), seed F-200 was added to ca. 30% coverage, while seed B-7 was not added extra emulsifier

(before during competing growth experiments). The emulsifiers for B-6 and F-200 were added dissolved in 100 ml of water while to B-3+5 and B-MIX it was added in solid form.

Designation	B-3+5	B-MIX	B-6	B-7	F-200
Seed a or b	a	a	b	b	b
$\bar{D}_v$ (Å)	1003	1150	2175	2320	2390
$N^w \times 10^{-16}$ (part./L H_2O)	8.20	5.30	4.21	4.57	3.30
Spread on $\bar{D}_v$ (Å)	72	ca. 100	132	146	156
Conversion (g PVC/L H_2O)	61	59	323	423	333
Surface area x 10^{-23} ($Å^2$/L H_2O)	2.59	2.17	6.30	7.72	5.90

Table VII. Overview of seed latexes.

The initiator amounts in molar units are:

1,63 g = 6,0 10^{-3} mol

0,815 g = 3,0 10^{-3} mol

0,203 g = 7,5 10^{-4} mol

Common to all seed experiments were the following conditions:

Total amount of water:	700 g
Vinyl chloride:	500 g/L H_2O
Buffer (borax):	0,30 g/L H_2O
Emulsifier:	80% dekning ved start
Temperature:	50,0 ± 0,3 °C
Pressure:	7,5 – 8,0 ato
Stirrer speed:	500 rpm = 8,22 s^{-1}
pH:	8,1 – 8,2

Fatty alcohol in experiment F-205 and F-206: 2x amount of emulsifier in moles (2X)

The amounts of seed for the various experiments were calculated from the conversion and the particle number (see section 4.5.3 and Appendix 4.5). An overview of the experiments is given in Table VIII.

Exp.	Seed a	Seed b	$N_a^w \times 10^{16}$ (L^{-1})	$N_b^w \times 10^{16}$ (L^{-1})	P_a^0 (g/L)	P_b^0 (g/L)	$Ar \times 10^{-23}$ ($Å^2$/L)	C_{in} (g/L)
B-9	B-3+5	B-7	0.50	0.50	3.70	45.3	1.01	0.815
B-10	″	″	1.00	″	7.40	″	1.16	″
B-11	″	″	0.50	″	3.40	″	*	″
B-12	″	″	1.00	″	7.40	″	*	″
B-13	″	B-6	0.50	0.39	3.70	29.2	0.73	″
B-14	″	″	2.00	″	15.0	″	1.20	″
B-15	″	″	5.04	″	37.9	″	2.16	″
B-16	″	″	0.53	0.53	4.00	40.2	0.96	″
B-17	″	″	2.94	0.53	22.1	22.1	1.36	″
B-18	″	″	0.81	0.81	6.05	60.9	1.45	″
B-19	B-MIX	F-200	1.65	0.50	18.4	50.4	1.68	1.63
B-20	″	″	″	″	″	″	″	0.203
B-21	″	″	″	″	″	″	″	0.815
F-205	″	″	″	″	″	″	″	″
F-206	″	″	0.42	0.64	4.72	64.2	1.32	″

* - uncertain due to coagulation

Table VIII. An overview of the experiments

All values for a-particles in Table VII and VIII are based on the diameters given in Table VII. If the diameter is higher, these values will change. Values for respectively 1100 Å and 1200 Å for latex B-3+5 and B-MIX are given in Appendix 6 together with the experimental results.

6.4 Methods of analysis

6.4.1 Total conversion

Total conversion during polymerization was measured on samples taken out through the bottom valve of the autoclave. The amount ranged from 3 to 10 grams with an average of 6 grams. Due to the instantaneous evaporation of vinyl chloride during sampling, there was a strong foaming in the test beaker. 150 and 100 ml beakers were used with a watchglass as a lid.

The test beakers were weighed in advance (weight P_0) and were immediately after sampling put in a heating cabinet at 50°C for 5 minutes to allow residual vinyl chloride to evaporate. The glass was then set to cool, and then weighed (without lid, weight P_1). The water was evaporated off in a heating cabinet at 65 °C. This took a maximum of 1 day. After cooling, the glasses were weighed again (weight P_2). The amount of solids in the sample could thus be determined according to the formula

$$P_t' = \frac{P_2 - P_0}{P_1 - P_2} 10^3 \ \text{(g/L } H_2O\text{)} \qquad (6:1)$$

as the density of water is set to 1.0 g/cm^3

The amount of PVC is obtained by subtracting the amount of emulsifier (P_e), initiator (P_{in}), and buffer (P_{bu}):

$$P_t = P_t' - (P_e + P_{in} + P_{bu}) \ \text{(gPVC/L } H_2O\text{)} \qquad (6:2)$$

6.4.2 Particle size by microscopy

Particle sizes were determined by electron microscopy. Some of the latex from the pressure samples, or the final latex, were diluted with redistilled water to a solids content of 10-15 g/L H_2O (varying between 1:10 and 1:30 depending on the solids content of the latex). This was then usually set in an ultrasonic bath for approx. 20 minutes to disperse any agglomeration (except when this was to be studied). Using a special spray dispenser, some of this latex was sprayed onto a pre-prepared microscope grid of copper, which was then used directly in the microscope.

The copper grid (Athens, type new 200, diameter 2.30 mm, 13 threads) was coated with a thin sheet of Formvar (polyvinyl formaldehyde) (prepared from chloroform solution) which was strengthened by evaporation of carbon.

The images were taken at a magnification of 2600 or 8000 (preferably the last) and were enlarged 2 to 6 times during copying, depending on the particle size. Thus, for each latex, 2 - 4 images were taken, depending on the number of particles in the images.

The particle diameter was measured on the particle size analyzer as described under section 5. On images of starting seed, it approx. 1000 particles were measured, and on images from experiments with competitive growth, approx. 500 of each size when the images contained that many of each, otherwise all the particles in the images were measured. The measurements took 50-60 minutes per. 1000 particles.

Mean diameters and spread were calculated on a computer according to the formulas in section 4.5.3. In addition, the percentage and weight percent of particles with a diameter greater than $\bar{D}_n + \sigma$ and less than $\bar{D}_n - \sigma$ (σ is the spread) were calculated. This is designated by H and L, respectively. The relationship between H and L expresses the distribution curve's symmetry around $\bar{D}_n$ (one should note that discrete distributions have been used so that H and L can be somewhat different even if the curve is symmetric if $\bar{D}_n$ is close to the middle of an interval, else see the program FKHPART).

6.4.3 Soap titration

Soap titration was used primarily to determine the amount of emulsifier to be added to the seed in competitive growth experiments. In this connection, a survey was also conducted to see if emulsifier (especially sodium octyl sulfate) diffuses out in the dialysis process. The titration itself was performed as follows:

In a small crystallization dish (about 5 cm diameter), 2-10 grams of latex was weighed out, depending on the particle surface (smallest amount for large surface area). Two parallels of different sizes were weighed out. After measuring the surface tension with (see section 5), they were added 5, respectively, 10 ml of 0.2 M sodium chloride solution, with the smallest parallel being added 10 ml and the largest 5 ml to get the greatest possible difference between the parallels. The parallels were then titrated with a solution of 10 g/L sodium lauryl sulfate and 0.2 M sodium chloride. After each addition, it was stirred 3 - 5 minutes to obtain equilibrium (magnetic stirring), and then the surface tension was measured. The platinum ring of the tensiometer was washed in distilled water and ethanol and burned in a gas flame after each measurement.

The calculation of S_a was done as explained in section 4.5.3. When a quantity of emulsifier was to be added during the seed experiments, only added emulsifier was taken into consideration, as any sodium octyl sulfate was neglected. This size is denoted by S_a'. To check the surface per. molecule, a_s, $\overline{D}_{ar}$ (also called D_s) could be calculated from S_a by equation (4:164).

In order to investigate the significance of any residual sodium octyl sulfate and if this disappears during dialysis, an experiment was made with the addition of sodium octyl sulfate to a latex. Latex V-1-10 was used with 1.90 10^{24} Å^2 /L H_2O and 492 gPVC/L H_2O. This is made with sodium lauryl sulfate as an emulsifier and it had a coverage of 4.4% (stated) when a_s is set equal to 45 Å^2. In order to compare the results with titration of latex B-3, V-1-10 was diluted to give the same surface as B-3. This was done by diluting 75 g of latex with 318 ml of water. A 40 ml sample was taken and 0.368 g of sodium octyl sulfate was added. This corresponds to 1.1 g per L water. After dissolving the octyl sulfate, a new sample was taken and the two samples were soap titrated in the usual manner. The last sample was allowed to stand for 6 weeks for a possible equilibrium to be established and was titrated again. The results are given in section 7.2.

6.5 Methods of calculation

As mentioned in section 6.4.2, the calculation of mean diameters, spread and similar were calculated on computer using the FKHPART program (written in ALGOL66). This is a modified version of a similar program previously used by the institute. The program is given in Appendix 7.

For the experimental order x of the volume growth with respect to the diameter (equation 4:49), both integral and differential values were calculated. The integral values were calculated from equation (4:56) in the way that for given values of D_a^0 and D_b^0, a table was written of the values of D_b/D_a as a function of D_a/D_a^0 (in steps of 0.01) and x (in step of 0.1).

The range of variation was usually $1 < D_a/D_a^0 < 3.5$ and $0 < x < 3$. These tables were printed by the computer and give the function (4:56) in the same way as for example Figure 6. The tables are not attached, as they would require too much space, but as an example, one page of each of the tables for $D_a^0 = 1003$ Å and $D_b^0 = 2175$ Å and for $D_a^0 = 1100$ Å and $D_b^0 = 2175$ Å (alternative values for D_a^0, Appendix 8). The computer program (FKHDP1) is also enclosed in Appendix 7. The curve for $D_a^0 = 1003$ Å and $D_b^0 = 2175$ Å is given in Figure 26 with some plotted test results.

Differential values for x were calculated by fitting a parable to the function $D_b = f(D_a)$ according to least squares method as specified in section 4.3.2, and x was calculated from equation (4:62). To get comparable values for the same seed, the parabola was forced through the point (D_a^0, D_b^0). The fitting was made using the CURFIT subroutine in the program library at the NTH computing center (17). The program is enclosed in Appendix 7 (Program Name: XBER).

From the theoretical expressions derived in section 4.3.4, one could calculate D_b as a function of D_a and the corresponding differential values of x. The method described in the same location was used, and the values for D_p, k_{tp}, ρ^w, diameters and particle numbers were varied to some extent. This calculation was also done on a computer and the program, FKHTEO, is enclosed in Appendix 7.

This program was extended and modified by Lervik (15) for calculation after the extended theory given in section 4.3.6 (different kinds of radicals). Due to difficulties with solving the linear equation system (library program), the execution of the program at this time of writing is still somewhat uncertain (need for debugging).

To show the experimental relationship between the exponent x and the variables in the experiment (D_a, D_b, N_a^w, N_b^w) a regression analysis was performed where x was assumed to be a linear function of the four variables. The library program REGANA (18) was used, which itself provides data input and prints results.

(A notice for present day readers: At the time of execution of this thesis, 1970, programs and data were read from punched cards and all computing done on a mainframe computer. The results were printed on paper by the computer. All runs were done in batch. The programming language used in this thesis was ALGOL66).

7 Results

Section 7.1 and 7.2 give results from the experiments with the production of seed and soap titration that are related to the experimental performance of the work and are believed to be of interest in this connection. The actual results from competitive growth experiments and the calculations are given in section 7.3.

7.1 Preparation of seed

The experiments include B-1 - B-8, additionally V-16 and F-200. The conditions are given in section 6.3.2 (Table VI). The results are given in Table IX below (in the order they are performed).

Exp.	Reac. time (min)	Conv. at end (g/L)	Diam. at end (Å)	Spread. σ (Å)	Spread σ (%)	N^w x 10^{-16} (L^{-1})	Ar x 10^{-23} ($Å^2$/L)
V-16	280	379	1870	144	7.74	7.85	8.57
B-1	320	434	2472**	199	8.09	3.89	7 .42
B-2		705	1764	137	84	17.36	16.90
B-3	100	61	1003	72	7.23	8.19	2.55
B-4	434	692	precip.	-	-	-	-
B-5	100	60	ca. 1000	-	-	-	-
B-6*	350	449	2175	132	6.07	5.93	8.76
B-7	350	423	2321	147	6.37	4.58	7.72
B-9	100	59	1240	79	6.37	4.17	2.01
F-200	340	444	2391	156	6.56	4.40	7.86

Table IX.

* - Before adding emulsifier dissolved in water

** - Probably too high because of under-focusing images. Particle numbers and surfaces are therefore also uncertain.

All values are given before dialysis. For data for seed after dialysis, see Table VII, section 6.3.3. In some of the experiments, a pressure samples were taken during the run. The data for these are given in Table X below.

Figures 13 and 14 show images of typical seed latexes (B-3 and B-7). In Figure 15, the kinetics curves for the tests V-16, B-1, B-4, and B-6 are plotted. The other experiments follow

the B-4 curve up to the given conversion (B-4 and B-6 also follow the same curve). B-4 gave a "max" start after approximately 390 minutes of reaction time and the latex coagulated immediately after this time. The conversion as a function of time in the experiments where it was measured is given in Appendix 2 and the results of the particle measurements in Appendix 12.

Exp./ sample	Reac.time (min.)	Conv. (g/L)	Diam. (Å)	Spread (Å)	Spread (%)	N^w x10^{-16} (L^{-1})	Ar x10^{-23} ($Å^2$/L)
V-16/1	203	195	1552	102	6,59	7,06	5,32
B-1/1	218	212	1257	80	6,39	14,47	7,15
B-4/1	350	450	2077	133	6,41	6,80	9,18

Table X

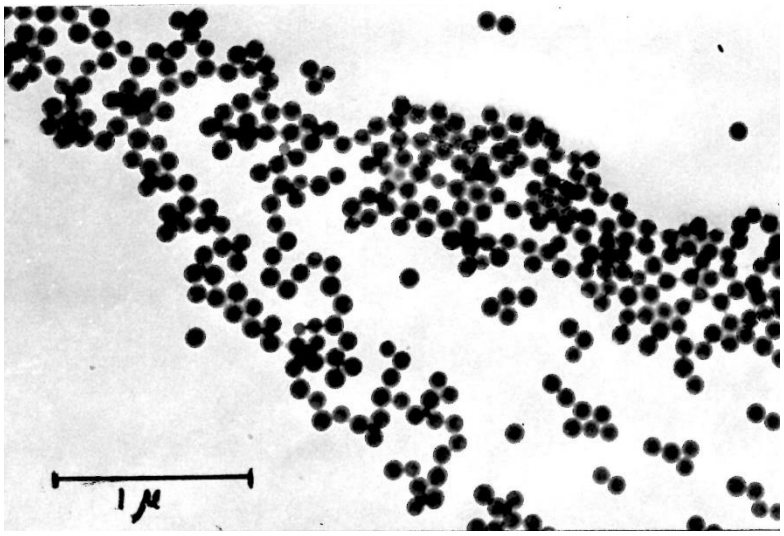

Figure 13

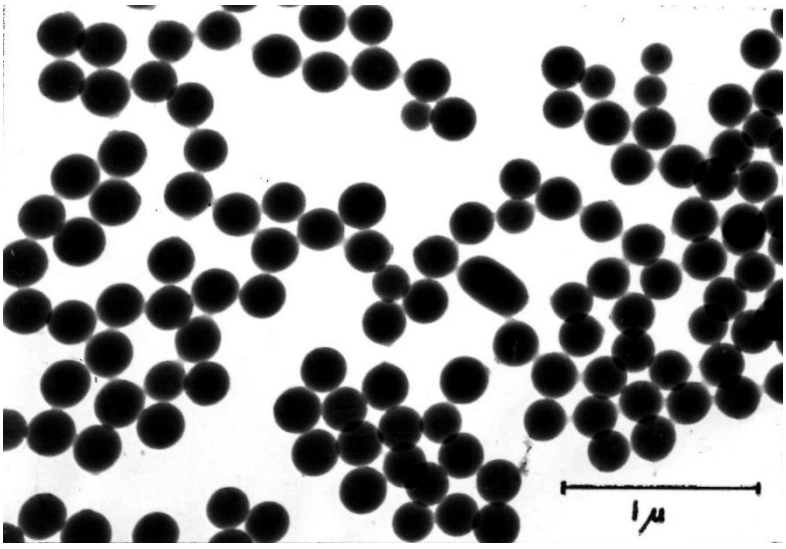

Figure 14

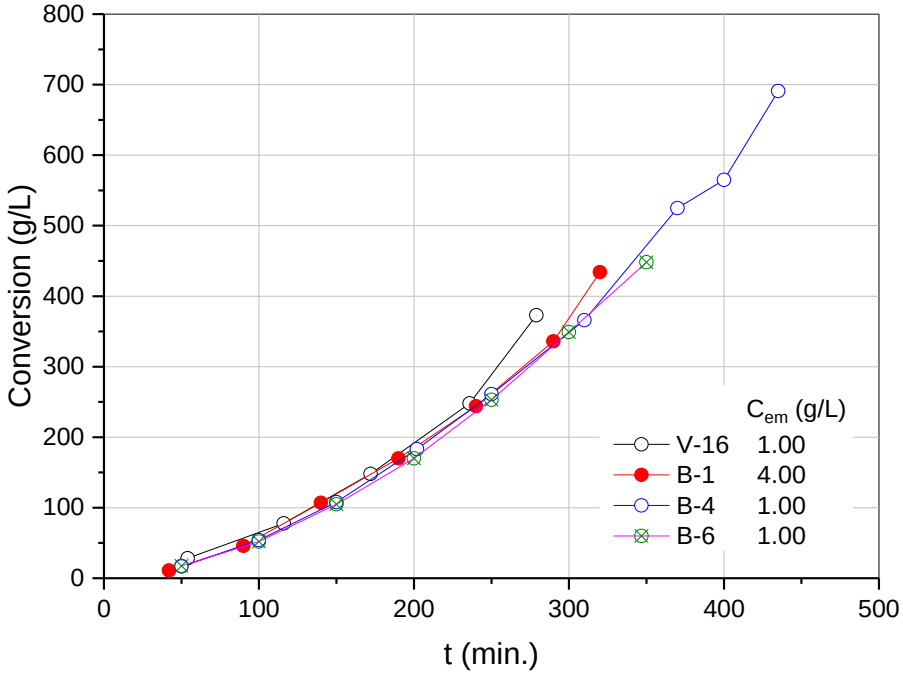

Figure 15. Preparation of seed. Conversion as a function of time during normal polymerization. Variation of the amount of emulsifier. Emulsifier: Sodium octyl sulfate, initiator concentration 6.0 10^{-3} mol/L H_2O

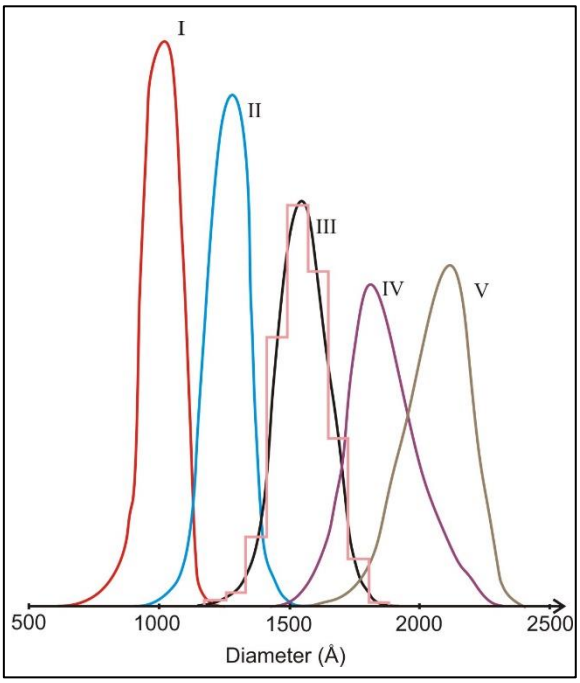

Figure 16. Distribution curves from seed production experiments.

Curve no	Exp.	Time (min)	Conv. (g/L)	$C_{em.}$ (g/L)	Com.
I	B-3	100	60	1.00	Bef. max
II	B-1	218	211	4.00	Press. samp.
III	V-16	203	195	1.00	Press. samp.
IV	V-16	279	373	1.00	End samp.
V	B-4	350	450	1.00	Press. samp.

Some of the distribution curves from the experiments are shown in Figure 16. To show the width of the measurement intervals and the method of drawing of the distribution curves, the histogram is entered for experiment V-16, sample 1 (curve III). To facilitate the overview,

this is not done for the other curves. All curves are measured at the same image magnification (24000x).

7.2 Soap titration, surface coverage

Some of the seed latexes were soap titrated as explained in section 6.4.3. Titration curves and forms are shown in Appendix 3.1. The titrations gave the following result:

Experiment	S_a x 10^5 (mol/gPVC)	S_a' x 10^5 (mol/gPVC)	D_s (Å)	N^w_s x 10^{-16} (L^{-1})
B-1	10.8	6.9	1320	26
B-2	8.8	6.4	1610	26
B-3	20.2	11.5	700	24
B-3 d	-	11.2	-	-
B-7 d	6.10	5.03	-	-
V-FT	15.5	14.8	-	-
V-FT m	22.0	14.0	-	-
V-FT m*	21.7	13.7	-	-
F-200	-	6.20	-	-
F-200 **	-	3.30	-	-
F-200 d	-	4.25	-	-

Table XI

d - Dialyzed

m - Added sodium octyl sulfate

* - After 6 weeks

** - After addition of emulsifier to stabilize the latex

S_a' – Added amulsifier t0 100 % coverage in totration

D_s is calculated from = 50 $Å^2$/molecule

V-FT is the name of the experiment with the addition of sodium octyl sulfate to a latex, see section 6.4.2 and Appendix 3.3.

7.3 Competitive growth

A total of 15 experiments were made with competing growth. The experimental conditions for these are given in Section 6.3.3. Experiments B-11 and B-12 were run with seed latex B-7 (large particles) after it had coagulated (creamy consistency), and these resulted in the formation of new particles. No measurements were made on images from these experiments (only images were created to show the new formation). Figure 17 shows typical images from experiments with competitive growth (experiment B-10), and Figure 18 shows images from the experiments that gave new nucleation (somewhat after start and at the end).

The kinetics curves for the competitive growth experiments are given in Figures 19, 20, 21 and 22. Data are given in tabular form in Appendix 5.

Tables of results are given in Appendix 6, while printouts of the individual counts are given in Appendix 13. As the diameter of the small particles at start (D_a^0) was somewhat uncertain, the results are calculated for two value sets of D_a^0, 1003 Å on B-3+5 and 1150 Å of B-MIX, respectively 1100 Å and 1200 Å (calculation of B-MIX, see Appendix 4.4). See also section 8.4.

The diameters (D_b as a function of D_a) are given in Figures 23, 24 and 25 for the experiments with three different seed mixtures. The reaction time is thus eliminated. This is given in the tables in Appendix 6.

Figure 26 gives the reference curves for D_b/D_a as a function of D_a/D_a^0 and x according to equation (4:56) for seed B-3+5 (1003 Å) and B-6 (2175 Å) in the same manner as given by Vanderhoff et al. (4), (5). In comparison with their results, points have been inserted for experiment B-13. The values for x calculated in this way are given in Figure 28. For the various experiments, such integral values of x are given in Figures 27, 28, 29 and 30. For all experiments in the one figure, the same seed latexes are used. For experiments B-13 - B-18, x is calculated and drawn for two alternate values of D_a^0, 1003 Å and 1100 Å (Figures 28 and 29). See also section 8. For the experiments B-19 - F-206, as mentioned, x was calculated for two values for D_a^0. As the difference here is smaller (50 Å), the largest values of D_a^0 (1200 Å) are not plotted (see Appendix 6).

Differential values for x are given for most experiments in Figures 31, 32 and 33. Figures 31 and 32 show the differential values from experiments B-13 - B-18 for the two alternative D_a^0, 1003 Å and 1100 Å while Figure 33 shows values from experiments B-19 - F-206 with D_a^0 = 1150 Å. Values for D_a^0 = 1200 Å and for experiments B-9 and B-10 are given together with the other values in Appendix 9.

Figures 34, 35 and 36 show values of x (differential) calculated from the theoretical derivations in section 4.3.4 as explained in section 6.5. By using this program (FKHTEO), one may, if desired, vary all parameters, both constants and experimental variables. Figure 34 shows how the variation of some of the constants affects x at experimental conditions corresponding to run B-13. The increase of ρ^w corresponds to multiplication of 3.4, which corresponds to the effect of vinyl chloride at the disintegration rate of the initiator. k_{tp} = 2.8

10^8 L/mole s equals a value of 5 10^{-13} L/mole. h (multiplied by 3.4) used by Ugelstad et al. (2). k_{tp} = 3.6 10^8 L/mole s is a corrected value used by Ugelstad et al. in later work. The value D_p = 2 10^{-11} L/mole s is the most likely value of this constant. See also section 8. Figure 35 shows the variation in x by variation in the experimental conditions corresponding to experiments B-13 - B-16. The figure also shows how x changes when it is assumed that the absorption rate is proportional to the particle surface instead of the particle radius. Figure 36 shows how a variation of D_b affects x when V_{pb}^0 is constant. This could, for example, be due to coagulation of large particles (see also section 8).

(In Figure 24, D_b as a function of D_a is plotted for two different D_a^0 and different D_p to directly compare the diameters. Further calculated values for the diameters and x together with $\bar{n}_a$ and $\bar{n}_b$ are given in Appendix 11) (not shown here).

The regression analysis gave the following correlation between x and experimental variables:

Experiment B-13 - B-18

I: D_a^0 = 1003 Å, D_b^0 = 2175 Å

$$x = 1{,}43 - 6.72\ 10^{-4}\ D_a + 6.06\ 10^{-4}\ D_b + 4.05\ 10^{-18}\ N_a^w + 3.09\ 10^{-17}\ N_b^w \qquad (7{:}1)$$

II: D_a^0 = 1100 Å, D_b^0 = 2175 Å

$$x = 2{,}04 - 6.97\ 10^{-4}\ D_a + 4.92\ 10^{-4}\ D_b + 6.24\ 10^{-18}\ N_a^w + 3.80\ 10^{-17}\ N_b^w \qquad (7{:}2)$$

The full printouts with correlation coefficients, F levels, etc. are given in Appendix 10. For documentation, see (18).

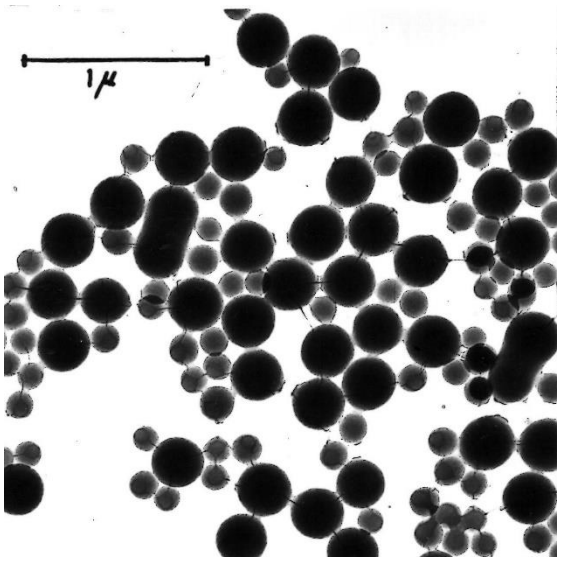

90 min

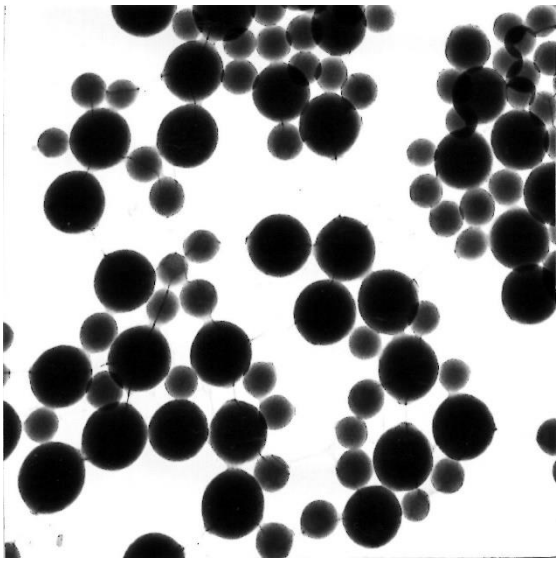

170 min

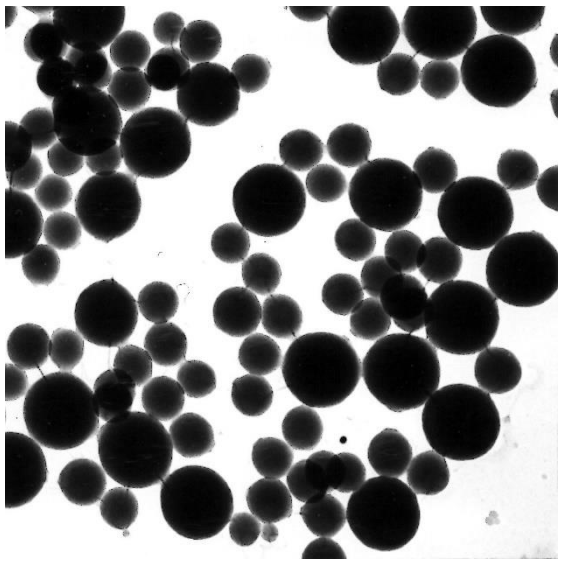

250min

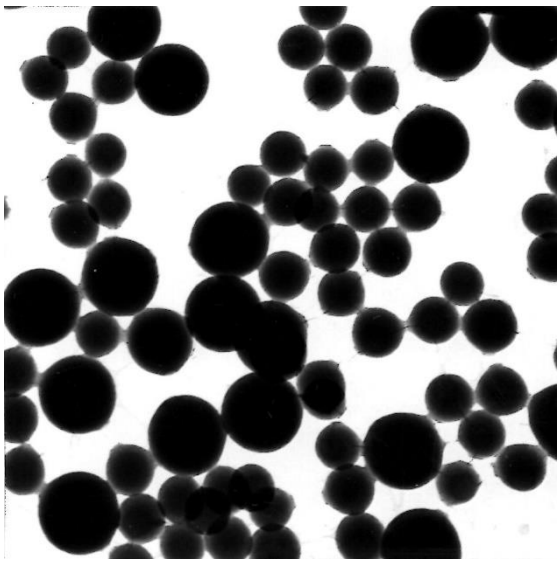

340 min

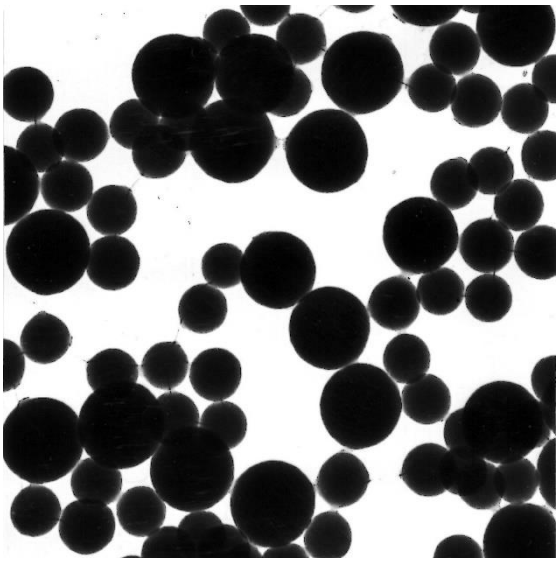

430 min

Figure 17

Example of images from competitive growth.

Experiment B-10

Magnification 24000x

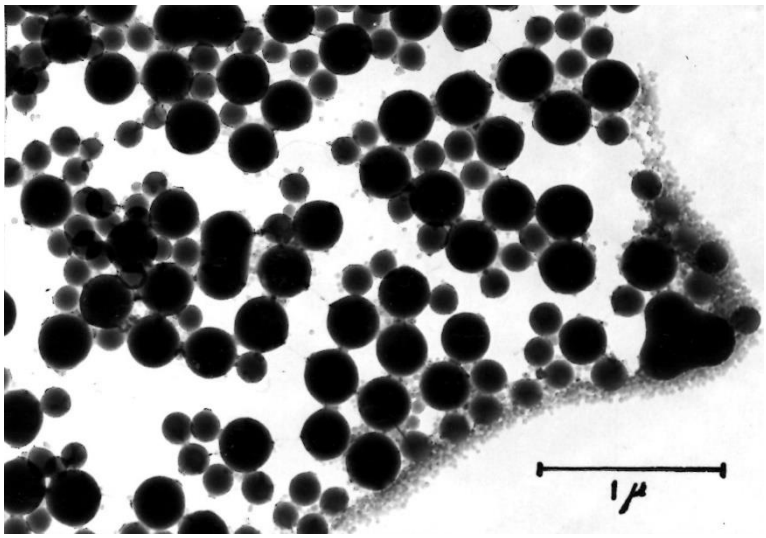

B11/1 90 min.

Figure 18

New formation in seed experiments.

Magnification 24000x

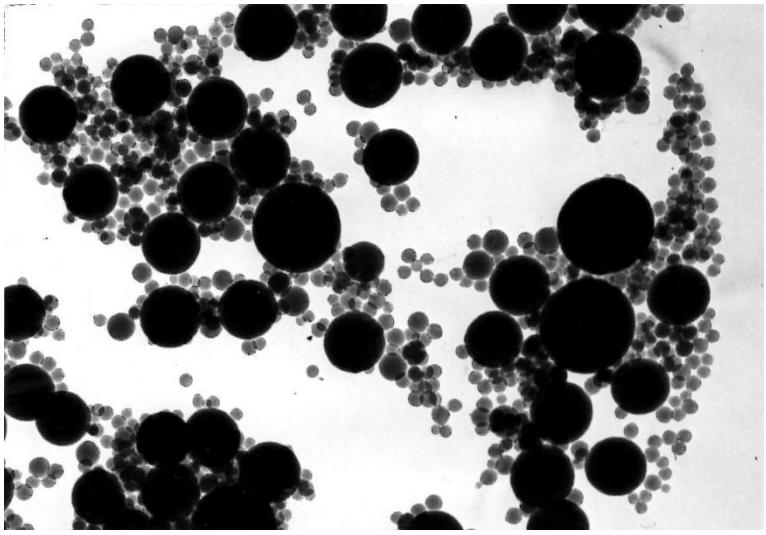

B12/5 420 min.

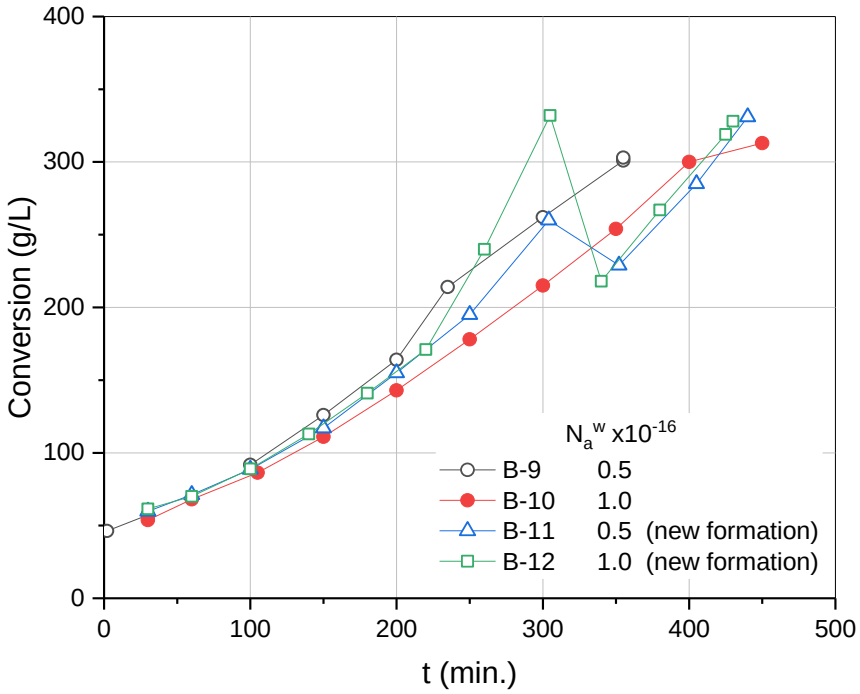

Figure 19. Kinetics of competitive growth at two different particle numbers and ratios. Effect of new formation on conversion curve. Seed B-3+5 og B-7.
N_b^w = 0.5 x10^{16} L^{-1}, C_i = 3.0 10^{-3} mol/L.

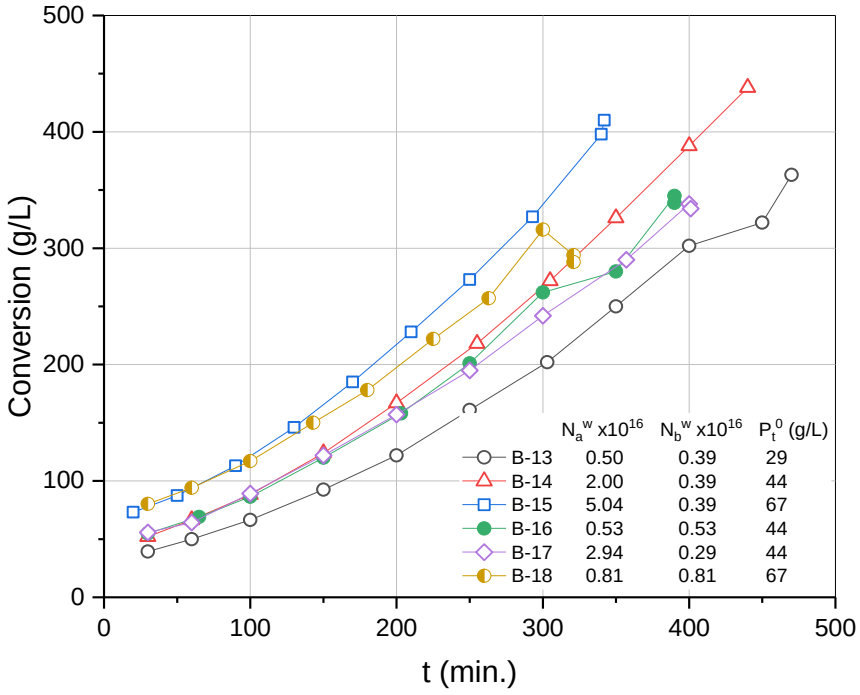

Figure 20. Kinetics of competitive growth at varying particle numbers and ratios. Seed B-3+5 and B-6. C_i = 3.0 10^{-3} mol/L.

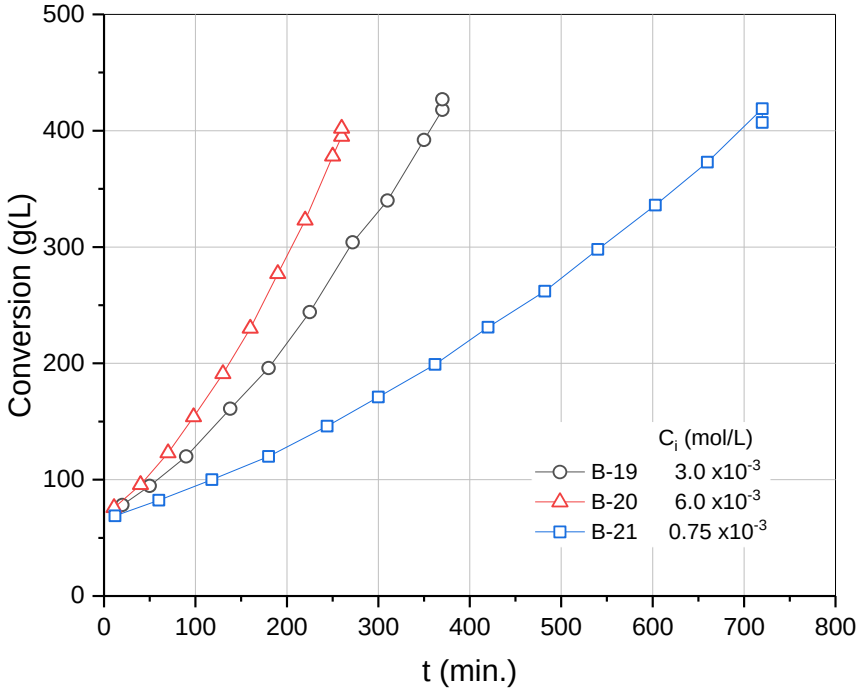

Figure 21. Kinetics of competitive growth. Effect of initiator concentration. Seed B-MIX og F-200.

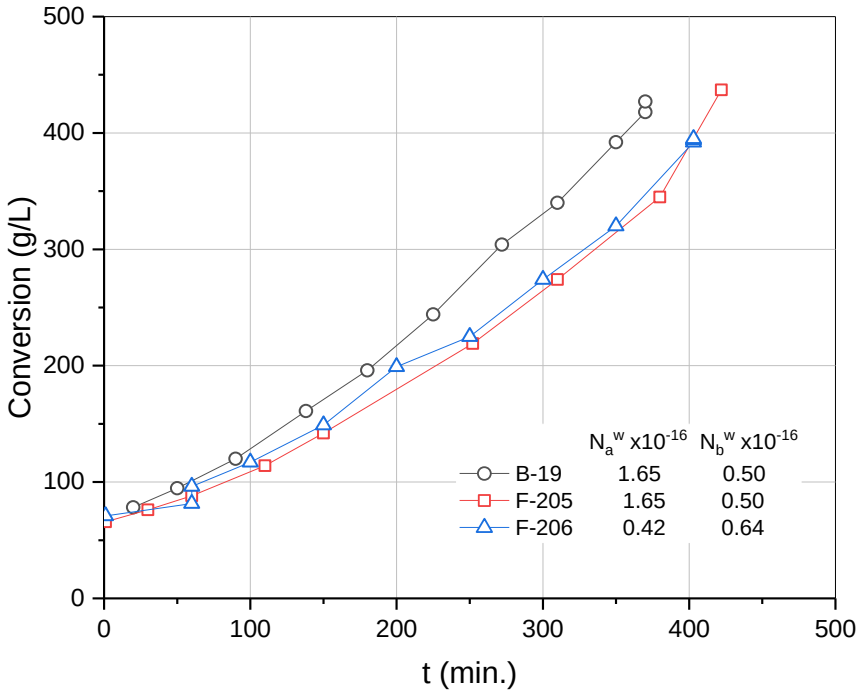

Figure 22. Kinetics of competitive growth. Effect of fatty alcohol. Seed B-MIX og F-200. C_i = 3.0 x10^{-3} mol/L, P_t^0 = 69 g/L.

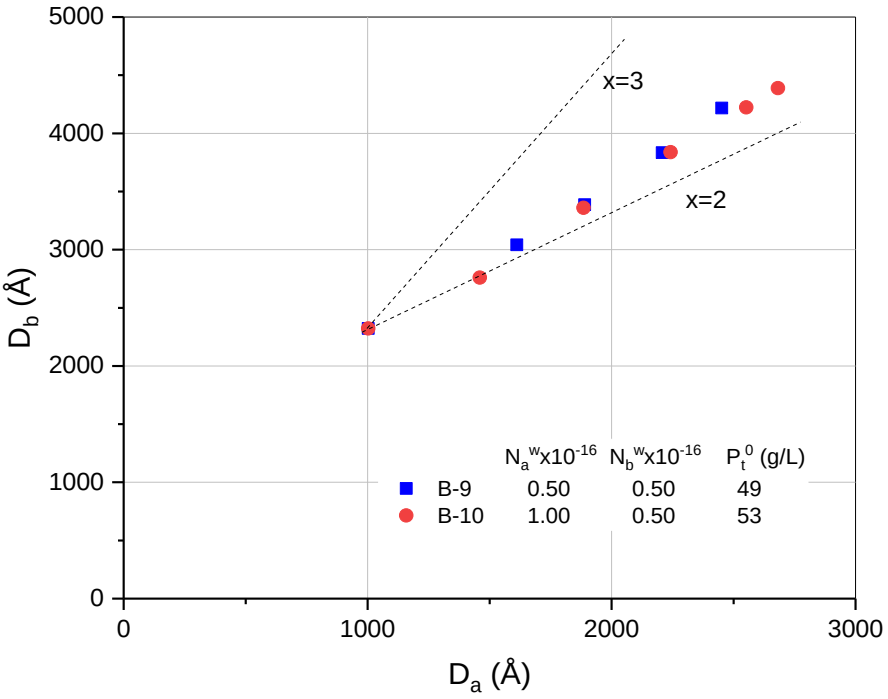

Figure 23. Diameter of large particles as a function of diameter of small particles. For experiments B-9 and B-10. C_i = 3.0 10^{-3} mol/L. Theoretical lines for x=2 og x=3.

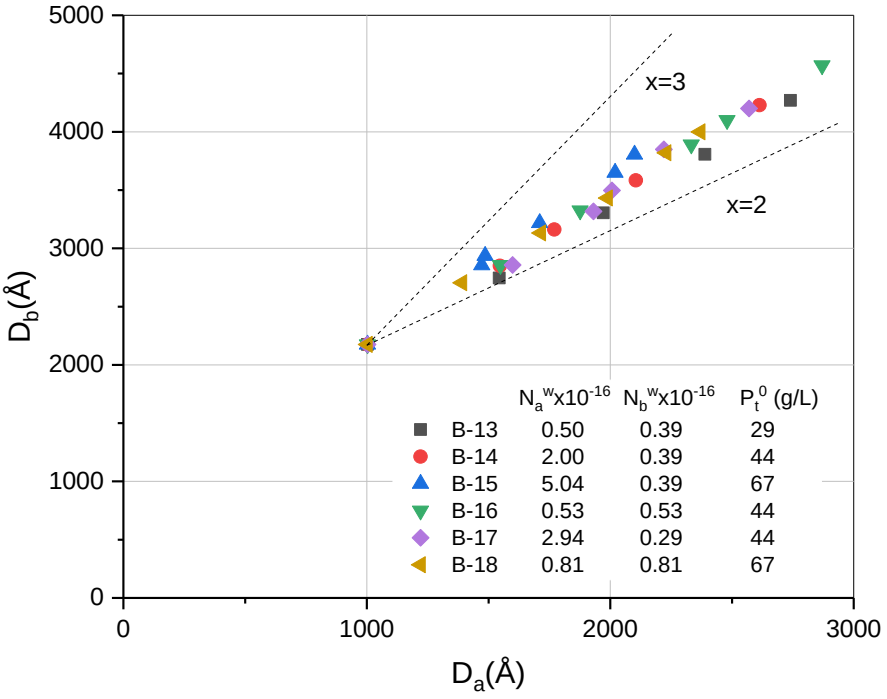

Figure 24. Diameter of large particles as a function of diameter of small particles at varying particle numbers and ratios. C_i = 3.0 10^{-3} mol/L. Theoretical lines for x=2 og x=3.

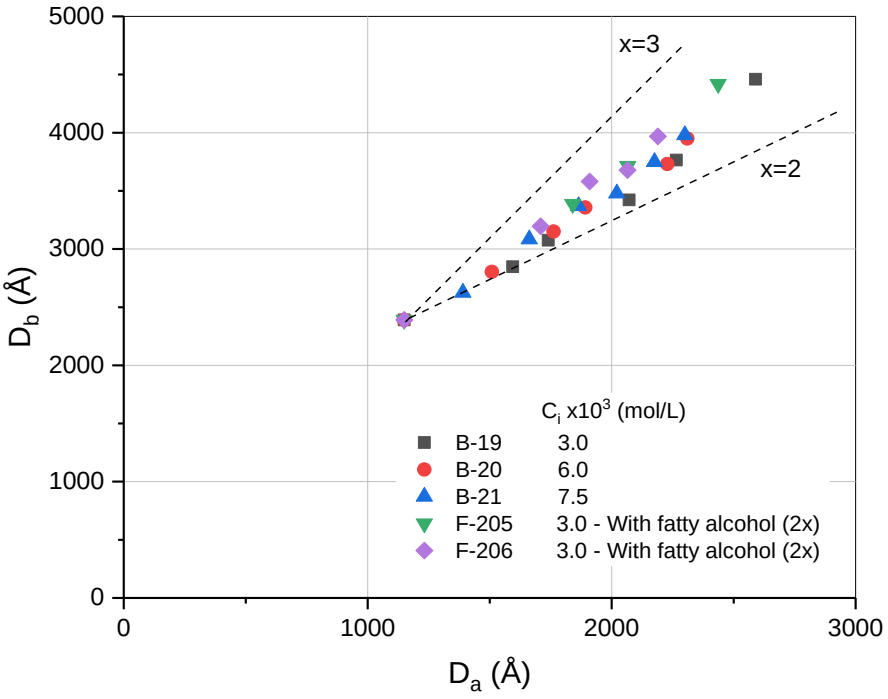

Figure 25. Diameter of large particles as a function of diameter of small particles at varying initiator concentration and experiments with fatty alcohol.

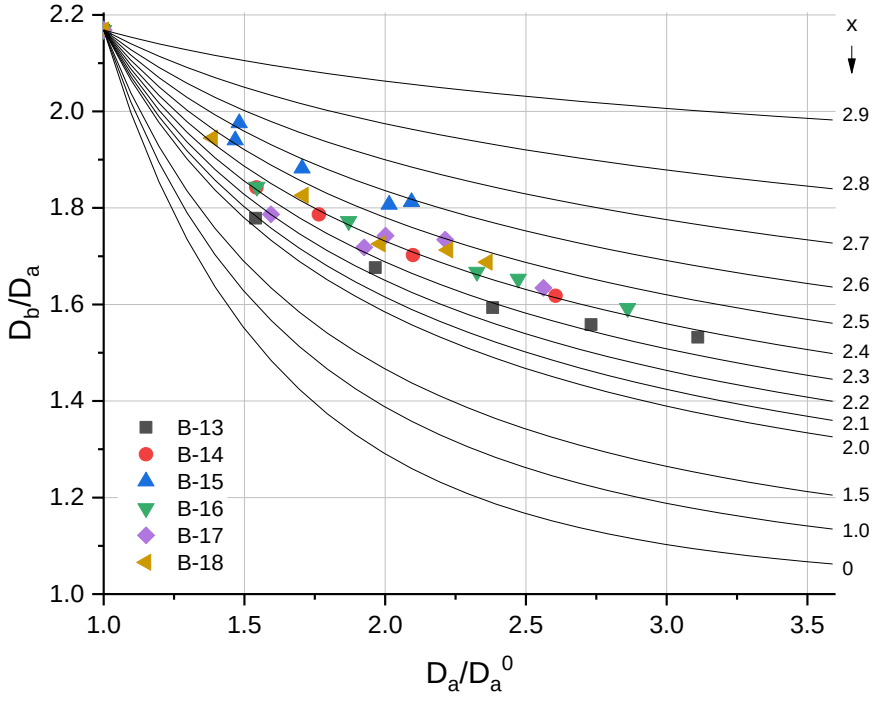

Figure 26. D_b/D_a as a function of D_a/D_a^o. Results from experiments B-13 - B-18 and theoretical reference curves for different x from equation (4:56). Variation of particle numbers and ratios. Seed a: B-3 + 5, seed b: B-6.

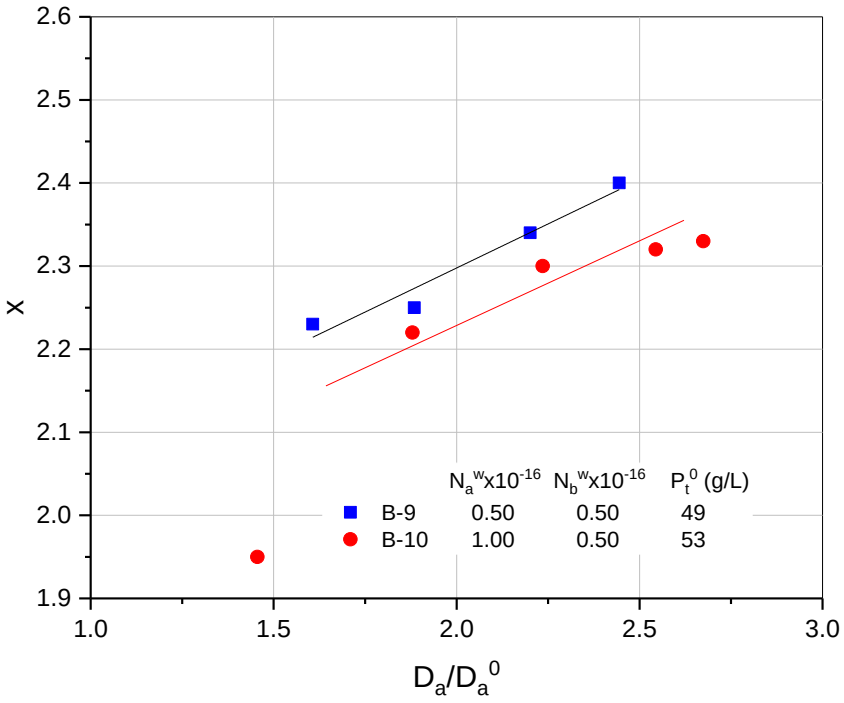

Figure 27. The exponent x as function of D_a/D_a^0 for experiments B-9 and B-10. Seed a: B-3+5, seed b: B-7. C_i = 3.0 10^{-3} mol/L.

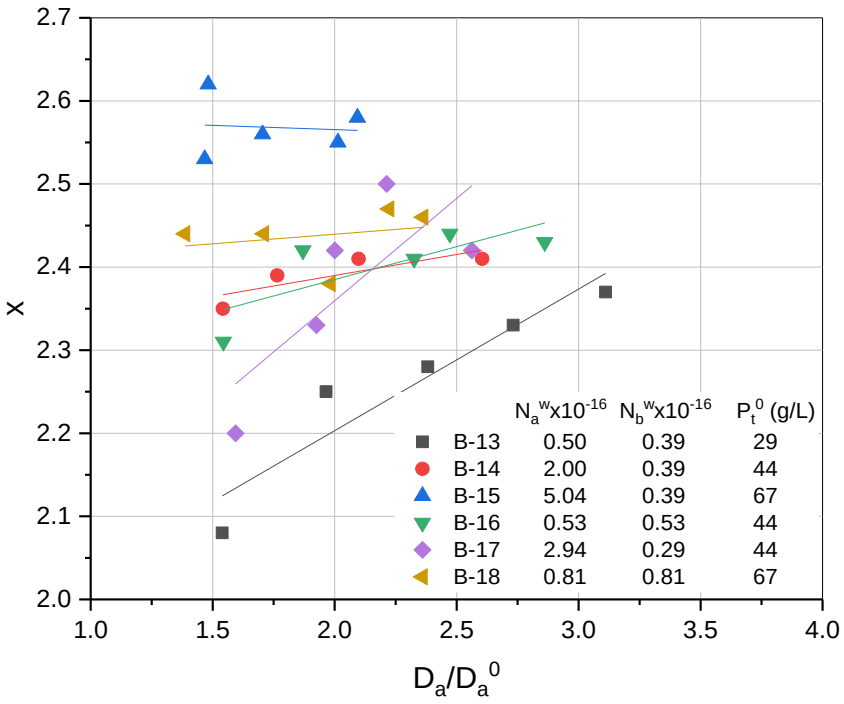

Figure 28. The exponent x as function of D_a/D_a^0 for experiments B-13 - B-18 with varying particle number and ratios. Seed a: B-3+5 med D_a^0 = 1003 Å, seed b: B-6 (2175Å). C_i = 3.0 10^{-3} mol/L.

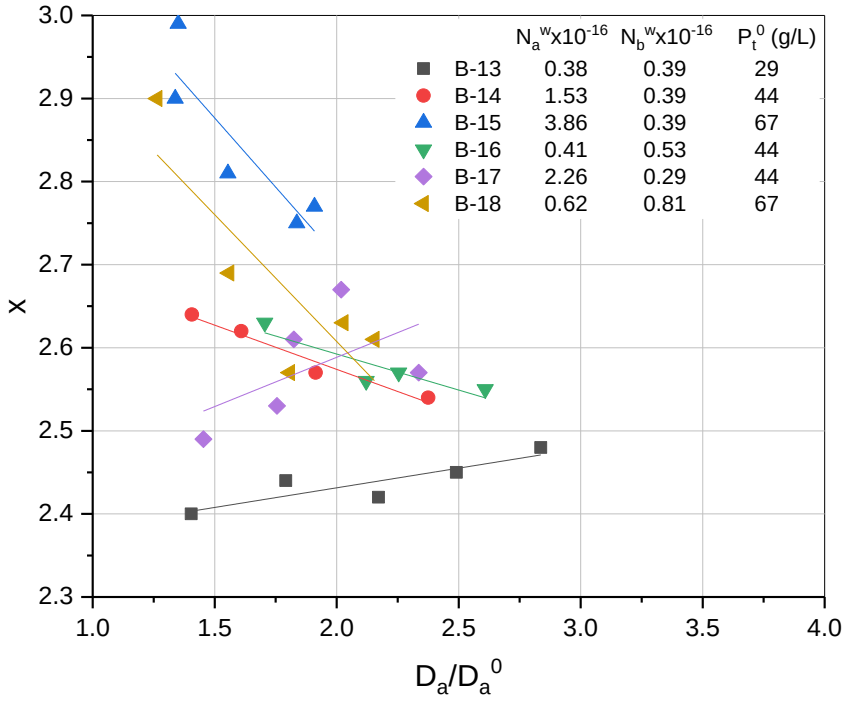

Figure 29. The exponent x as function of D_a/D_a^0 for experiments B-13 - B-18 with varying particle number and ratios. Seed a: B-3+5 med D_a^0 = 1100 Å, seed b: B-6 (2175Å). C_i = 3.0 10^{-3} mol/L

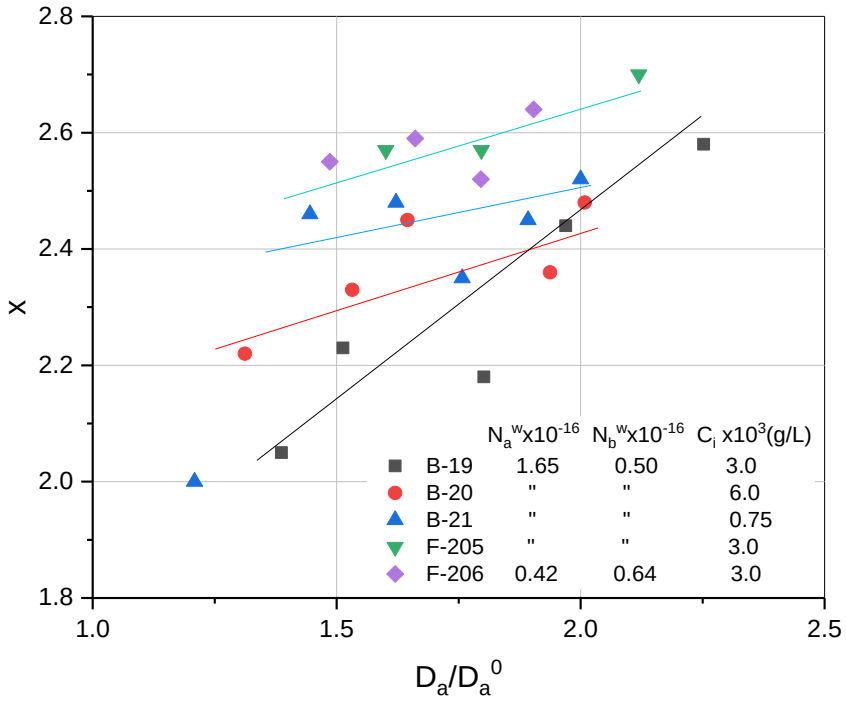

Figure 30. The exponent x as function of D_a/D_a^0 for experiments with varying initiator concentration and with fatty alcohol (2X). Seed a: B-MIX, seed b: F-200. P_t^0 = 69 g/L

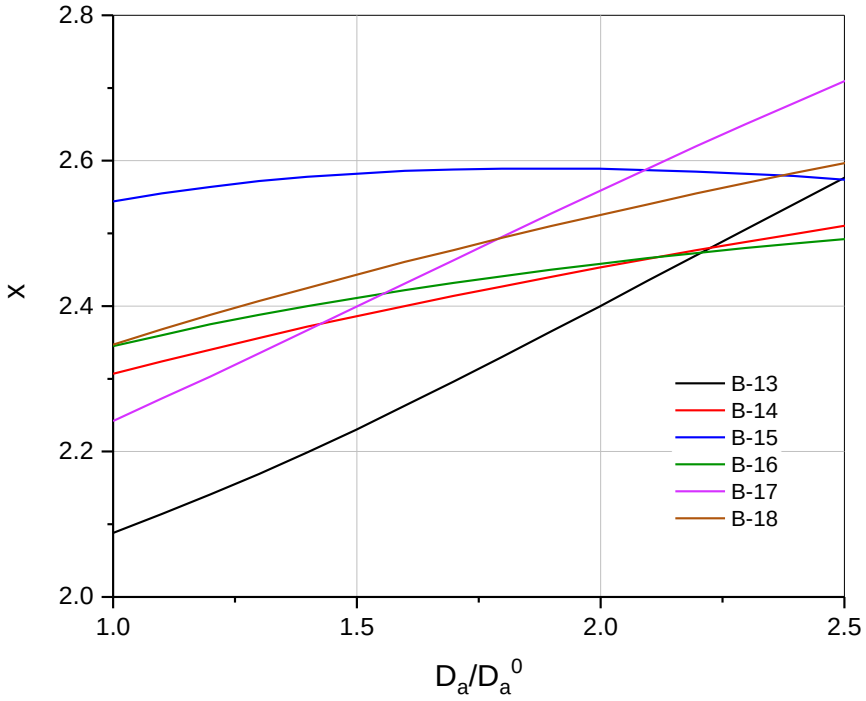

Figure 31. Differential values of the exponent x for experiments with varying particle numbers and ratios. Calculated by fitting parables to experimental data. Seed a: B-3+5 with D_a^0 = 1003Å, Seed b: B-6 (2175Å).

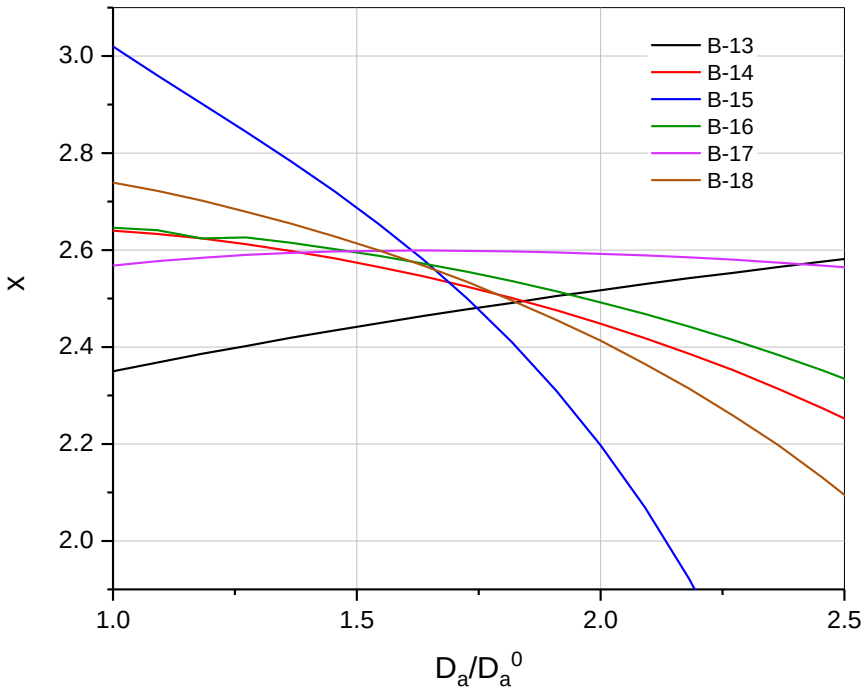

Figure 32. Differential values of the exponent x for experiments with varying particle numbers and ratios. Calculated by fitting parables to experimental data. Seed a: B-3+5 with D_a^0 = 1100 Å, Seed b: B-6 (2175Å).

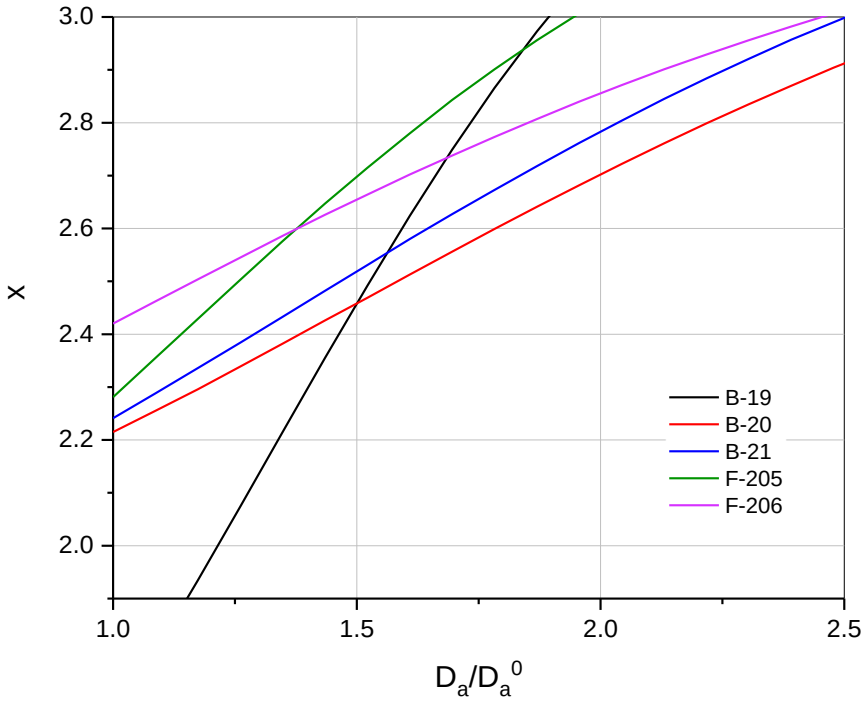

Figure 33. Differential values of the exponent x for experiments with varying particle numbers and ratios. Calculated by fitting parables to experimental data. Seed a: B-MIX (1150Å), Seed b: F-200 (2390 Å).

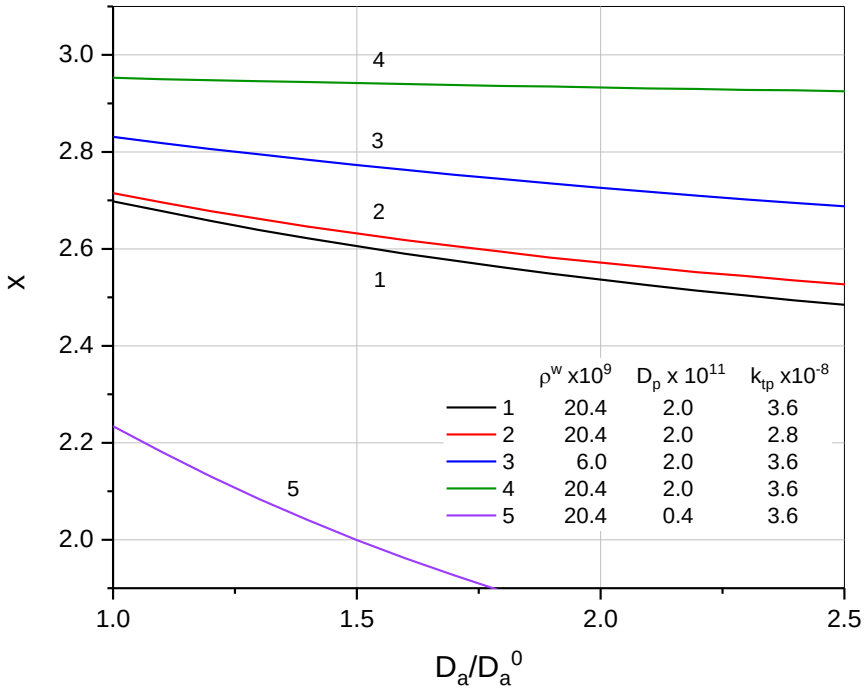

Figure 34.Technical curves for the exponent x as a function of D_a/D_a^0 calculated from Bessel functions. Variation of the constants at the same particle diameter and number as in experiment B-13. D_a^0 = 1003Å, D_b^0=2175Å, N_a^w= 5.0 10^{15} part./L, N_b^w= 3.9 10^{15} part./L Dimensions: ρ^w[=]mol/L s, D_p[=]dm^2/s, k_{tp}[=]L/mol s.

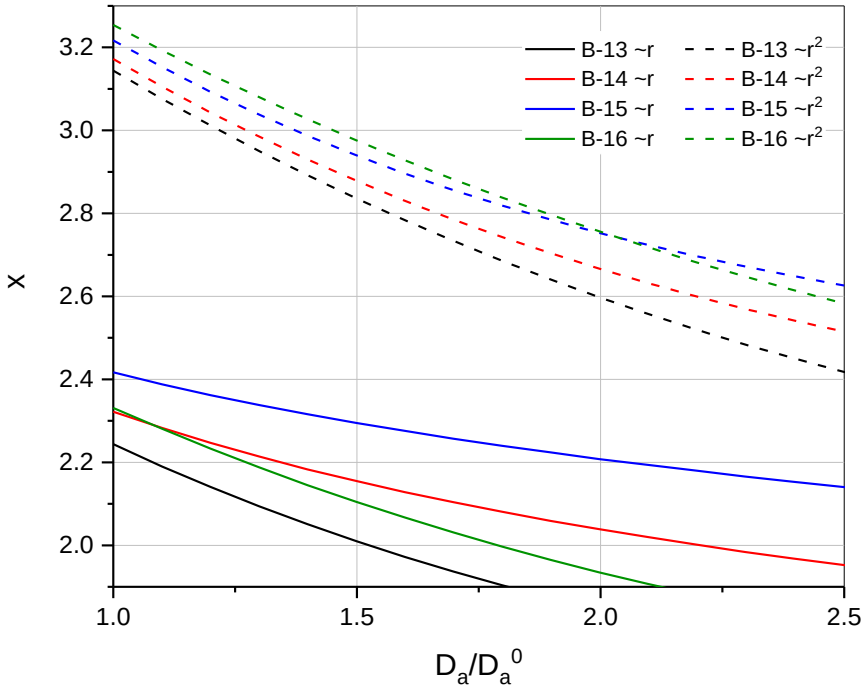

Figure 35. Theoretical curves for the exponent x as a function of D_a/D_a^0 calculated from Bessel functions. Variation of constants at particle numbers and ratios by the rate of absorption proportional to the radius and the surface. Corresponding conditions as in experiments B-13 - B-16. $\rho^w = 20.4\ 10^{-9}$ mol/L s, $D_p = 0.4\ 10^{-9}$ dm^2/s, $k_{tp} = 3.6\ 10^8$ L/mol s.

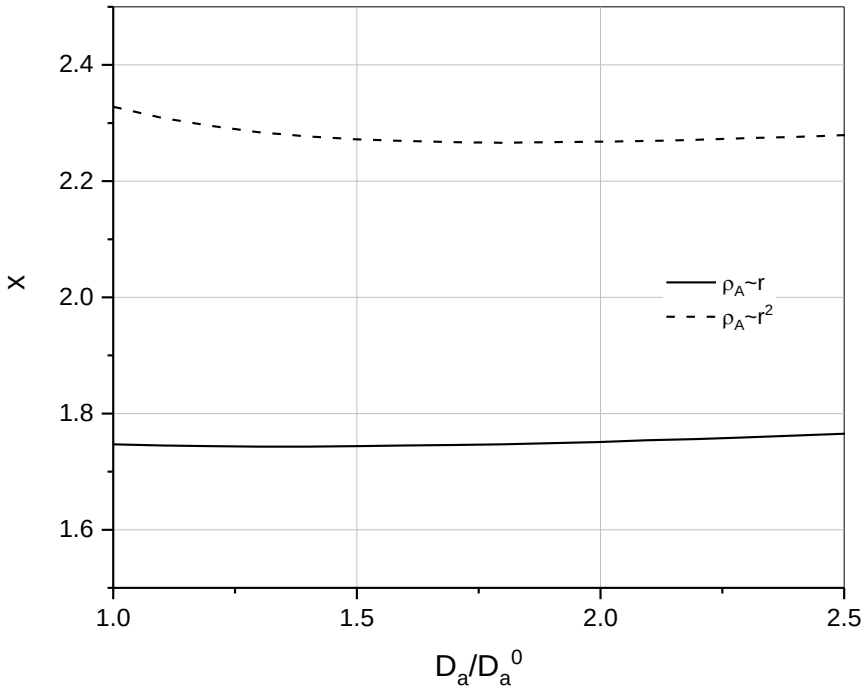

Figure 36. Theoretic curves for the exponent x as a function of D_a/D_a^0 calculated from Bessel functions. Variation of the diameter of large particles at constant total particle volume. Effect of the absorption rate dependence on the particle radius.
$D_a^0 = 1003$ Å, $D_b^0 = 21750$ Å, $N_a^w = 5.3\ 10^{15}$ part./L, $N_b^w = 5.3\ 10^{12}$ part./L

8 Error calculations and discussion

8.1 Kinetics curves

8.1.1 Error calculation

In the method used to determine the PVC content of the latex during the reaction, there are many sources of error of different importance; weighing errors are in the weight of empty beaker, in the weight of glass with latex and in the weight of glass with PVC (+ additives). The actual reading uncertainty on the weight (± 0.5 mg) is insignificant with the weights involved here (> 1 g) and reproducibility is good (better than ± 1 mg). At the sampling there is always some latex left in the valve from the previous sample. The significance of this error is difficult to estimate and will vary, but it hardly accounts for more than about 0.1% of P_t (leading to a lower P_t). Remaining vinyl chloride in the sample before drying will give a somewhat lower P_t (equation 6:1) but this is hardly significant. The main sources of error will be the evaporation of water from the samples and possible incomplete drying. This last can be avoided by weighing the samples several times after successive drying. Experiments showed that this does not matter when the results appear reasonable and the samples appear to be completely dry (at least 3 hours at 65 °C for small samples (1-2 g), longer for larger samples). Contamination of the sample and test tube is considered to be insignificant for most samples, but may lead to random major deviations in P_t. This might be seen in the conversion curve.

Evaporation of water from the sample already begins as the sample is removed and continues until the sample is dried. The water that evaporates until the wet sample is weighed (P_1) will cause a systematic error in P_t (too high P_t). Until the samples have been removed from the heating cabinet (50 °C), this error will be approximately the same on all samples (absolute). As the samples are left to cool for different periods, different amounts of water will evaporate. The error in P_t will have the same sign for all the samples, so that the uncertainty in P_t (standard deviation) when calculating the rate curves becomes less than the real error. However, the curve will be offset against higher values of P_t. When weighing a sample beaker, lid is removed, and this results in a faster evaporation. A vaporization rate of 1.4 mg H_2O/min. at 25 °C (150 ml beaker) was found. Some water will be left on the lid, this was found to be about 1 mg. Weighing of all glasses with the lid could eliminate this last error.

Even with lid, some water will evaporate. This was measured by placing a glass of sample and lid on the weight (with both glass doors open) and was weighed at regular intervals for 1/2 hour (17 °C). This gave a vaporization rate of 40 mg H_2O/hour. Assuming that the greatest difference in the cooling time of the glasses is 1 hour, $\Delta P_1 = 0.04$ g. Upon repeated drying, $\Delta P \approx 0.004$ g was found. Partial derivation gives:

$$\Delta P_t = \left[\left(\frac{P_t}{P_1 - P_2} \Delta P_1 \right)^2 + \left(\frac{P_1 - P_0}{(P_1 - P_2)^2} \Delta P_2 \right)^2 \right]^{\frac{1}{2}} \qquad (8:1)$$

when we set $\Delta P_0=0$ and disregard errors in weighed addition amounts. With values for P_1= 66 g, P_2=61 g and P_0=60 g (common values) we get:

P_t = 200 g/L and $\underline{\Delta P_t = 2 \text{ g/L}}$

ΔP_2 can be anticipated is due to weak hygroscopic properties of the PVC particles. ΔP_t calculated from this is therefore not so large, it will also decrease with P_t.

Some points on the rate curves may differ more than this from the smooth curve. One assumes that this is due to random conditions such as fowling (lumps) in the latex, contamination of the sample and the like. By fitting the rate curve a parable by least squares method, one could calculate the standard deviation of P_t, as the fit with smooth curves became very good. The standard deviation was usually found to be about 1 g/L, that is, somewhat less than ΔP^t, but of the same order of magnitude. (The program and printouts are not attached, as the program was also used for other calculations not included in this report).

8.1.2 Kinetics with new nucleation

The kinetics curves, both in normal experiments and in competitive growth, usually become even and smooth, as ΔP_t as seen is relatively small (except for some random major deviations). However, in experiments that gave new formation (B-11 and B-12) the kinetic curves have a different course. As seen in Figure 19, the curves follow the approximate course of B-9 up to 200-250 g PVC/L H_2O. Thereafter, the course is then uncertain (two of the samples from B-12 seem unusually high) until approx. 350 g PVC / L H_2O. Then the curve has sunk down to another level, and then looks again to have a steady rise. This tendency can hardly be due to errors in the sampling, as experiments B-11 and B-12 gave the same result. For obvious reasons, the solids content in the total latex cannot decrease, so that it must be the samples giving a lower result than the total solids content of the latex.

A possible explanation for this may be that the formation of new particles leads to the coagulation of a part of the latex due to the fact that the surface coverage of emulsifier becomes very low when the new particles have reached a certain size (large surface area per liter of water). The part of the latex that has coagulated can therefore be flung out against the wall of the autoclave (low effect of the flow breakers). In the middle of the bottom of the autoclave where the sample is taken, there will be less solids than the average of the latex and the measured conversion becomes too low. It appeared that the amount that was precipitated then did not increase significantly, as the conversion again increased relatively smoothly. The final latex from B-11 and B-12 also showed a very strong lump formation. It is possible that it is the large particles that mostly coagulates, as it appears to be very few particles on the images (see Figure 18, B-12/5). The ratio at start was 2: 1 between the number of small and

large particles. However, this cannot be said with certainty, as the preparation for microscopy may possibly shift the relationship somewhat.

An alternative explanation may be that even if the centrifugal force from the stirring may not cause a solids gradient in the reactor, large lumps will not get into the sample in any case, as the bottom valve opens very little when the samples are withdrawn (high pressure). Large lumps will hardly get through this opening.

8.1.3 Reproducibility, order

The experiments B-11 and B-12 are reproductions of B-9 and B-10, respectively. These were conducted to investigate the reproducibility of the experiments, especially as regards competitive growth, but also on overall rate. As both of these experiments gave new nucleation of particles, one had to switch to another large particle seed (B-6) and it was found that time did not allow further experiments to test reproducibility.

The aforementioned experiments were done especially because B-9 and B-10 clearly yielded deviant kinetics, although according to the results of previous workers (Ugelstad et al.) these should only differ insignificantly (twice as many small particles would yield a somewhat higher rate for B-10). Further experiments (B-13 ...) show that the B-10 curve is abnormally low and that B-9 probably has the correct course. The reason that B-10 was unusually slow may be possible errors in initiator amount, possible contamination or the like. The rate otherwise shows the same trend as one would expect (steady increase).

The experiments B-13 - B-18 show that the dependency of the rate on the particle number and volume is approximately the same as one would expect from the results of Ugelstad et al. for ordinary emulsion polymerizations (maximum order for V_p equal to ½ and for N_t^w equal to 1/6). Experiments B-13, B-14 and B-15 show a slight increase of dV_p/dt at the same V_{pt} when V_{pa}^0 increases and V_{pb}^0 is constant. The order regarding N_t^w is about 0.1. Experiments with the same V_{pt}^0, but with different particle ratios (i.e. different N_t^w) usually showed an increasing rate with increasing particle numbers. Here, one can compare the experiments B-15 with B-18 and B-14 with B-16 and B-17 (see Figure 20). B-15 and B-18, respectively B-14 and B-16, show an increasing rate with increasing N_t^w when V_{pt}^0 is constant. It should also be expected that B-17 would go faster than B-14, but the opposite was the result. This shows that the reproducibility of the experiments are sometimes poor, but is mostly good. The results with B-17 may have the same reason as B-10, although N_a^w/N_b^w here is completely different.

With variation in the initiator concentration (Figure 21) we see that the order with respect to the initiator is quite close to ½, as the rate increases by a factor of 1.4 when ρ^w is doubled, and by 2 when ρ^w is quadrupled. In the experiments with fatty alcohol (Figure 22), a decrease in speed is obtained in the same way as in other alcohol fatty tests carried out at the institute (personal communication). F-205 and F-206 have virtually the same rate (F-206 somewhat higher starting volume, although theoretically it should be the same, this may be due to the weighing).

When considering the kinetics curves, we see that the measurement points lie on a smooth curve almost all the way to the end of the reaction, but the last samples can give some varying values, especially too low. Special tests taken from the final latex show such a tendency. This is probably due to fouling during the polymerization. When sampling from the final latex, it was attempted to avoid lumps, resulting in a non-representative solids content (too low). However, samples containing such lumps showed too high values (B-14, Figure 20). It also seems that experiments with low N_a^w/N_b^w gave more fowling than experiments with higher ratios. This may be due to the fact that the large particles will have a higher tendency for agglomeration (orhokinetic agglomeration), as the images indicate (increasing N_a^w/N_b^w ratio). However, this can also be due to the preparation. The experiments with seed B-MIX and F-200 gave very little coagulation. This may be because the coverage of B-MIX is higher than 80% as mentioned in Appendix 4.2. It may also be due to the fact that F-200 was stabilized against coagulation by addition of additional emulsifier prior to dialysis. An initial coagulation of the seed latex may then be continued during polymerization despite the addition of extra emulsifier.

In order to investigate whether there was such a latex coagulation that led to new particle nucleation in experiments B-11 and B-12, this latex was photographed (by institute employees) with and without ultrasonic treatment and with and without added emulsifier. It was not found any significant difference to these images, but there were some larger lumps. It is also possible that the agglomerates are so large that they do not come on the grid during preparation. In any case, it is difficulty imagining any other reason that experiments B-11 and B-12 should cause new nucleation. It was also found some nucleation in experiment B-13, but it is believed that this is due to the fact that it is on the border of too low seed quantities (too low $N^w r$), as P_t^0 was only 29 g PVC/L H_2O.

8.2 Soap titration, surface coverage

8.2.1 Error calculation

The amount of sodium lauryl sulfate to be added to the latex to obtain a certain coverage is calculated from the soap titrations as mentioned in section 6.4.3. These titrations will have some uncertainty which gives an uncertainty in the sizes calculated from them. Possible sources of error are: Error in latex weighing, titration errors, measurement error of surface tensions, and evaporation of water from the sample during titration. Titration errors and measurement errors in the surface tension will cause an inaccurate determination of the break point and hence of C_a. One can also get systematic errors due to inaccurate concentration of the titration solution.

Based on the titrations of B-3 (dialyzed) and V-FT (with sodium octyl sulfate), a reasonable uncertainty in the determination of the break point was found at ±2 when the reproducibility in the measurements of the surface tension is set to 0.3 dynes/cm (a reasonable value). See also the V-FT curves in Appendix 3.1 where the maximum errors in drawing the lines are indicated. The uncertainty in calculated amount of water in the latex at the

breakpoint can be neglected, with water added with the sodium chloride solution and water in the diluted 1atex dominating (negligible measurement and weighing errors). Therefore, the uncertainty in C_a (g emulsifier/L H_2O at the breakpoint) is also 2%, as we have

$$C_a = \frac{10V_k}{W_k} \qquad (8:2)$$

V_k – titration volume at the breakpoint
W_k g H_2O in 1atex at the breakpoint
(it is 10 g/L lauryl sulfate in the titration solution)

All other errors than ΔV_k can be considered negligible in relation to this, therefore,

$$\frac{\Delta C_a}{C_a} = \frac{\Delta V_k}{V_k} \qquad (8:3)$$

If we plot ΔC_a error bars for C_a as a function of the polymer content we can draw lines with minimum and maximum slopes. For V-FT^m we get:

Maximum slope: $S_a' = 15{,}0\ 10^{-5}$ mol/g PVC

Minimum slope: $S_a' = 12{,}7\ 10^{-5}$ mol/g PVC

with a mean of 13,8 10-5 mol/g PVC, close to the found value of 13,7 10-5 mol/g PVC.

The uncertainty in i S_a' can then be set to

$\Delta S_a' = ½\ (15{,}0 - 12{,}7)\ 10^{-5} = \underline{1{,}15\ 10^{-5}\ \text{mol/g PVC}}$

or ca. 8 % of S_a'

The uncertainty will increase with increasing V_k, but it can be reduced by making multiple titrations (parallels). The titration of B-3 (dialyzed) was also checked, and this gave the same result. It therefore seems that $\Delta S_a'$ of approx. 8% is reasonable.

When using soap titrations to determine average surface diameter, the sum $C_a + C_i$ is used for the calculation of S_a, D_s and N_s^w. C_i is calculated from the original amount of emulsifier in the latex, which is weighed, and also from the same weights and titration volumes that are used to calculate C_a. The error in C_i therefore becomes insignificant when the latex is not dialyzed, and the error in $C_a + C_i$ becomes less than the error in C_a. $\Delta C_i = 0$ gives

$$\Delta(C_a + C_i) = \Delta C_a$$

If for instance $C_a \approx C_i$ we get

$$\frac{\Delta(C_a + C_i)}{(C_a + C_i)} = \frac{\Delta C_a}{2C_a} = \frac{1}{2}\frac{\Delta C_a}{C_a} \qquad (8:4)$$

The error in D_s and N_s^w thus becomes half the error in S_a' (relative) at 50% coverage on the original latex. D_s will thus vary from approx. 8% and downward depending on the latex being

titrated. In the competitive growth experiments, a coverage of 80% of the emulsifier added is used for titration to 100% coverage. The uncertainty in the coverage will then be:

80 % • 0,08 = 6,4 % ≈ 6 % absolute

8.2.2 Dialysis, V-FT

In dialysis, initiator and buffer are removed from the latex, but the emulsifier may not be removed, and if this happens, it may not be complete. The reason for this may be that the emulsifier will be adsorbed to the particles and/or that the emulsifier molecules are so large (C_8 and C_{12}) that they do not diffuse through the cellulose membrane.

In the titrations of B-3 before and after dialysis, S_a' was found equal to 11.5 and 11.2 10^{-5} mol/g PVC, respectively. The difference is within the experimental error, and this may indicate two things; either the octyl sulfate will not disappear in dialysis, or the octyl sulfate is adsorbed to the particles to such a small the extent that titration with or without octyl sulfate (about 1 g/L) will give the same result. It is known that sodium octyl sulfate is relatively soluble in water, and that it usually would be much more present in the solution than adsorbed to the particulate surface (soap titration with this is therefore not favorable). To investigate whether the octyl sulfate disappears during dialysis, the experiment V-FT was performed as described in section 6.4.3 and Appendix 3.3. The titrations before and after addition of octyl sulfate gave S_a' equal to 14.8 and 14.0 10-5 mol/g PVC. The difference is also within the experimental error, and this shows that octyl sulfate in this case (small surface area per liter of water) is only to a small extent adsorbed to the surface or that it may be replaced during titration. In this case, this should be visible from the curves, but they show no difference.

After the octyl sulfate sample had been left for 6 weeks, it was titrated again, which gave S_a' = 13.7 10^{-5} mol/g PVC. The difference from the previous titrations is also within the experimental error, but there is a slight decreasing trend in S_a' (insignificant). This shows that the equilibrium of adsorption of emulsifier on the surface is set rapidly, probably within a few minutes, confirming the earlier assumptions that the octyl sulfate is only adsorbed to a small extent. We cannot, therefore, from this determine if the emulsifier disappears at the dialysis.

Results from the titrations of seed latex F-200 (curves in Appendix 3.1) before and after addition of sodium lauryl sulfate and after dialysis, indicate that sodium lauryl sulfate is partially removed by dialysis (S_a' = 3.30 and 4.25 10^{-5} mol/g PVC before and after dialysis, respectively). It is therefore likely that sodium octyl sulfate, which are smaller molecules, is also removed by dialysis. This justifies the simplification that has been done in calculating surface coverage for competitive growth, where possible octyl sulfate has been neglected. It would be interesting if experiments could be done where sodium octyl sulfate in the latex, optionally the dialysis water, could be analyzed by other methods than by soap titration.

When looking at D_s calculated by the titrations and comparing with $\bar{D}_{ar}$ calculated from the microscopic measurements (Appendix 12), we see that D_s will be lower than $\bar{D}_{ar}$, but the difference decreases with increasing diameter. This is probably due to the assumption

that in the calculation of D_s, a_s is assumed to be a constant, while a_s for sodium octyl sulfate will be lower than for lauryl sulfate (smaller molecules). As the diameter (surface area) increases, the impact of the octyl sulfate will decrease and D will approach $\bar{D}_{ar}$. One could possibly correct for this by replacing $S_a a_s$ in equation (4:164) by $\sum S_a a_s$ and using a lower a_s for octyl sulfate. Probably, $a_s = 50 Å^2$ for lauryl sulfate is also somewhat high and may also vary somewhat (with, for example, the salt concentration).

8.3 Correlation methods, experimental conditions

With regard to experiments with competitive growth, many different methods can ve used to correlate the results. The number of variables increases compared to ordinary emulsion polymerization, in addition, the number and diameter of small and large particles can be varied. It is therefore a question of what is the best method for systematizing the results. One can for example calculate experimental orders on the different variables, such as V_{pt}, V_{pa}, N_a^w, N_b^w, D_a, D_b, initiator concentration, etc. However, it is uncertain how much such orders will tell, and moreover, how accurately they can all be determined from a relatively small number of measurement points. Regarding the total variables V_{pt} and N_t^w, one will probably get about the same orders as with ordinary experiments; this will also apply to the initiator concentration, as shown in section 8.1.3. As for D_a, D_b, etc., one is primarily interested in the relative growth of D_a compared to D_b, how, for example, the relationship between them will change over time and with the experimental conditions. Plotting for instance D_a as a function of time gives a relatively poor overview, it is much better if D_b is plotted as a function of D_a or vice versa. We will then more easily be able to evaluate the relative growth. The model used by Vanderhoff et al. will, as mentioned in section 4.3.2, give a very good overview of the experimental results and it has the advantage of being quite simple. Of course, other models can be set up, for example, particle numbers and initiator concentrations can be included, but such models will hardly be more physically correct than a simple model because the real relationships are much more complicated. Instead, in this work the model used by Vanderhoff et al. has been used as a focus in the treatments, considering equation (4:51) as the definition equation for x. As an additional treatment, D_b is also set up as a function of D_a, since equation (4:52) can be used directly. In terms of equations that describe growth more precisely so that also the other experimental variables can be considered, the theoretical derivations given in section 4.3.3 and following, have been used. These have the advantage that they are based on real physical conditions.

In calculations from particle measurements, the different kinds of mean diameters $\bar{D}_n$, $\bar{D}_v$, etc. are calculated. It is then generally believed that it is most correct to use $\bar{D}_v$ in calculations of the kind used here. For some monodisperse latexes, the difference between the different diameters will not be so large that it would give major deviations if other mean diameters were used, but it is assumed that generally $\bar{D}_v$ it is the most correct here.

In the experiments, all experimental conditions can be varied within certain limits so that the relative growth under many different conditions can be determined. Conditions that are particularly relevant to vary are N_a^w, N_b^w, D_a, D_b and initiator concentration (possibly also

temperature and emulsifier coverage). It is then useful to systematize the experiments by keeping most of the parameters constant, while only few, preferably just one, are varied. This will then show the influence of this factor (but interactions may confound this). When such a factor is varied, derived factors will also vary, such as N_t^w, V_{pt}, etc. It will be difficult, however, to vary only one factor, as for example V_{pt}^0 will vary with N_t^w when N_a^w, N_b^w, D_a, and D_b are constant. This can be remedied by reading the reaction time from the kinetics curves at the same V_{pt}, then find D_a/D_a^0 from D_a as function of time, and then x. In similar ways, one can keep other factors constant, for example D_a, V_{pa} etc. There are therefore many ways to treat the test results, but due to the time available, there was no opportunity to do all such treatments.

After the seed experiments did not produce particularly useful results, it was found that first and foremost the particle numbers and total seed quantities should be varied, so that at the same total seed amount V_{pt}, experiments were performed with varying N_a^w/N_b^w. By then increasing or decreasing one of the particle numbers, another V_{pt}^0 resulted, and then another series could be run by varying N_a^w/N_b^w. As the amount of seed for these experiments (B-6) was limited, only six such experiments with total seed amounts between about 30 g and 70 g could be run (experiments B-13 - B-18).

After a new seed b was produced (F-200), it was also possible to run experiments with varying initiator concentrations, doubling and decreasing to the fourth of what was commonly used (3.0 10-3 mol/L H_2O). This latex also gave enough seed for two experiments with fatty alcohol addition where N_a^w/N_b^w was varied while V_{pt}^0 was kept constant. As the experiments and processing of the results were very time consuming, there was no time for more experiments, for example, with variation in particle size and variation of N_a^w/N_b^w and V_{pt} across a wider area.

8.4 Diameter measurements, errors in x

By measuring the particle diameters by the particle size analyzer, as mentioned in section 6.4.2, approx. 1000 particles of the seed latexes and approx. 500 of each size per. sample during the experiments with competitive growth. As long as an infinite number of measurements cannot be made, the mean diameter (calculated according to the various expressions) and the distribution curve, will always be subject to some uncertainty, and this will decrease the more particles being measured. This has been dealt with by Montgomery (19), which has calculated how many particles that has to be measured with 99% certainty to find an average diameter, respectively, a distribution curve, with a maximum error of 5%. He has calculated curves of the required number of measurements as a function of characteristic variables in the distribution function (how much of the particles have a diameter larger, possibly less, than a given part of the total number). Following these curves, one should, in the given cases, measure approx. 50 particles to get a maximum of 5% error. He also states that, for halving the error, the number must be quadrupled. Now, an error of 5% is too big to be accepted without further ado in these experiments; to find approximately how many particles should be measured, tests were done on the B-9/4 sample and also some samples

from other experiments if the particles appeared blurred. On B-9/4, the registry status was written down after approx. 50, 100, 300 and 450 particles were measured (see Appendix 12). It was then obtained a men diameter that decreased from 2290 Å at 50 particles to 2280 Å at 455 particles. If one assumes that this last one is most correct, the error at approx. 50 particles is 90Å, or 4%, so it seems that the specified curves by Montgomery are correct. It is also seen that after 300 particles, $\bar{D}_v$ changes very little (8Å, about 0.4% from 301 to 455 particles). From B-9/2 (large particles, samples 3 and 4), it is found that $\bar{D}_v$ changes from 3114 to 3042 Å (about 2%) when the number of particles measured increases from 346 to 520. In B-9/5 (small particles, samples 1, 2 and 3) $\bar{D}_v$ changed only slightly from 2477 at 147 particles to 2452 at 545 particles (about 1%).

It appears that the mean diameter of any experiment is almost constant after a few hundred particles are measured, while in other experiments it constantly changes, and usually in the same direction. This is probably due to the sharpness of the images, and if all the images are taken at the same focus. Usually, not enough particles were obtained by measuring only one image, and if we go to other images that are not focused in the same way, it may be possible to get a constant increase or a decrease when constantly more particles are measured and these add to the old ones. It is therefore important that all the images have the same focus. It seems that $\bar{D}_v$ with an error of ± 1% after measuring 300-500 particles can be obtained. Therefore, this was considered satisfactory in the experiments with competitive growth, as an increase in the number of particles measured would significantly increase the work of the measurements. Thus, it was possible to achieve a relative accuracy in D_a and D_b relative to each other of 1%, i.e. an accuracy in D_b/D_a of $1 \cdot \sqrt{2} = 1{,}4$ %. This is because D_b/D_a will be independent of the magnification of the images when the relative accuracy of the measurements is the same.

Now, the error in the exponent x due to error in D_b/D_a and D_a/D_a^0 can be found, when absolute errors in D_a^0, D_b^0, and D_a are neglected. To find x, parts of the reference curves are shown in Figure 26 on an enlarged scale for two areas of D_a/D_a^0, 1,5 and 2,5. A mean value of x equal to 2.4 is chosen.

$D_a/D_a^0 = 1.5$ gives:

$D_a = 1.5 \cdot 1003 \approx 1500$ Å

$D_b = 2830$ Å as $D_b/D_a = 1.886$

We have: $\Delta\left(\frac{D_a}{D_a^0}\right) = \frac{D_a}{D_a^0}\left|\frac{\Delta D_a}{D_a}\right|$ (8:5)

$= 1.5 \cdot 0.01 = 0.015$

$$\Delta\left(\frac{D_b}{D_a}\right) = \frac{D_b}{D_a}\left[\left(\frac{\Delta D_a}{D_a}\right)^2 + \left(\frac{\Delta D_b}{D_b}\right)^2\right]^{\frac{1}{2}} \qquad (8:6)$$

$$= \sqrt{2}\,\frac{D_b}{D_a}\left|\frac{\Delta D_a}{D_a}\right| \qquad (8:7)$$

$$= \sqrt{2} \cdot 1.886 \cdot 0.01 = \underline{0.027}$$

as $\frac{\Delta D_b}{D_b} = \frac{\Delta D_a}{D_a}$ in this case (1 %).

When the deviation of D_b/D_a is the most positive, at the same time, the deviation of D_a/D_a^0 will be the most negative (D_a at the minimum) and the maximum error in x can be found by drawing the diagonal in the error rectangle of Figure 37 below, from the upper left to the bottom right corner. From the figure, we find

$\Delta x = 0.07$

$D_a/D_a^0 = 2.5$ gives in the same way

$D_a = 2.5 \cdot 1003 = 2500$ Å

$D_b = 4080$ Å as $D_b/D_a = 1.631$

$$\Delta\left(\frac{D_a}{D_a^0}\right) = 2.5 \cdot 0.01 = 0.025$$

$$\Delta\left(\frac{D_b}{D_a}\right) = \sqrt{2} \cdot 1.631 \cdot 0.01 = 0.023$$

Which from the figure gives $\Delta x = 0.04$

Δx calculated in this way will increase with decreasing D_a/D_a^0. When D_b/D_a increases, we will get higher values for x. $\Delta(D_b/D_a)$ will also increase, but at the same time the distance between the lines for the different x will increase, so that Δx will not change significantly, at least as long as $2 < x < 3$.

The error calculated above is the lowest uncertainty that may be achieved if the uncertainty in D_a^0 and D_b^0 is zero and if there is no error in the image magnification. If reliable values for D_a^0 and D_b^0 can be found, but there is an error in the image magnification of e.g. 5%, this will not cause greater errors in D_b/D_a because D_b and D_a will change relatively the same while ΔD_a will become 5% so that $\Delta(D_a/D_a^0) = 5$ %. This is independent of $\Delta(D_b/D_a)$, which has the same value as above. By plotting $\Delta(D_a/D_a^0)$ on the figure for the two values of D_a/D_a^0, $\Delta x = 0.10$, resp. 0.04 (mean value). To find the total Δx in the two cases, we must set

$\Delta(D_a/D_a^0) = 1.5$: $\Delta x = (0.07^2 + 0.10^2)^{1/2} = 0.12$

$\Delta(D_a/D_a^0) = 2.5$: $\Delta x = (0.04^2 + 0.04^2)^{1/2} = 0.06$

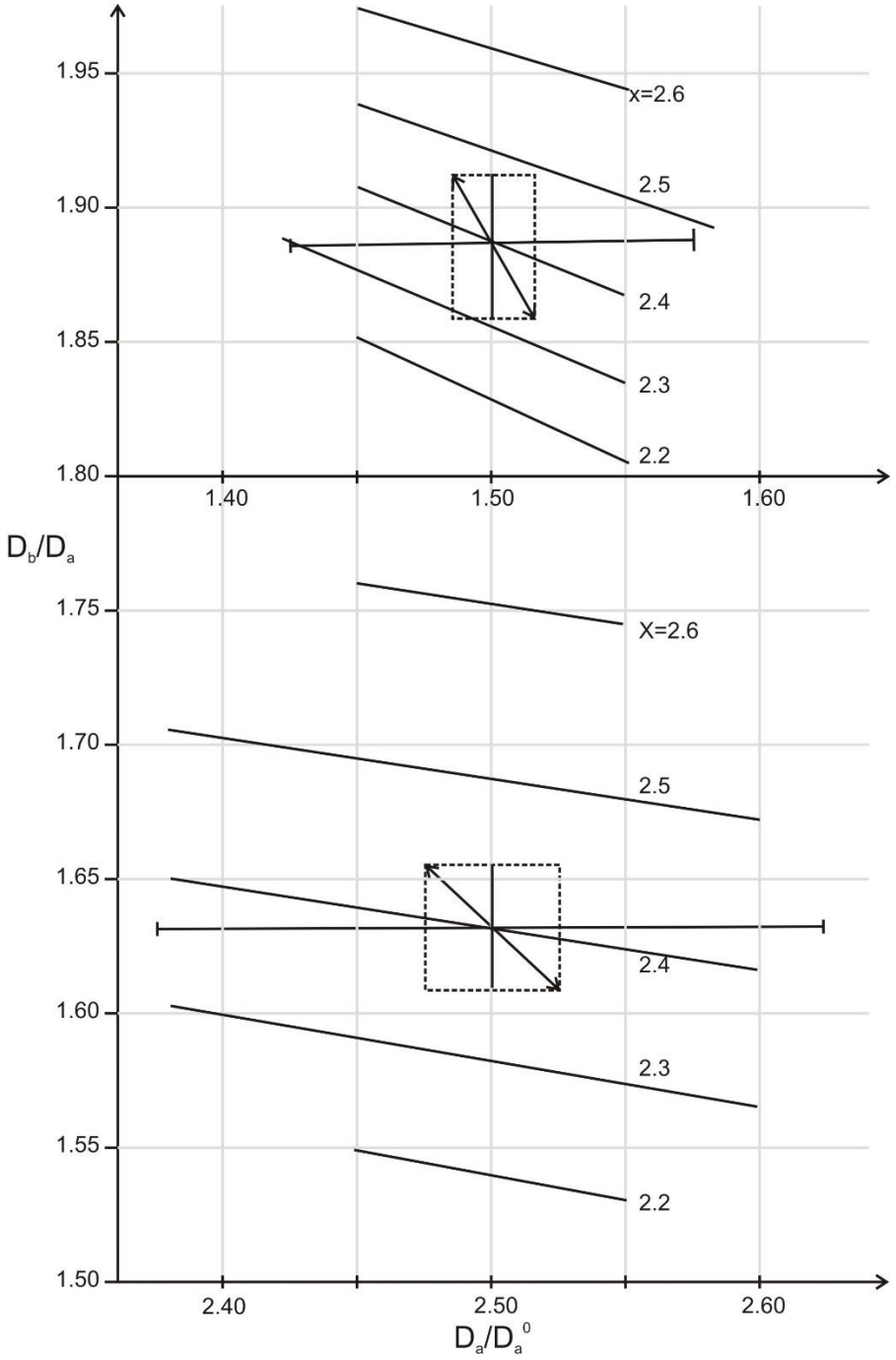

Figure 37. Calculation of error in x. Reference curves with drawn error rectangles and areas.

It is seen that an error in magnification at low $\Delta(D_a/D_a^0)$ can cause major errors in x while the error gets smaller at higher D_a/D_a^0. If e.g. the magnification (on D_a and D_b) higher than given, D_a/D_a^0 be too large and x therefore too large. This can be seen from the equation

$D_r = D_f/L$ (8:8)

D_r – real diameter of particle
D_f - diameter measured on image, D_r [=] D_f
L - image magnification

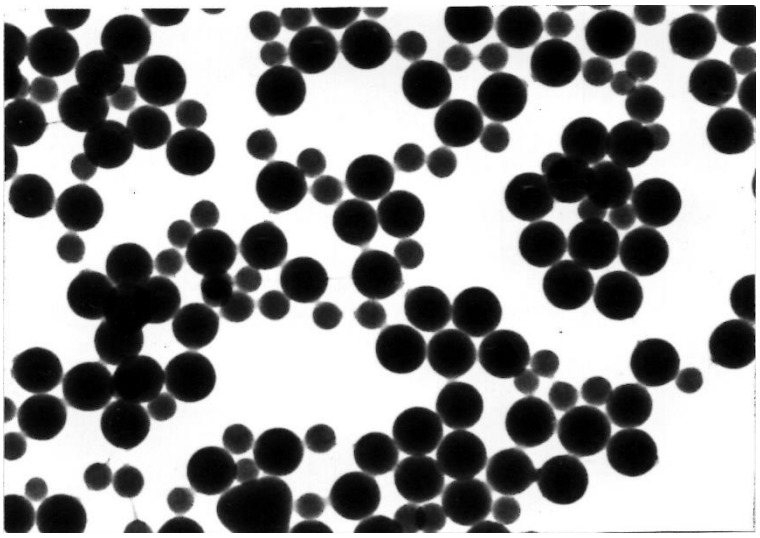

Figure 38. Image taken at 6x2600x magnification (B-18/5).

All photos of seed were measured at 24000x magnification (8000x on the microscope and 3x on the magnifier). Images from competitive growth experiments were also measured by this magnification until the large particles became too large to be measurable (see Figure 17) ($D_f \geq 10$ mm). These images were instead enlarged twice on the magnifier (16000x). As the particles were so large, more images (4 - 5) had to be taken of the same sample to get the desired 300-500 of each size. Instead, therefore, these images were taken at 2600x on the microscope and then enlarged 6 times (15600x). This resulted in a much larger particle count (up to 9 times as many) per negative, and therefore two negatives per sample were sufficient. However, it turned out that these images gave too large particle diameters so that x after what is shown above became too high along with D_a/D_a^0. The points on the curves for $x=f(D_a/D_a^0)$ therefore moved upwards to the right. By measuring the same particles taken at 24000x and 15600x, it was found that this last magnification would correspond 17200x if one assumed that the images taken at 24000x had the correct magnification. D_r should therefore be about 10% less, and as mentioned above, this should apply to both large and small particles. The measurements made at 15600x magnification were therefore corrected to 17200x. This is marked with a K in the forms in Appendix 6. Whether it is the microscope or magnifier that is responsible for this error is hard to say, but after measurements it can probably be assumed that the error is in both. It may also be that the subjective assessment of the particle sizes in the measurements is important even though the images were relatively sharp, see Figure 38 (B-18/5). An error only due to the magnification will cause a displacement of the points in Figure 23-25 along a line through the origin (constant D_b/D_a).

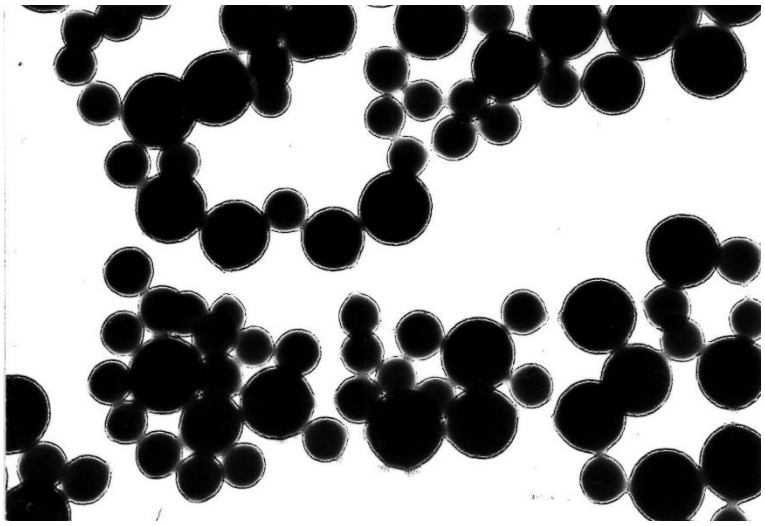

Figure 39. Example of highly overfocused image.

Measurements on images at 16000x (performed on the particle size analyzer) also gave a deviation from the measurements of images at 24000x. Here, the magnification of the microscope will not play a role and measurements made directly with a mm-ruler on the same images enlarged 2 and 3 times showed no significant difference in calculated D_r. It is therefore possible that it is the assessment of the particle size in the measurements that come in play, in particular for the small particles. If these are judged too large, as shown above, x will be too small when the large particles are judged correctly. However, there may also be errors in the large particles and the final result is difficult to predict. The error can then easily exceed 1% as found above. Such an error is likely, as the tests F-205 and F-206 where the measurements were made by departmental staff gave a negative P_t (calculated - measured). The assessment of particle size was clearly different here.

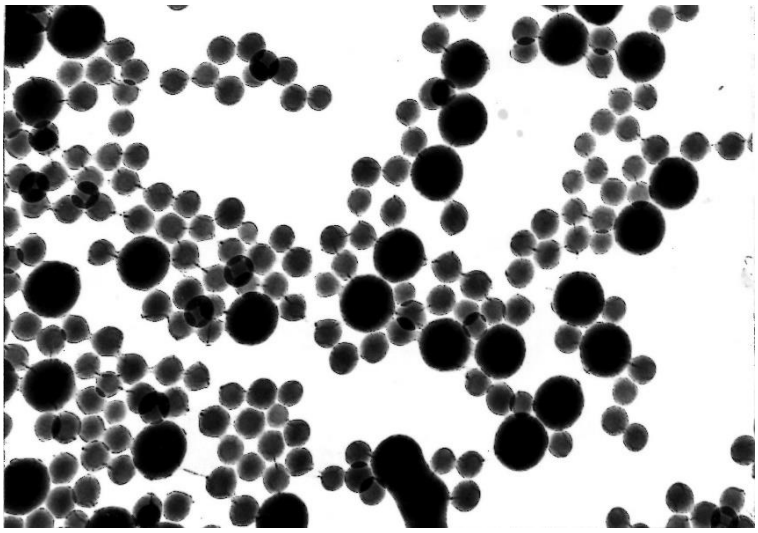

Figure 40. Probably overfocused image from B-15/1 that gives too high D_a.

Another possibility of error is the focus of the electron microscope. An error in the focus will cause an error in magnification, and this error can be significant. An overfocus will cause a ring around the particles, and the magnification becomes too large, see Figure 39. The same is true of underfocusing where the images get somewhat blurred. In this case it is also difficult to adjust the spot on the particle size analyzer correctly and the diameter is easily measured incorrectly. If the images from the same sample are not equally focused, it might result in a large spread of the diameter (large σ) and the diameter will change with the number of measured particles when measuring on multiple images with different focus. This is probably the case for e.g. sample B-9/4 as mentioned above. The data in Appendix 12 also shows that σ_a here varies relatively strongly. With such an error in focus, we will get an equal absolute error in D_a and D_b in addition to the relative error in D_a due to the magnification. If an image e.g. has rings around the particles, the magnification will be too large, i.e. D_a becomes relatively too large, and x too large. The absolute error, however, will cause too low D_b/D_a, as D_a the most affected. This will cause x to decrease. Therefore, the final effect on x is hard to predict, but it may not be that large. However, D_a/D_a^0 will surely be too large. A typical example of this is sample B-15/1, in Figures 20 and 21 (curves) and Figure 40 (image). By comparison with the other samples, we see that this point has an overly high value for D_a/D_a^0. x is somewhat uncertain, as the other points also contain the usual uncertainty.

It has also been noticed that on some images there seems to be some kind of coating on the particles, a kind of skin that gives unclear particles and also gives too high diameter. A good example of this is latex B-MIX where the coverage of emulsifier according to Appendix 4.2 is higher than 80%. Figure 41 shows this. Calculation of D_a^0 for this from measurement of B-8 and B-3 (Appendix 4.4) gave a diameter about 1150 Å (max 1200 Å). However, measurements on B-MIX (added emulsifier) gave 1300 Å in diameter, i.e. even higher than B-8 (1240 Å). This is probably due to the coating seen in the figure. It is somewhat uncertain what this may be due to, but one might imagine that the emulsifier possibly binds some water (hydrophilic properties) despite the high vacuum in the microscope (?). There are currently investigations at the department of the importance of the emulsifier on the diameter measurements.

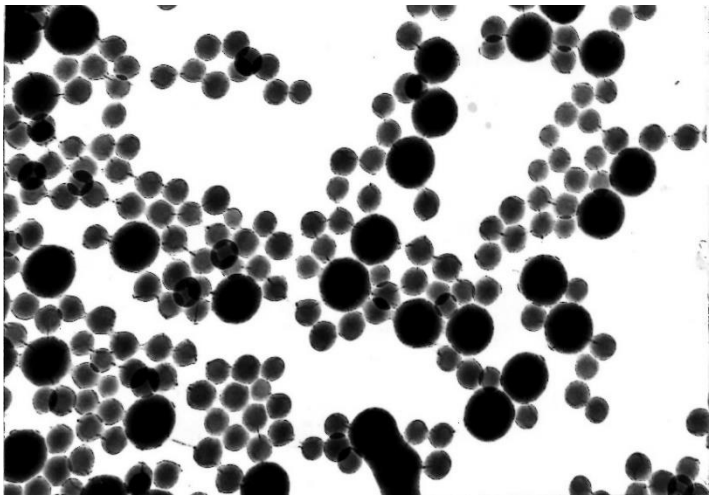

Figure 41. Coating that gives unclear and too large particles. B-MIX.

The values used for the diameter corresponding to the different intervals of the particle size analyzer at a given magnification were given by the department. However, after a while, it was discovered that these values were probably too high. Measurements of the largest and smallest diameter of the spot on the analyzer gave limiting values of 1.0 and 10.0 mm, while the values used were 1.1 and 10.3 mm, respectively (the manufacturer of the instrument states 0.7 and 9 mm, but this cannot be correct). As this was discovered so late in the work, it was decided that there was no particular purpose in correcting all the calculated diameters and print new tables for calculating x. A change in diameter also affects all the derived variables, such as for example, N^w. All diameters will be somewhat smaller (3 - 5%, largest deviation for small particles). B-3+5 and B-6 will have $\bar{D}_v$ equal to 955 and 2113 Å, respectively. This gives

$D_b^0/D_a^0 = 2.212$

B-13/3 gives $D_a = 2324$ Å

$D_b = 3724$ Å

$D_a/D_a^0 = 2.433$

$D_b/D_a = 1.603$

x = 2.2 gives $D_b/D_a = 1.570$

x = 2.3 gives $D_b/D_a = 1.617$

I.e. $$x = \frac{1,603 - 1,570}{0,1(1,617 - 1,570)} + 2,20 = \underline{2.27}$$

The old values gave x = 2.28

The conclusion is that x will therefore change little, and it was chosen to use the old values. The correction of the figures that gives D_b as a function of D_a is also not so big, and the points will be shifted approximately along the line from (D_a^0, D_b^0) (this is the reason for the slight shift in x).

As long as D_a^0 and D_b^0 are correct, the error in x will vary somewhat, it is usually around 2 - 3%, but can in unfavorable cases become considerably larger (up to 10%) as explained above. However, the results obtained eventually gave an indication that the values of D_a^0 on seed B-3+5 and seed B-MIX were too low. First, it seems that D_a increases unusually fast at the start of the reaction up to the first pressure sample. This is evident, for example, in Figure 28, as the distance from start to sample one is always greater than from sample one to two, although the time difference is the same. This tendency does not continue with the following samples (see Appendix 6). A similar tendency can be seen in Figure 24, as the curvature of the $D_b = f(D_a)$ curve is usually largest at the start.

Another suggestion that D_a^0 is too small appears when considering seed B-MIX. Calculations (Appendix 4.4) gave a mean diameter of 1150 Å and spread at 140 Å. A distribution curve with two peaks should also be expected, however, measurement on B-MIX

yielded a mean diameter of 1300 Å, as mentioned, and a spread of 94 Å. The distribution curve has only a peak. The high diameter may be due to the factors mentioned, but the spread should not change as much as this. There is therefore a possibility that the diameter of B-3+5 is greater than 1003 Å, the maximum that can be anticipated is 1100 Å. This will give a spread of B-MIX about 100 Å and a calculated diameter of approx. 1200Å. This seems to be in better accordance with the other diameters. A higher diameter (spread) on B-3+5 can either be due to errors in the images of B-3 and/or that 1atex B-5 (which was not photographed and mixed with B-3), had a higher mean diameter. B-5 was made in the same way as B-3, and the diameter should therefore be the same, but as B-8 differed significantly, it might also be thought that B-5 differed somewhat.

Due to the uncertainty in D_a^0 as explained, it was most appropriate to make the calculations of, among other things, x, with both the alternate values. The correct value may then be located somewhere between these limits. The influence of D_a^0 on x can be found by comparing the values calculated for the two different diameters, for example by comparing Figures 28 and 29. The increase in D_a^0 by 10% will obviously cause an increase in x, and this increase is largest, 0.3 - 0.4, at low D_a/D_a^0 (0.3 - 0.5). It decreases with increasing D_a (about 0.1 at $D_a/D_a^0 = 3.0$), which corresponds to approx. 15 to 4% x. The trend in x will then be different, see section 8.5.

An error in D_b^0 could also imagined. It is in fact seen that calculated and measured dry matter are badly matched, which may be due to high N^w. This applies in particular to seed experiments (B-13 - B-18). Now, the compliance becomes better when D_a^0 is increased, as N_a^w then decreases. There will nevertheless be some difference between P_t (calc) And P_t (measured). This will increase with increasing conversion, which may be due to the fact that D_b^0 is too low. If D_b^0 is increased, N_b^w will decrease and compliance will improve. However, x will again decrease, which may seem less likely. It is therefore possible that the reproducibility of D_b^0 in the production of seed is not as bad as has been thought, but that the error can be elsewhere (microscopy). It is also seen that the seed with the largest mean diameter (F-200, 2390 Å) sometimes gives negative P_t (calc - measured) and that B-7 (2320 Å) does not give as much discrepancy as B-6 (see experiments B-9 and B-10).

An indication of the influence of changes in D_a^0 and D_b^0 on x can be found in Figure 42. Here, the differential values of x are calculated in the described way for two different values of D_a^0 and two of D_b^0 (10% difference), i.e. for 4 combinations. The differential values of x will vary more than the integral values (see also section 8.6), while the initial values and trend are the same. Data from experiment B-13 (corrected values) have been used. The same trend as described above is clearly see; higher D_a^0 will give higher x while higher D_b^0 will work in the opposite direction. Changes in D_b^0 (relative) give the largest change in x (because D_b^0 is largest). When the ratio D_b^0/D_a^0 is approximately constant, it is seen that x will not change much (only D_a/D_a^0 changes). It is also seen that at $D_a/D_a^0 \approx 2.3$, the approximately same value for x will be obtained for all four combinations. This may indicate that x approaches an approximately constant value, which also indicated by the calculated integral

values (Figure 42 does not apply to fits much above $D_a/D_a^0 = 2.5$ because the curves then become extrapolations that are very inaccurate).

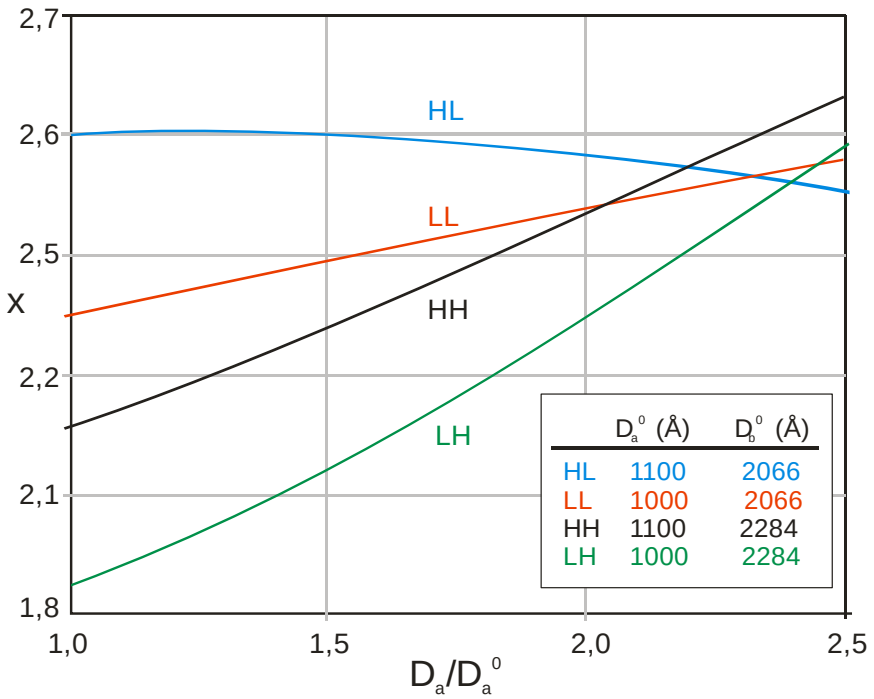

Figure 42. Error calculation on run B-13. Differential values of the exponent x calculated by matching parables to experimental data: $D_b = C_1 + C_2 D_a + C_3 D_a^2$.
The curves show the influence of D_a^0 and D_b^0 on x.

From what is mentioned above, it is understood that the uncertainty in x is quite large, but the order of magnitude is quite certain. In all the experiments (with a few exceptions) the value of x was between 2 and 3. It is also seen that the difference in x between the different experiments decreases with increasing conversion. The order of magnitude found fits well with what could be expected from ordinary polymerizations, Figure 16. After what is mentioned by Ewart and Carr, the spread of the distribution curves will increase when $x > 2$, and such a trend is evident in Figure 16. From the figure it is also seen that in the "max" region the distribution curve will widen faster than usual, so x will be higher. This may have several reasons, and it is therefore difficult to say something specific about it. This effect has not been included in this investigation, as all samples for microscopy were taken out before "max" as mentioned in section 6.2.1.

The absolute spread of the diameter during competitive growth is seeing to increase, while the relative spread (1%) shows a marked declining trend. We thus see the same tendency as under normal polymerizations. This fits well with the results of the experiments conducted by Ewart and Carr and by Vanderhoff et al. as mentioned in section 3.1. Vanderhoff et al. found for styrene a value of x between 2 and 2.5, while Ewart and Carr found that the spread on the diameter increased, which corresponds to $x > 2$. The same has been achieved here, even though the results are not quantitatively compliant. This would not be expected either.

As for the variation of x with conversion, this will, as has been seen, depend on D_a^0, which is uncertain. However, a certain trend is the effect of the amount of seed. There was a clear increase in x when the number of particles, i.e. also V_{pt}^0, was increased. Particularly this is shown by the experiments B-13 - B-15. Experiments B-14, B-16, and B-17 are all done with the same V_{pt}^0 (P_t^0 = 44.3 g PVC/L H_2O). B-14 and B-16 show a clear compliance despite different N_a^w/N_b^w (5:10 and 1: 1, respectively). B-17 differs somewhat from these, especially in the first two samples. Now, however, B-17 was centrifuged because $N_a^w/N_b^w \approx 10$ and it would then be very few large particles compared to small ones, such as in B-15. These pictures were somewhat unclear, especially the small particles, and were similar to the pictures of the B-MIX. It is therefore possible that the small particles here are too large and therefore x too low (section 8.4). B-18 was slightly lower than B-15 despite the same V_{pt}^0. Particle numbers are lower here, but this should not be as important as found in the foregoing. However, very good reproducibility should not be expected in the experiments because of all the sources of error present and discussed, among other things, in section 8.4. When experiments with the same starting volume of the two latexes (same amount of PVC) especially B-17, are considered, it is also seen that the small particles will grow fastest; even in B-14 it is seen that the small particles, which initially make up a smaller volume than the big ones, will eventually pass the big ones in volume. This is a natural consequence of the magnitude found of x, since the ratio between the volumes will only be constant when x = 3.

To investigate a little more exactly how the four variables D_a, D_b, N_a^w, and N_b^w are affecting x, the described regression analysis was performed. As mentioned above, this will only provide linear correlations, but will also say something about the tendency in x within the limits of the experimental conditions. However, one should be careful to use the found equations substantially outside this range. The equations show that D_a and D_b will have an opposite effect on x, and this will be of the same order of magnitude. That there is such a connection is also clear from Figure 37. However, that a change in D_a^0 and/or D_b^0 would have a similar effect, cannot be deduced from this, in that case experiments with varying starting diameters would have to be made. The most interesting result of this analysis, however, is the influence of N_a^w and N_b^w. It is clear that x increases with both of these factors, which also could be concluded from the forgoing. It turns out, however, that N_b^w has much greater influence than N_a^w. This is probably due to the fact that the b particles have so much greater volume than the a particles (about 10 times with the original diameters). The order x will thus depend mostly on the amount of seed and not so much on the number of particles. The same result was obtained by a direct comparison of B-14 and B-16 as mentioned above. The found equations describe the experimental results quite well, explaining the uncertainty in x as a result of uncertainties in D_a and D_b, the equations can thus be used very easily for error estimation.

Regarding the reliability of the regression analysis, it seems satisfactory. The values of the F-level provide a measure for this (analysis of variance). One must consider the final values (F-levels for the final regression) and not so much the values that are found in each step in the analysis (see (18)) as this will not give an unambiguous result, as they are

depending on the order of the inputs of the four variables (4 steps). Without going into the theory, one can say that the system will have a number of degrees of freedom, ν_1 and ν_2. Here $\nu_1 = 1$ because in the analysis the variation in x for one variable at a time is considered, and $\nu_2 = 24$, i.e. the number of measurements (29) minus the number of variables (5). From statistical tables can be found values for F, here $F_{1,24}$ (F-distribution). These values will depend on the wanted degree of confidence in the analysis, as increasing degree of confidence will give increasing F. If we wish with 95% probability that the correlation will not be worse than found, F = 4.26. 97.5% probability gives F=5.72, 99.0% gives F=7.82 and 99.9% gives F=14.03. Analysis no. 1 yields higher F values than analysis no. 2, but the result is as seen satisfactorily (better than 97.5% for most cases). The multiple correlation coefficient (1 at 100 correlation) is also satisfactory so that the found equations explain most of the variation in x.

The experiments with variation in initiator concentration gave somewhat uncertain results. It is thought that may be due to uncertainty in the particle measurements. According to the theory (see next section), x should increase with decreasing initiator concentration to x = 3 when $\bar{n}<<1$. However, both B-20 and B-21 gave higher x than B-19. The results from B-21 are fairly satisfactory, although the variation is somewhat less than expected. However, it is not possible to conclude with certainty about B-19 and B-20 because of uncertainties in the measurements.

The experiments with fatty alcohol gave somewhat higher x than B-19 - B-21. This is as expected, as previous experiments at the institute have given an indication of this, however, the effect is not so great. A higher coverage of fatty alcohol should give even higher x. The reason for this effect has not yet been clarified, but may be due to the absorption rate of particles in the particles increasing against proportionality to the surface. However, there is no clear reason for this to occur.

8.5 Differential values, theoretical calculations

The calculations from the theoretical outlines in section 4.3.4 did not match well with the experimental data. To compute values of x directly, one had to calculate differential values, and this was done according to the described method. These differential values gave about the same tendencies in x as the integral values, while the variation with D_a/D_a^0 is greater, as may be expected. The fitting of the parabola turned out to be easy and achieved a good result, while some experiments gave curves that had a different course than one should expect when comparing the integral values of x. However, an accurate result it should not be expected when the number of measurement points is so small and the accuracy of D_a and D_b is not better. Even using a parabola, only one point that deviates greatly from the others can significantly affect the curve. Instead use a straight line might be used, but then the discrepancy between real and fitted curve shape would be too big. Moreover, it would always give a decreasing x.

When comparing these differential values with the values calculated using Bessel functions, it is seed that the compliance is better with D_a^0 on seed B-3+5 equal to 1100 Å than

to 1003 Å. This is again an indication that 1100 Å is more correct than 1003 Å. The order of magnitude of the calculated x is, however, the same as the experimental, and the theory of desorption and reabsorption of radicals can therefore give a partial explanation of why the growth is as found. This appears as a result of the fact that the mean number of radicals are much higher in large than in small particles. This is again due to the fact that the rate of absorption will be greatest for the large particles, while the desorption rate and the termination rate will be lower due to larger particle volumes (lower concentrations). The difference is however, not so large that the relative volume growth of large particles is as high as for small particles, and D_b/D_a will therefore decrease with increasing conversion. The value of $\bar{n}$ is approximately consistent with what can be calculated from the kinetics curves and equation (4:4) (precise calculations have not been made). The constants used in the calculation are somewhat uncertain, especially D_p, so that the exact magnitude of x as well can fit. However, the tendency is not entirely consistent with the experiments. In particular, this is seen on B-15. Now the actual method of determining the differential x from experimental data is not quite satisfactory, but it is difficult with so few samples to find a better method. The curvature of the curves is not very important, as it cannot be expected for a parabola to provide a good fit for the second derivative. In order to directly compare calculated values with experimental, it would therefore be advantageous to compare the diameters directly. This is done in Figure 24 for two different values of D_p (for run B-13). It can be seen that with the lowest value of D_a^0, there is no good match, while D_a^0 = 1100 Å gives a much better result. It is therefore possible that the discrepancy is mostly due to experimental errors.

In the experiments with seed B-MIX and F-200 a stronger increase of x (Da = 1150 Å) has been obtained than in the other experiments. This can also be due to experimental errors (D_a and D_b^0). It seems that this is also the reason for the discrepancy between the different experiments. From Figure 34, it is seen that a decrease in initiator concentration (decreases in ρ^w, i.e. in α') would increase x, while any distinct difference in the experimental curves cannot be found (when ignoring a stronger increase in B-19).

From Figure 35, it can also be seen that if ρ_A is proportional to the particle surface instead of the radius, a higher x would result, while the decrease would be stronger. The experiments with fatty alcohol gave as seen in Figure 33 slightly higher x, but the increase is not large. Therefore, it cannot be drawn particularly certain conclusions from this.

The possibility for agglomeration of large particles may also be suggested; loose agglomerates that could dissolve by ultrasonic treatment at the time of preparation or just by dilution. Experiments carried out at the department did not give results that could point in this direction. To investigate how such agglomeration would affect the calculated x, a calculation was made where the diameter of the large particles increased 10 times and the particle number decreased to 1/1000 (constant V_{pb}^0). The result of this calculation is seen in Figure 36. The decreasing trend in x is then replaced with an almost constant value. This fits better with the experimental results, but it is unlikely that it is a good explanation.

A better explanation of the discrepancies may be that the situation considered in the theoretical derivations is not completely realistic, but that it should be distinguished between

different kinds of radicals as discussed in section 4.3.6. As mentioned in section 7.3, the calculation for this system has at the time of writing not yet gone through on the computer, and the result is therefore uncertain.

The results of Vanderhoff et al. have arrived at for styrene are similar in many respects to what has been found here, although styrene differs in many ways from vinyl chloride in behavior by emulsion polymerization. Even though the mechanism of desorption and reabsorption does not apply, values of x between 2 and 2.5 can still be obtained, namely if $\bar{n} > 1$ (4.3.5 and 4.4). The variation with the conversion can then be thought of as a variation of the rate of absorption between proportionality to the radius and to the surface. However, this seems unlikely because Vanderhoff et al. operated with highly diluted latexes. A better explanation of why x exceeds 2 is that all of their polymerizations were driven to virtually complete conversion, i.e. through the "max" region. But in this region, both for vinyl chloride and probably also for styrene there will be an abnormally strong increase in x, which may be due to the fact that the monomer concentration in large and small particles differs. It may also have other reasons. When Gerrens states that they have obtained lower x for smaller particle sizes, this may be due to $\bar{n}$ decreasing against ½ when the particle size decreases, i.e. x approaches zero as the lower limit. Gerrens' explanation of their high values of $\bar{n}$ is that they operate with so low particle numbers and high initiator concentrations. It is then also reasonable that they for the smallest particles found an increase in x with increasing initiator concentration, as x with low concentrations may approach zero because then $\bar{n} = ½$.

However, this does not seem to be the case with vinyl chloride. The variation of x with the initiator concentration and the amount of solids is reversed by what one would expect if $\bar{n} >> 1$. This gives a clear indication that desorption and reabsorption of radicals is a much more likely explanation of the observed order than $\bar{n} >> 1$. According to that, x could not become larger than 2.5, while this was achieved here (though with some uncertainty).

9 Conclusion

1. In competitive growth experiments an experimental order x of the volume growth with respect to particle diameter in the range 2 to 3 has been obtained.
2. This order increases with increasing amount of seed against a possible upper limit of 3.
3. Inaccuracies in the analytical methods make it difficult to say anything about the variation of the order with the conversion.
4. A mechanism of desorption and reabsorption of radicals can explain the magnitude and variation of x much better than a high radical number in the particles, but it cannot be said anything about the compliance with increasing conversion.

10 References

1. J. Uge1stad, P.C. Mørk, and J.O. Aasen, J. Polymer Sci., A-1, 5, 2281 (1967).
2. J. Uge1stad, P.C. Mørk, P. Dahl, and P. Rangnes, J. Polymer Sci., C 27 49 (1969).
3. J. Uge1stad and P.C. Mørk, British Polymer J., 2, 31 (1970).
4. J.W. Vanderhoff, J.F. Vitkuske, E.B. Bradford, and T. Alfrey, JR., J. Polymer Sci., 20, 225 (1956).
5. J.W. Vanderhoff and E.B Bradford, TAPPI, 39, 650 (1956).
6. G. Gatta, G. Benetta, G.B. Talamini, and G. Vianello, Advances in Chemistry Series, No. 91.
7. H. Gerrens, Advances in Polymer Science, Band 1, Heft 2 (1958-1960).
8. R. H. Ewart and C.I. Carr, J. Phys. Chem., 58, 640 (1954).
9. J. Ugelstad, H. Lervik, B. Gardinovacki, and E. Sund, to be published.
10. W.H. Stockmayer, J. Polymer Sci., 24, 314 (1957).
11. J.T. O'Toole, J. Polymer Sci., 2, 1291 (1965).
12. W.D. Harkins, The Physical Chemistry of Surface Films, Reinhold Publishing Corp., New York, 1952.
13. a) W.V. Smith and R. H. Ewart, J. Chem. Phys., 16, 592 (1948). b) J. Am. Chem. Soc., 70, 3695 (1948). c) J. Am. Chem. Soc., 71, 4077 (1949).
14. F. A. Bowey et al., Emulsion Polymerization, Interscience publishers, Inc., New York, 1955, First ed.
15. H. Lervik, unfinished work.
16. R. Byron Bird, W.E. Stewart, and E.N. Lightfoot, Transport Phenomena, John Wiley & Sons, Ind, New York.
17. Documentation for the program CURVEFIT (N0062), Computing center, NTH.
18. A.O. Østlie, Documentation for the program REGANA (N0175), Computing center, NTH.
19. D.W. Montgomery, Bulletin Technique Zeiss, No. 44, Carl Zeiss, Oberkochen/Württ.